ABSTRACT

GALVÃO, RAFAELO MARQUES. Discovery of a New Family of Protein Kinases Containing Phosphoinositide 3/4-Kinase and Ubiquitin-Like Domains. (Under the direction of Wendy F. Boss.)

This thesis is focused on the characterization of new protein kinases from plants. Here, I show that the Arabidopsis *UbDKγ4* and *UbDKγ7* (ubiquitin-like domain kinases), which were originally identified as putative phosphatidylinositol 4-kinases, have protein kinase activity. As the proposed name UbDK suggests these protein kinases have ubiquitin-like domains in addition to the catalytic phosphoinositide 3/4-kinase domain. In depth characterization of UbDKγ4 revealed its interacting proteins and substrate. UbDKγ4 interacts directly with proteins involved in the ubiquitin/proteasome system. Ubiquitin fusion degradation 1 (UFD1), one of UbDKγ4 interacting partners, was identified as a UbDKγ4 substrate and the UFD1 phosphorylation sites were mapped. My thesis is that UbDKγ4 and UbDKγ7 are founding members of a new family of protein kinases.

Analysis of protein-protein interactions, gene expression and preliminary characterization of transgenic plants expressing *UbDKγ4*-derived polypeptides suggested that UbDKγ4 may be involved in protein degradation during the unfolded protein response in plants. Specifically, we propose that UbDKγ4 is implicated in the recognition and delivery of ubiquitinated proteins derived from the endoplasmic reticulum-associated degradation (ERAD) pathway for degradation via the 26S proteasome.

Discovery of a new family of protein kinases containing phosphoinositide 3/4-kinase and ubiquitin-like domains

by

Rafaelo Marques Galvão

A dissertation submitted to the Graduate Faculty of
North Carolina State University
In partial fulfillment of the requirements for the degree of
Doctor of Philosophy

Plant Biology

Raleigh, NC
August 16, 2007

Approved by:

Rebecca S. Boston

Ralph E. Dewey

Imara Y. Perera

Dominique Robertson

Wendy F. Boss
Chair of Advisory Committee

DEDICATION

To my wife Rita,

my grandparents,

my parents and brothers.

BIOGRAPHY

Rafaelo was born in the coastal city of Vitória, southeastern Brazil, on November 26th 1974, son of loving and dedicated parents, Elizeu and Angela Galvão. Rafaelo attended the Colégio Nossa Senhora da Penha – Marista for his education from kindergarten to high school. At the age of 17, he moved away from his hometown to Viçosa, a small college town in the country, to pursue B.S. degree in Biology at the Universidade Federal de Viçosa. His interest in science leaded him to join the laboratory of Dr. Eliane Menin in the end of his freshman year. In Dr. Menin's lab Rafaelo was awarded with a one-year undergraduate research scholarship to study the anatomy of the digestive track of a tropical freshwater fish. Also as undergraduate student, Rafaelo became later involved in other extracurricular activities such as an environmental education program at the Serra da Canastra National Park and a research project on systematic and ecology of Bromeliaceaes and Orchidaceaes. In his last two years as undergraduate student, Rafaelo worked as teaching assistant for the "BIO111" laboratory. BIO111 was a freshmen level cell biology course. Through that experience Rafaelo became interested in cellular and molecular biology. Early 1997, soon after graduation, Rafaelo was recruited as a research technician in the laboratory of Dr. Elizabeth Fontes. That experience gave Rafaelo a chance to discover the fascinating wonders of the recombinant DNA world. One year later Rafaelo was accepted to the graduate school with full scholarship to pursue M.Sc. degree in Genetics. Under guidance of Dr. Fontes, Rafaelo worked for his thesis in the discovery and characterization of new strains of tomato viruses. During the many years that Rafaelo lived in Viçosa he had the opportunity to explore his passion for music, photography and capoeira (the Brazilian martial art). The years that Rafaelo spent in there gave him also something so precious that no word (in English or Portuguese) can express the value. It was in Viçosa where Rafaelo met Rita, the woman that became his wife and the love of his life. After getting his M.Sc., Rafaelo sought for professional experience outside of the academia. Early 2000 he moved to Londrina, southern Brazil, to join the laboratory of Dr. Luiz Gonzaga Vieira and Dr. Luiz Filipe Pereira at the Instituto Agronômico do Paraná (IAPAR). There Rafaelo had the opportunity to work with applied plant molecular biology and biotechnology. He was specifically involved in a research project aiming the investigation of fruit ripening and ethylene biosynthesis in coffee. In the year of 2001, Rafaelo applied for a

full scholarship to pursue doctoral degree abroad from a training program sponsored by the National Council for Scientific and Technological Development (CNPq). Rafaelo was awarded with the scholarship and in January 2002 he came to the United States and joined Dr. Wendy F. Boss' laboratory in the Department of Plant Biology at North Carolina State University.

ACKNOWLEDGMENTS

I would like to thank my thesis advisor Dr. Wendy F. Boss for welcoming me in her laboratory and for providing guidance, enthusiasm, patience and encouragement to pursue my research project.

I want to thank the Department of Plant Biology of the North Carolina State University and its graduate program for the opportunity.

I am grateful to the National Council for Scientific and Technological Development (CNPq), the Brazilian funding agency that, generously, provided the scholarship for my training.

Many thanks to the members of my thesis advisory committee Dr. Rebecca S. Boston, Dr. Ralph E. Dewey, Dr. Imara Y. Perera, and Dr. Dominique Robertson for their help, advise and support.

Many thanks also to my former mentors Dr. Elizabeth Fontes, Dr. Luiz Gonzaga Vieira, and Dr. Luiz Filipe Pereira, without whom I would not have gotten this far in my career.

I would like to thank also the following people:

The current and past members of Dr. Boss' laboratory including Catherine Beck, Irena Brglez, Dr. Amanda Spell-Davis, Chiu-Yueh Hung, Dr. Yang Ju Im, Dr. Imara Perera and Dr. Brian Philippy for the help, fruitful discussions and friendship; The talented undergraduates that in many ways helped me in my research, including Jonathan Davis, Keriann Paul, Casey Lowder and Aaron Lomax; My colleagues of the Plant Biology graduate program and the Metabolic Engineering personnel, particularly, the members and former members of Dr. Boston and Dr. Dewey's laboratories for the friendship and help; The administrative staff of the Department of Plant Biology, in particular, Sue Vitello who, from day one, guided me with my academic responsibilities; Dr. Susan Carson and Dr. Joanna Miller for mentoring me during my year as Teaching Assistant in the Biotechnology program; Dr. Michael Goshe, Dr. Norma Houston, Eric Soderblon, and Uma Kota for the valuable collaboration; My dear Brazilian friends Matias and Mariana Kirst, Patrick and Gisele Gurgel, Luiz and Rita Maia, Rodrigo and Debora Lourenço, with whom my wife and I

shared many great moments; My family in Brazil, particularly, my parents for their support and encouragement despite the distance.

Finally, I want to thank my wife Rita for her unconditional love and friendship and for always being there for me.

TABLE OF CONTENTS

LIST OF FIGURES

CHAPTER 1

CHAPTER 2

LIST OF TABLES

LIST OF SYMBOLS AND ABREVIATIONS

ABRC	Arabidopsis Biological Resource Center
ATM	ataxia telangiectasia mutated
ATR	ATM and Rad3 related
Act	actin
CDC	cell cycle division
C_T	cycle number at the threshold fluorescence
DNA-PK	DNA dependent protein kinase
ER	endoplasmic reticulum
ERAD	ER-associated protein degradation
GST	glutathione S transferase
GFP	green fluorescent protein
Ins(1,4,5)P_3	Inositol 1, 4, 5 trisphosphate
KDa	kilo Dalton
KD	kinase dead
LC	liquid chromatography
LC/MS/MS	liquid chromatography-tandem mass spectrometry
MS	mass spectrometry
PCR	polymerase chain reactio
PLC	phospholipase C
NPL	nuclear protein localization
PI	phosphoinositide
PI3K	Phosphatidylinositol 3-kinase
PI4K	phosphatidylinositol 4-kinase
PI3/4K	phosphoinositide 3/4- kinase
PIKK	phosphoinositide kinase-related protein kinase
PIP5K	phosphatidylinositol phosphate kinase
PtdIns	phosphatidylinositol
PtdIns(4)P	phosphatidylinositol 4 phosphate
PtdIns(4,5)P_2	phosphatidylinositol 4, 5 bisphosphate
PUX	plant UBX domain-containing protein
Rad	radiation sensitive
RP	regulatory particle
RPN	RP non-ATPase
RPT	RP ATPase
RT-PCR	reverse transcription – polymerase chain reaction
SDS-PAGE	sodium dodecyl sulfate polyacrylamide gel electrophoresis
SMG1	suppressor with morphogenetic effect on genitalia
std	standard deviation
TAIR	The Arabidopsis Information Resource
Tm	tunicamycin
TRRAP	transactivation/transformation-domain-associated protein
TOR	target of rapamycin
UBA	ubiquitin associated

UbDK	ubiquitin-like domain kinase
UBL	ubiquitin-like
UBX	ubiquitin regulatory X
UFD	ubiquitin fusion degradation
UIM	ubiquitin interactin motif
vWA	von Willebrand A

CHAPTER 1

Phosphoinositide 3/4- kinase and ubiquitin-like domains and the discovery of new plant protein kinases

Introduction

The work presented here started as an attempt to characterize new plant phosphatidylinositol (PtdIns) 4-kinases (PI4Ks). PI4Ks are the enzymes that catalyze the phosphorylation of PtdIns to PtdIns(4)P, the first committed step of the lipid-mediated synthesis of the second messenger inositol (1,4,5) trisphosphate ($InsP_3$). The motivation for this work comes from the fact that not only $InsP_3$ but also other phosphoinositides are important signaling molecules in the life of eukaryotic cells (Carpenter and Cantley, 1996; Toker and Cantley, 1997; Fruman et al., 1998; Stevenson et al., 2000; Cantrell, 2001; Cockcroft and De Matteis, 2001; Cantley, 2002; Roth, 2004; Boss et al., 2006). Thus, knowing and understanding how plants and other organisms evolved toward using a wide repertoire of enzymes, including phosphoinositide kinases, to control the turnover of these metabolites is an important step in understanding life itself.

Enzymes with PI4K activity have a catalytic domain described as the phosphoinositide 3/4- kinase (PI3/4K) domain (InterPro - IPR000403 and pfam - PF004540). As the name suggests, some proteins containing the PI3/4K domain phosphorylate the inositol ring of inositol phospholipids in the 3-OH or 4-OH position. Intriguingly, a group of proteins containing the PI3/4K domains, the phosphoinositide kinase-related kinases (PIKK) have phosphotransferase activity toward Ser and Thr residues of proteins and not toward inositol phospholipid headgroups. To make matters more complicated, a select group of PI3Ks can phosphorylate both inositol phospholipids and other proteins.

In this introductory chapter I will start by briefly reviewing the current knowledge on PI3/4K domain-proteins and describe how the idea of characterizing a new group of PI4Ks from plants came about. Later, I will summarize the key findings of my thesis work and explain how the characterization of plant PI4Ks turned into the discovery of the ubiquitin-like domain kinases (UbDKs), a new family of protein kinases. Finally, I will discuss the biological impact of my thesis work, the potential connection between UbDKs and the ubiquitin/proteasome system and ER-associated protein degradation and future directions.

PI3/4K domain-proteins, a fine line between lipid and protein kinase activity

PI3/4K proteins can be divided into 3 major groups of enzymes: PI3K, PI4K and PIKK (Figure 1). This diverse group of proteins share in common not only their catalytic domain but also their involvement in cellular signaling (Fruman et al., 1998; Abraham, 2004; Balla and Balla, 2006; Wullschleger et al., 2006).

PI3Ks

PI3Ks catalyze the phosphorylation at the 3'-OH position of the inositol ring of PtdIns, PtdIns(4)P or PtdIns(4,5)P_2, producing three lipid products: PtdIns(3)P, PtdIns(3,4)P_2 and PtdIns(3,4,5)P_3. There are multiple isoforms of PI3Ks in mammalian cells, and they fall into three different classes (I, II and III) (Fruman et al., 1998; Vanhaesebroeck and Waterfield, 1999; Cantrell, 2001). Class I PI3Ks are heterodimers composed of regulatory and catalytic (p110) subunits and are subdivided into 2 classes, Ia and Ib. Class Ia enzymes (PI3Kα, β and δ) are activated by receptor tyrosine kinases and Rho family GTPases. Class Ib enzymes (PI3Kγ) are activated by heterotrimeric G-proteins. Both class Ia and Ib enzymes can be activated by p21-ras and use PtdIns, PtdIns(4)P and PtdIns(4,5)P_2 as substrates (Vanhaesebroeck and Waterfield, 1999; Cantrell, 2001; Wu et al., 2007).

Class II PI3Ks (PI3KC2α, β and δ) are monomeric enzymes with higher molecular weights than the class I PI3Ks, and they preferentially phosphorylate PtdIns and PtdIns(4)P (Vanhaesebroeck and Waterfield, 1999; Cantrell, 2001; Falasca and Maffucci, 2007). Both class I and II PI3Ks have Ras-binding, C2 and lipid kinase unique (LKU) domains (referred also as helical domain) in addition to the catalytic PI3/4K domain. Class II PI3Ks have an additional C-terminal PX domain and an N-terminal Pro-rich sequence (Djordjevic and Driscoll, 2002) (Figure 1).

The class III PI3K, also known as Vps34 (for vacuolar protein sorting 34) or Vps34-like PI3K, is the only PI3K found in yeast and plants. It uses only PtdIns as substrate and is involved in vesicle trafficking. In yeast and mammals class III PI3K is associated with Vps15 and p150, respectively, which are membrane-targeted Ser/Thr kinases (Herman and Emr, 1990; Vanhaesebroeck and Waterfield, 1999; Yan and Backer, 2007).

Figure 1. Linear representation of the domain structure of PI3/4K domain-proteins and the UbDK.
PI3/4K domain-proteins are divided into 3 major families: PI3K, PIKK and PI4K. The domains shown are, (PI3K) Ad, adaptor binding; Ras, Ras binding; C2 domain; LKU, lipid kinase unique domain (referred also as helical domain); PX, Phox homology domain; Pro-R, proline-rich motif; (PIKK) HEAT-R, HEAT (Huntingtin, elongation factor 1A, protein phosphatase 2A A subunit, TOR) repeats; FAT, FRAP, ATM and TRRAP domain; FATC, FAT domain C-terminal; (PI4K) PH, pleckstrin homology domain; RS, repetitive sequence; Glu-R, glutamic acid-rich motif and UBL, ubiquitin-like domain. The PIKK DNA-PK has armadillo motif repeats instead of HEAT repeats. The presence of RS in the type III PI4Kβ is based on the plant amino acid sequence as denoted by Xue et al. (1999).

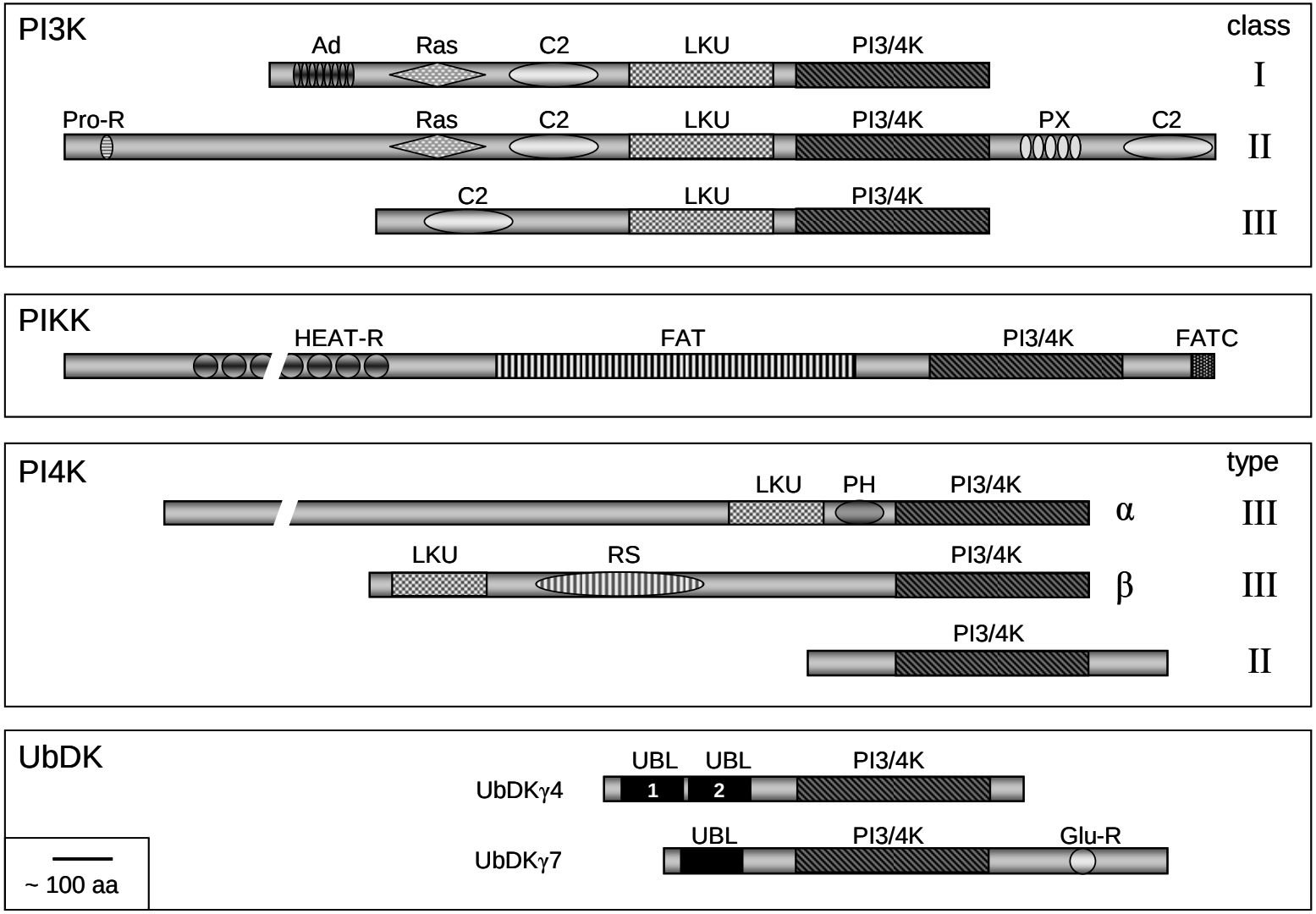
PI3K
class
Ad
Ras
C2
LKU
PI3/4K
I
Pro-R
Ras
C2
LKU
PI3/4K
PX
C2
II
C2
LKU
PI3/4K
III
PIKK
HEAT-R
FAT
PI3/4K
FATC
PI4K
type
LKU
PH
PI3/4K
α
III
LKU
RS
PI3/4K
β
III
PI3/4K
II
UbDK
UBL
UBL
PI3/4K
UbDKγ4
1
2
UBL
PI3/4K
Glu-R
UbDKγ7
~ 100 aa

In plants PtdIns 3-kinase activity is essential for normal plant growth (Welters et al., 1994). Immunodetection of PI3K revealed nuclear localization of this enzyme associated to active nuclear/nucleolar transcription sites (Bunney et al., 2000). PI3K (and PI4K) activity associated with Arabidopsis extracts can be enhanced by the addition of recombinant SSH (Soybean SEC14 homolog) a putative plant phosphatidylinositol transfer protein (Monks et al., 2001). Similar to the yeast and mammalian homologs, plant PI3K may be also involved in vesicle trafficking (Hong and Verma, 1994; Matsuoka et al., 1995).

It is noteworthy that several class I PI3Ks have the ability to phosphorylate protein substrates in addition to the 3'-OH position of phosphoinositides. For example, class Ia PI3Kα can phosphorylate its p85 adaptor subunit (Dhand et al., 1994) and class Ib PI3Kγ can phosphorylate non-muscle tropomyosin (Naga Prasad et al., 2005). In addition, Class III PI3Ks will autophosphorylate (Stack and Emr, 1994), but no phosphotransferase activity toward other proteins has yet been demonstrated.

PIKKs

The phosphoinositide kinase-related kinases (PIKK) are PI3/4K domain-proteins with Ser/Thr kinase activity. They have been also referred to as "class IV" PI3K, but so far no lipid kinase activity has been reported for members of this family of enzymes (Vanhaesebroeck and Waterfield, 1999; Abraham, 2004). PIKKs are considered atypical eukaryotic kinases due to both their similarities to lipid kinases and lack of similarity to typical Ser/Thr or Tyr protein kinases (Manning et al., 2002).

PIKKs are in general large proteins (>250 kDa) with a conserved C-terminal domain organization containing the PI3/4K catalytic domain flanked on the N- and C-terminal sides by the FAT (FRAP, ATM and TRRAP) (pfam02259) and FATC (FRAP, ATM and TRRAP C-terminal) (pfam02260) domains, respectively. Most of the PIKKs have long stretches of HEAT (Huntingtin, elongation factor 1A, protein phosphatase 2A A subunit, TOR) repeats in the remaining sequence (Figure 1). Functionally and structurally, PIKKs can be divided into six distinct groups TOR, ATM, ATR, TRRAP, SMG1 and DNA-PK. The latter, DNA-PK

DNA dependent protein kinase) is not represented in plant genomes (Templeton and Moorhead, 2005); therefore, it will not be discussed further here.

TOR (target of rapamycin) was the first PIKK identified. As the name indicates, these PIKK family members are the protein targets of the potent antifungal and immunosuppressive agent, rapamycin. TOR orchestrates signaling cascades as part of multiprotein complexes (TORC for TOR complex) and has an essential role in regulating cell growth and metabolism by modulating transcription, translation, ribosomal biogenesis and cell morphology (Harris and Lawrence, 2003; Inoki and Guan, 2006; Wullschleger et al., 2006). TOR in plants is encoded by a single gene, which in the case of Arabidopsis (AtTOR), is 39% identical to human TOR (mTOR or HsTOR). Disruption of *AtTOR* via T-DNA insertion causes premature arrest of endosperm and embryo development. *AtTOR* is expressed in primary meristem, embryo, and endosperm, but not in differentiated cells. Curiously, AtTOR is insensitive to rapamycin (Menand et al., 2002; Templeton and Moorhead, 2005).

ATM (ataxia telangiectasia mutated) and ATR (ATM and Rad3-related) are part of a genome integrity surveillance mechanism. Both play important roles in controlling cell cycle progression, DNA repair and controlled cell death. ATM and ATR have many known substrates, some of which are shared by both kinases. ATM and ATR are activated by DNA damage caused by ionizing radiation, UV light, reactive oxygen species and radiomimetic chemicals (Abraham, 2001; Shiloh, 2003; Abraham, 2004; Kurz and Lees-Miller, 2004). Arabidopsis ATM and ATR homologs (AtATM and AtATR) have been identified and were found to be involved in conserved functions (Garcia et al., 2000; Garcia et al., 2003; Culligan et al., 2004; Templeton and Moorhead, 2005; Ricaud et al., 2007).

TRRAP (transactivation/transformation-domain-associated protein) is a PIKK with no phosphotransferase activity. TRRAP appears to be involved in transcription as a molecular scaffold. Specifically, TRRAP affects transcription by means of histone modification, as part of multiprotein complexes containing histone acetyltransferase activity (Herceg and Wang, 2005). SMG1 (suppressor with morphogenetic effect on genitalia) is the most recently identified member of the PIKK family. SMG1 plays a role in nonsense-mediated mRNA decay, a process by which mRNA containing premature termination codons

are preferentially degraded (Abraham, 2004). TRRAP and SMG1 putative homologs have been identified in Arabidopsis and rice, respectively; however, to date, nothing has been published about their function in plants (Templeton and Moorhead, 2005).

PI4Ks

The phosphorylation of PtdIns to PtdIns(4)P is catalyzed by two independent groups of PI4Ks designated type II and III (type I PIK activity is PI3K) (Fruman et al., 1998; Heilmeyer et al., 2003; Balla and Balla, 2006) (Figure 1). The type III PI4Ks were the first to be characterized at the molecular level. In yeast there are two type III PI4Ks, STT4 and PIK1. They are responsible for the synthesis of independent pools of PtdIns4P, and therefore, display non-overlapping functions. PIK1 is involved in Golgi integrity and Golgi to membrane trafficking, while STT4 is a critical regulator of vacuole morphology and actin cytoskeleton organization (Audhya and Emr, 2002). The mammalian orthologs of STT4 and PIK1 are, respectively, PI4KIIIα and PI4KIIIβ.

LSB6, the *S. cereviseae* type II PI4K, was first identified in a two hybrid screen by using LAS17, an organizer of the cortical actin network (WASp ortholog in yeast), as bait (Madania et al., 1999). The function of LSB6 in yeast cells is proposed to be associated with endosome motility mediated by actin, a function which, intriguingly, is independent of its PI4K activity (Chang et al., 2005). Mutant studies suggested that the type II PI4K LSB6 accounts for a very small percentage of PI4K activity in *S. cereviseae* cells.

The mammalian type II PI4Ks, similar to the type III PI4Ks, exist as α and β isoforms (PI4KIIα and PI4KIIβ). In contrast to yeast cells, the type II PI4Ks in mammalian cells account for a significant amount of PI4K activity; they are the prevalent source of PtdIns4P in selected tissues and organs such as the brain (Guo et al., 2003). Early localization studies by Wong et al. (1997), indicated that PI4KIIIα was found primarily in the ER while PI4KIIIβ was in the Golgi. However, localization studies with the type II enzymes in mammalian cells have yielded conflicting results depending on the approach (endogenous versus over-expressed enzymes) (Minogue et al., 2001; Balla et al., 2002; Wei et al., 2002; Wang et al., 2003). The only enzyme that has been shown to translocate to the plasma membrane in

stimulated cells is the PI4KIIβ (Wei et al., 2002). PI4KIIβ translocation is proposed to occur via a Rac-dependent mechanism (Wei et al., 2002). More recent data (Balla et al., 2005), using inhibitors and RNAi, suggest that PI4KIIIα is the source of PtdIns4P re-synthesis in the plasma membrane of cells after Ca^{++}-mediated PLC stimulation by ionomycin treatment. Of interest with regard to regulation of PI4KIIIβ, recombinant PI4KIIIβ undergoes autophosphorylation via an intramolecular reaction. Furthermore, PI4KIIIβ autophosphorylation decreases its PI4K activity and is inhibited by the presence of lipid substrate (Zhao et al., 2000).

Pioneering work in plant PI metabolism (Sommarin and Sandelius, 1988; Chen and Boss, 1990; Gross et al., 1992; Xu et al., 1992; Yang et al., 1993) established that PI4K activity was associated with microsomal, plasma membrane, nuclear and soluble cell fractions. The Arabidopsis type III PI4Kα1 (AtPI4Kα1), a STT4 homolog, was the first plant PI4K cloned (Stevenson et al., 1998). This enzyme is inhibited by its product PtdIns4P and featured a pleckstrin homology (PH) domain, a phosphoinositide binding domain and is recovered with F-actin *in vitro* suggesting that it might bind actin *in vivo* (Stevenson et al., 1998). The AtPI4Kα1 PH domain was shown to bind to PtdIns4P and to be essential for F-actin interaction (Stevenson-Paulik et al., 2003). Work by Dr. Jocelyn Malamy's group revealed that mutations in *AtPI4Kα1* caused altered lateral root development (unpublished data) in Arabidopsis plants. However, in collaboration with Dr. Malami's group, we showed that the mutations in the *lrd* (lateral root development) alleles of AtPI4Kα1 did not impact PI4K activity (Appendix 2). Therefore, the root phenotype must be derived from a secondary function of the protein – possibly actin binding.

AtPI4Kβ1, a PIK1 homolog was cloned few a years later and was found to have a unique repetitive motif (Xue et al., 1999). AtPI4Kβ1 is recruited to the cytoskeleton by AtPIP5K1 (Davis et al., 2007) and to the Golgi-derived secretory vesicles in the tip of growing root hairs by GTP-bound RabA4b (Preuss et al., 2006). Arabidopsis T-DNA insertion mutants, where both AtPI4Kβ1 and AtPI4Kβ2 are disrupted, have root hairs with aberrant morphology (Preuss et al., 2006). No cDNAs encoding AtPI4Kα2 (another putative type III PI4K) have been cloned and no EST from this gene has been found suggesting that *AtPI4Kα2* may be a pseudogene.

Plant putative type II PI4K

The *Arabidopsis thaliana* genome contains 8 putative type II PI4Ks (γ1 – γ8) (Mueller-Roeber and Pical, 2002). While the plant type III PI4Ks have been studied extensively, little is known about the type II PI4Ks. Two lines of evidence suggested the presence of type II PI4K in plants; i) genomic sequence comparisons with human and yeast indicated a conserved catalytic domain that could correspond to a type II kinase (Mueller-Roeber and Pical, 2002) and ii) a guard-cell enriched membrane protein fractions retained some wortmannin-resistant PI4K activity (Jung et al., 2002). Wortmannin is a potent inhibitor of PI3/4K activity but does not affect the activity of the type II PI4Ks.

My thesis work began with the hypothesis that the Arabidopsis genome, like those of yeast and metazoans, encoded active type II PI4Ks and that the type II PI4K activity in plants was, at least in part, responsible for providing discrete PtdIns4P pools associated with the plasma membrane. Of interest to my work was the observation that 5 out of 8 putative type II PI4Ks identified in the Arabidopsis genome contained N-terminal ubiquitin-like domains. These domains were not found in any other PI3/4K domain-proteins.

Ubiquitin-like domain and proteasome substrate delivery

Ubiquitin-like (UBL) domains consist of 70-100 amino acids that have significant identity with the primary sequence and structure of ubiquitin. UBL domain-proteins are not attachable to other proteins like ubiquitin itself or the type I ubiquitin-like proteins such as SUMO (small ubiquitin-related modifier). UBL domains are normally found at the N-terminus and are associated with a very diverse repertoire of other protein domains (Larsen and Wang, 2002; Hartmann-Petersen and Gordon, 2004; Walters et al., 2004).

The best known group of UBL domain-proteins is the group of the UBL/UBA proteins. In addition to the N-terminal UBL domain, the UBL/UBA proteins have one or two C-terminal ubiquitin associated (UBA) domain(s). A UBA domain is one of the many known ubiquitin binding domains. Functionally, the UBL/UBA proteins are thought to be involved in facilitating substrate delivery to the 26S proteasome (Figure 2). While the UBA domain

Figure 2. Ubiquitin/26S proteasome system and substrate delivery for protein degradation.
A. Proteins targeted to degradation are covalently linked to ubiquitin chains (ubiquitination) by the action of a series of enzymes; E1 (ubiquitin activating), E2 (ubiquitin conjugating) and E3 (ubiquitin ligase). Additionally, the requirement for an ubiquitin chain elongation factor (E4) has been proposed. Ubiquitinated proteins are delivered to the 26S proteasome where they are deubiquitinated and degraded by the action of the 20S catalytic core. Ubiquitin moietes and amino acids are then recycled. **B.** A lot of attention has been devoted to the investigation of the ubiquitination process. However, protein degradation is largely controlled at the level of substrate delivery. UBA/UBL domain-proteins bind to both the regulatory particle of the 26S proteasome (via UBL) and ubiquitinated proteins (via UBA). This dual binding capacity allows them to shuttle ubiquitinated proteins for degradation. RPN10 (via UIM – ubiquitin interactin motif) and UFD1 bind to ubiquitin chains of ubiquitinated proteins and they also facilitate delivery of proteasome substrate. RPN10 is itself a component of the regulatory particle of the proteasome and acts synergistically with UBA/UBL proteins. Via its von Willebrand A (vWA) domain and via UIM^{RPN10} – $UBL^{UBA/UBL\ protein}$ direct interaction, RPN10 promotes degradation of proteasome substrates. UFD1, as part of a multiprotein complex with chaperone activity (CDC48/UFD1/NPL4 complex), has been implicated in facilitating the degradation of ERAD-derived proteasome substrates. Whether UFD1 or CDC48/UFD1/NPL4 complex directly interact with the proteasome is unclear.

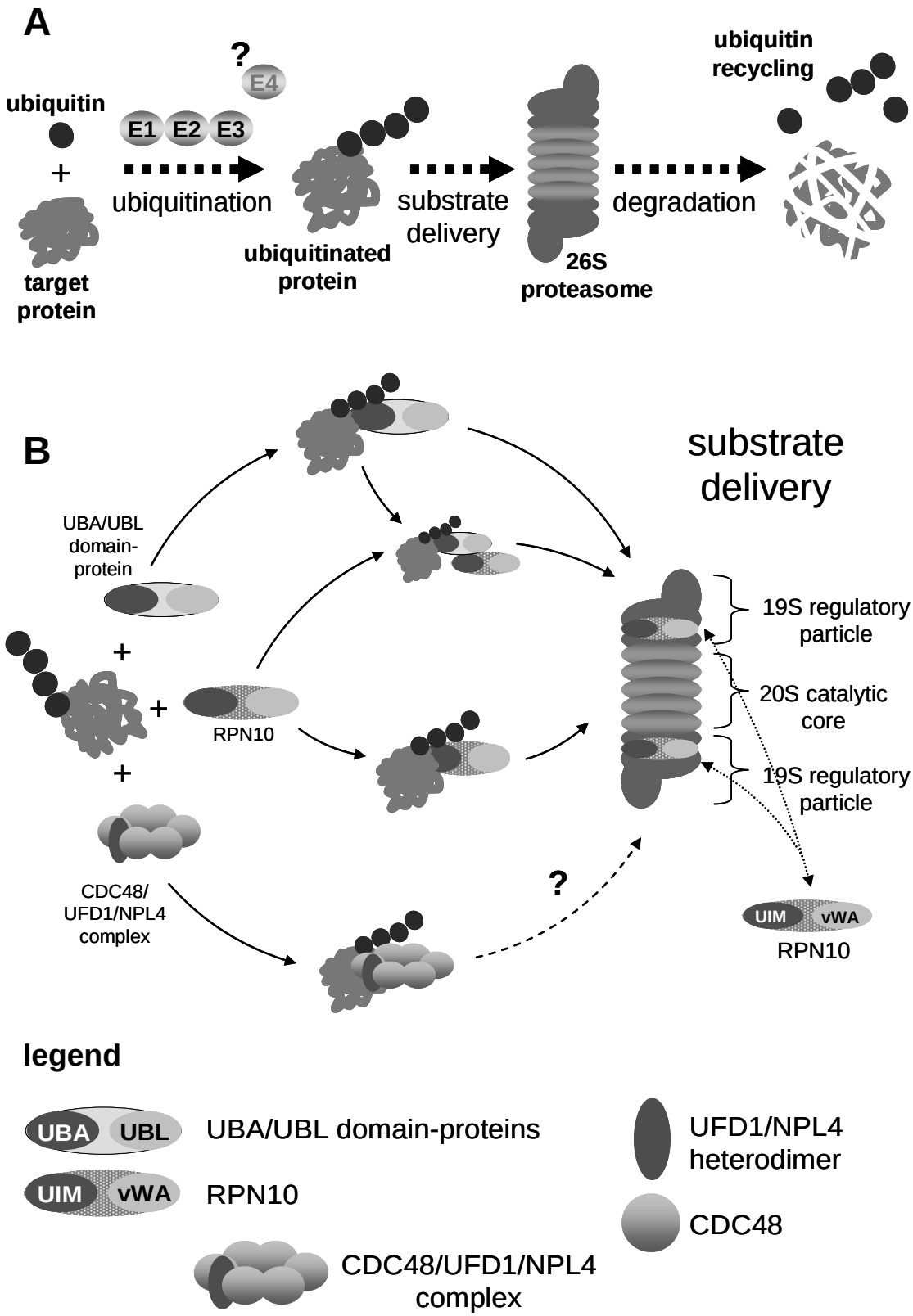
A
?
E4
ubiquitin
E1
E2
E3
+
ubiquitination
target protein
ubiquitinated protein
substrate delivery
26S proteasome
degradation
ubiquitin recycling
B
substrate delivery
UBA/UBL domain-protein
+
+
+
RPN10
CDC48/ UFD1/NPL4 complex
?
19S regulatory particle
20S catalytic core
19S regulatory particle
UIM
vWA
RPN10
legend
UBA
UBL
UBA/UBL domain-proteins
UIM
vWA
RPN10
CDC48/UFD1/NPL4 complex
UFD1/NPL4 heterodimer
CDC48

interacts with polyubiquitin chains of ubiquitinated proteins, the UBL domain interacts with the 19S regulatory particle (RP) of the 26S proteasome (Hartmann-Petersen et al., 2003; Hartmann-Petersen and Gordon, 2004, 2004, 2004; Walters et al., 2004; Kang et al., 2006). This dual binding property allows UBL/UBA domain-proteins to work as receptors of ubiquitinated substrates for the 26S proteasome. The exact docking site for UBL/UBA proteins in the 19S RP is still under debate. Both RPN1a and RPN10, non-ATPase components of the 19S RP, are potential candidates due to their ability to bind UBL domains (Elsasser et al., 2002; Elsasser et al., 2004; Madura, 2004); however, other components of the proteasome such as the ATPase components of the 19S RP, RPT5, cannot be excluded (Verma et al., 2004).

In addition to UBL/UBA proteins, other proteins with polyubiquitin chain binding properties have been characterized as substrate receptors for the proteasome such as RPN10 itself and the ubiquitin fusion degradation 1 (UFD1) (Figure 2). Verma et al. (2004), in one of the most complete functional analyses of different proteasome substrate receptors, established that multiple polyubiquitin chain binding proteins including the UBL/UBA proteins Rad23, Dsk2, as well as RPN10 and UFD1 (the latter most likely acting as part of a complex with nuclear protein localization 4 [NPL4] and the AAA-ATPase CDC48) determine substrate specificity for protein degradation via the 26S proteasome at the level of substrate delivery.

Discovery the of the ubiquitin-like domain kinases (UbDKs)

My thesis is that *AtPI4Kγ4* and *AtPI4Kγ7*, which were predicted to be part of the Arabidopsis type II PI4Ks gene family and which contain UBL domains, encode new bona fide protein kinases, designated UbDKγ4 and UbDKγ7 (ubiquitin-like domain kinase) (Figure 1). In addition, several lines of evidence suggest that UbDKγ4 may be involved in substrate delivery to the proteasome, in particular, the delivery of proteasome substrates from ER-associated protein degradation (ERAD).

In **Chapter 2**, my collaborators and I show that UbDKγ4 and γ7 phosphorylate protein substrates and that UbDKγ4 interacts directly with Arabidopsis UFD1 and RPN10

and uses these proteins as *in vitro* substrates. Furthermore, AtUFD1 phosphorylation sites targeted by UbDKγ4 protein kinase activity were identified by mass spectrometry. **Chapter 2 – "Characterization of a new family of protein kinases containing phosphoinositide 3/4-kinase and ubiquitin-like domains**" has been conditionally accepted for publication in the Biochemical Journal.

Chapter 3 introduces *in vivo* evidence that supports my thesis that UbDKγ4 may play a role in delivery of ERAD-derived proteasome substrates. Specifically, I confirmed that *UbDKγ4* is one of the up-regulated genes during the unfolded protein response (UPR). This observation was first reported by Martinez and Chrispeels (2003) using microarray-based gene expression analysis, but it was never verified by other methods. Also, transgenic tobacco (NT1) cells and Arabidopsis plants were generated expressing *UbDKγ4*-derived polypeptides fused with green fluorescent protein (GFP). Preliminary experiments indicated that in the transgenic cells and plants, accumulation of *UbDKγ4*-derived polypeptides produced minimal pleiotropic effects on growth and development. However, the transgenic Arabidopsis plants were remarkably more sensitive to tunicamycin, a UPR-inducing antibiotic, compared to control plants.

Appendix 1 highlights biochemical differences between UbDKγ4 and γ7. For example, while UbDKγ4 can use an intermolecular reaction to undergo autophosphorylation, UbDKγ7 appears to exclusively use an intramolecular autophosphorylation reaction similar to that found in mammalian PI4KIIIβ. Data presented in **Appendix 1** suggest that UbDKγ7 interacts with and is phosphorylated by a protein kinase present in the soluble fraction of Arabidopsis cells. This protein kinase, which is activated by hyperosmotic stress, phosphorylates recombinant UbDKγ7. These data suggest that UbDKγ7 may be part of a phosphorylation cascade activated by hyperosmotic stress.

The major impact of the work presented here is the discovery of new protein kinases and the connection of UbDKγ4 with the ubiquitin/proteasome system. The UbDKs are new atypical Ser/Thr kinases containing UBL domains that were never characterized before. This family of protein kinases is predicted to be present in other plant species and species of protozoans. Also, a wide range of tools have been generated that could, in the future, help unveil in more detail the regulation and function of the UbDKs in plants. Expression

cassettes for production of recombinant protein in *E. coli* and Sf9 insect cells have been produced. Transgenic NT1 cells and Arabidopsis plants producing truncations and a full-length kinase dead protein have also been made. An anti-UbDKγ4 antibody and RT-PCR primer sets are also among the tools described here that can be used for future research to define the role of the UbDK family of proteins in plants.

References

Abraham RT (2001) Cell cycle checkpoint signaling through the ATM and ATR kinases. Genes Dev 15: 2177-2196.

Abraham RT (2004) PI 3-kinase related kinases: 'big' players in stress-induced signaling pathways. DNA Repair (Amst) 3: 883-887.

Audhya A, Emr SD (2002) Stt4 PI 4-kinase localizes to the plasma membrane and functions in the Pkc1-mediated MAP kinase cascade. Dev Cell 2: 593-605.

Balla A, Balla T (2006) Phosphatidylinositol 4-kinases: old enzymes with emerging functions. Trends Cell Biol 16: 351-361.

Balla A, Tuymetova G, Barshishat M, Geiszt M, Balla T (2002) Characterization of type II phosphatidylinositol 4-kinase isoforms reveals association of the enzymes with endosomal vesicular compartments. J Biol Chem 277: 20041-20050.

Balla A, Tuymetova G, Tsiomenko A, Varnai P, Balla T (2005) A plasma membrane pool of phosphatidylinositol 4-phosphate is generated by phosphatidylinositol 4-kinase type-III alpha: studies with the PH domains of the oxysterol binding protein and FAPP1. Mol Biol Cell 16: 1282-1295.

Boss WF, Davis AJ, Im YJ, Galvao RM, Perera IY (2006) Phosphoinositide metabolism: towards an understanding of subcellular signaling. Subcell Biochem 39: 181-205.

Bunney TD, Watkins PAC, Beven AF, Shaw PJ, Hernandez LE, Lomonossoff GP, Shanks M, Peart J, Drobak BK (2000) Association of Phosphatidylinositol 3-Kinase with Nuclear Transcription Sites in Higher Plants. Plant Cell 12: 1679-1688.

Cantley LC (2002) The phosphoinositide 3-kinase pathway. Science 296: 1655-1657.

Cantrell DA (2001) Phosphoinositide 3-kinase signalling pathways. J Cell Sci 114: 1439-1445.

Carpenter CL, Cantley LC (1996) Phosphoinositide kinases. Curr Opin Cell Biol 8: 153-158.

Chang FS, Han GS, Carman GM, Blumer KJ (2005) A WASp-binding type II phosphatidylinositol 4-kinase required for actin polymerization-driven endosome motility. J Cell Biol 171: 133-142.

Chen Q, Boss WF (1990) Short-Term Treatment with Cell Wall Degrading Enzymes Increases the Activity of the Inositol Phospholipid Kinases and the Vanadate-Sensitive ATPase of Carrot Cells. Plant Physiol. 94: 1820-1829.

Cockcroft S, De Matteis MA (2001) Inositol Lipids as Spatial Regulators of Membrane Traffic. J of Membrane Biol 180: 187-194.

Culligan K, Tissier A, Britt A (2004) ATR Regulates a G2-Phase Cell-Cycle Checkpoint in Arabidopsis thaliana. Plant Cell 16: 1091-1104.

Davis AJ, Im YJ, Dubin JS, Tomer KB, Boss WF (2007) Arabidopsis phosphatidylinositol phosphate kinase 1 binds F-actin and recruits phosphatidylinositol 4-kinase β1 to the actin cytoskeleton. J Biol Chem 282: 14121-14131.

Dhand R, Hiles I, Panayotou G, Roche S, Fry MJ, Gout I, Totty NF, Truong O, Vicendo P, Yonezawa K, et al. (1994) PI 3-kinase is a dual specificity enzyme: autoregulation by an intrinsic protein-serine kinase activity. EMBO J 13: 522-533.

Djordjevic S, Driscoll PC (2002) Structural insight into substrate specificity and regulatory mechanisms of phosphoinositide 3-kinases. Trends in Biochem Sci 27: 426-432.

Elsasser S, Chandler-Militello D, Muller B, Hanna J, Finley D (2004) Rad23 and Rpn10 serve as alternative ubiquitin receptors for the proteasome. J Biol Chem 279: 26817-26822.

Elsasser S, Gali RR, Schwickart M, Larsen CN, Leggett DS, Muller B, Feng MT, Tubing F, Dittmar GA, Finley D (2002) Proteasome subunit Rpn1 binds ubiquitin-like protein domains. Nat Cell Biol 4: 725-730.

Falasca M, Maffucci T (2007) Role of class II phosphoinositide 3-kinase in cell signalling. Biochem Soc Trans 35: 211-214.

Fruman DA, Meyers RE, Cantley LC (1998) Phosphoinositide Kinases. Annu Rev Biochem 67: 481-507.

Garcia V, Bruchet H, Camescasse D, Granier F, Bouchez D, Tissier A (2003) AtATM is essential for meiosis and the somatic response to DNA damage in plants. Plant Cell 15: 119-132.

Garcia V, Salanoubat M, Choisne N, Tissier A (2000) An ATM homologue from Arabidopsis thaliana: complete genomic organisation and expression analysis. Nucleic Acids Res 28: 1692-1699.

Gross W, Yang W, Boss WF (1992) Release of carrot plasma membrane-associated phosphatidylinositol kinase by phospholipase A2 and activation by a 70 kDa protein. Biochim Biophys Acta 1134: 73-80.

Guo J, Wenk MR, Pellegrini L, Onofri F, Benfenati F, De Camilli P (2003) Phosphatidylinositol 4-kinase type II alpha is responsible for the phosphatidylinositol 4-kinase activity associated with synaptic vesicles. PNAS 100: 3995-4000.

Harris TE, Lawrence JC, Jr. (2003) TOR signaling. Sci STKE 2003: re15.

Hartmann-Petersen R, Gordon C (2004) Integral UBL domain proteins: a family of proteasome interacting proteins. Semin Cell Dev Biol 15: 247-259.

Hartmann-Petersen R, Gordon C (2004) Protein degradation: recognition of ubiquitinylated substrates. Curr Biol 14: R754-756.

Hartmann-Petersen R, Gordon C (2004) Proteins interacting with the 26S proteasome. Cell Mol Life Sci 61: 1589-1595.

Hartmann-Petersen R, Seeger M, Gordon C (2003) Transferring substrates to the 26S proteasome. Trends Biochem Sci 28: 26-31.

Heilmeyer LM, Jr., Vereb G, Jr., Vereb G, Kakuk A, Szivak I (2003) Mammalian phosphatidylinositol 4-kinases. IUBMB Life 55: 59-65.

Herceg Z, Wang ZQ (2005) Rendez-vous at mitosis: TRRAPed in the chromatin. Cell Cycle 4: 383-387.

Herman PK, Emr SD (1990) Characterization of VPS34, a gene required for vacuolar protein sorting and vacuole segregation in *Saccharomyces cerevisiae*. Mol Cell Biol 10: 6742-6754.

Hong Z, Verma DPS (1994) A Phosphatidylinositol 3-Kinase is Induced During Soybean Nodule Organogenesis and is Associated with Membrane Proliferation. PNAS 91: 9617-9621.

Inoki K, Guan KL (2006) Complexity of the TOR signaling network. Trends Cell Biol 16: 206-212.

Jung J-Y, Kim Y-W, Kwak JM, Hwang J-U, Young J, Schroeder JI, Hwang I, Lee Y (2002) Phosphatidylinositol 3- and 4-Phosphate Are Required for Normal Stomatal Movements. Plant Cell 14: 2399-2412.

Kang Y, Vossler RA, Diaz-Martinez LA, Winter NS, Clarke DJ, Walters KJ (2006) UBL/UBA ubiquitin receptor proteins bind a common tetraubiquitin chain. J Mol Biol 356: 1027-1035.

Kurz EU, Lees-Miller SP (2004) DNA damage-induced activation of ATM and ATM-dependent signaling pathways. DNA Repair (Amst) 3: 889-900.

Larsen CN, Wang H (2002) The ubiquitin superfamily: Members, features, and phylogenies. J Proteome Res 1: 411-419.

Madania A, Dumoulin P, Grava S, Kitamoto H, Scharer-Brodbeck C, Soulard A, Moreau V, Winsor B (1999) The *Saccharomyces cerevisiae* homologue of human Wiskott-Aldrich syndrome protein Las17p interacts with the Arp2/3 complex. Mol Biol Cell 10: 3521-3538.

Madura K (2004) Rad23 and Rpn10: perennial wallflowers join the melee. Trends Biochem Sci 29: 637-640.

Manning G, Whyte DB, Martinez R, Hunter T, Sudarsanam S (2002) The protein kinase complement of the human genome. Science 298: 1912-1934.

Martinez IM, Chrispeels MJ (2003) Genomic analysis of the unfolded protein response in Arabidopsis shows its connection to important cellular processes. Plant Cell 15: 561-576.

Matsuoka K, Bassham DC, Raikhel NV, Nakamura K (1995) Different sensitivity to wortmannin of two vacuolar sorting signals indicates the presence of distinct sorting machineries in tobacco cells. J Cell Biol 130: 1307-1318.

Menand B, Desnos T, Nussaume L, Berger F, Bouchez D, Meyer C, Robaglia C (2002) Expression and disruption of the Arabidopsis TOR (target of rapamycin) gene. PNAS 99: 6422-6427.

Minogue S, Anderson JS, Waugh MG, dos Santos M, Corless S, Cramer R, Hsuan JJ (2001) Cloning of a human type II phosphatidylinositol 4-kinase reveals a novel lipid kinase family. J Biol Chem 276: 16635-16640.

Monks DE, Aghoram K, Courtney PD, DeWald DB, Dewey RE (2001) Hyperosmotic stress induces the rapid phosphorylation of a soybean phosphatidylinositol transfer protein homolog through activation of the protein kinases SPK1 and SPK2. Plant Cell 13: 1205-1219.

Mueller-Roeber B, Pical C (2002) Inositol phospholipid metabolism in Arabidopsis. Characterized and putative isoforms of inositol phospholipid kinase and phosphoinositide-specific phospholipase C. Plant Physiol 130: 22-46.

Naga Prasad SV, Jayatilleke A, Madamanchi A, Rockman HA (2005) Protein kinase activity of phosphoinositide 3-kinase regulates beta-adrenergic receptor endocytosis. Nat Cell Biol 7: 785-796.

Preuss ML, Schmitz AJ, Thole JM, Bonner HK, Otegui MS, Nielsen E (2006) A role for the RabA4b effector protein PI-4Kβ1 in polarized expansion of root hair cells in *Arabidopsis thaliana*. J Cell Biol 172: 991-998.

Ricaud L, Proux C, Renou JP, Pichon O, Fochesato S, Ortet P, Montane MH (2007) ATM-mediated transcriptional and developmental responses to gamma-rays in Arabidopsis. PLoS ONE 2: e430.

Roth MG (2004) Phosphoinositides in constitutive membrane traffic. Physiol Rev 84: 699-730.

Shiloh Y (2003) ATM and related protein kinases: safeguarding genome integrity. Nature Rev Cancer 3: 155-168.

Sommarin M, Sandelius AS (1988) Phosphatidylinositol and phosphatidylinositolphosphate kinases in plant plasma membranes. Biochim Biophys Acta 958: 268-278.

Stack JH, Emr SD (1994) Vps34p required for yeast vacuolar protein sorting is a multiple specificity kinase that exhibits both protein kinase and phosphatidylinositol-specific PI 3-kinase activities. J Biol Chem 269: 31552-31562.

Stevenson-Paulik J, Love J, Boss WF (2003) Differential regulation of two Arabidopsis type III phosphatidylinositol 4-kinase isoforms. A regulatory role for the pleckstrin homology domain. Plant Physiol 132: 1053-1064.

Stevenson JM, Perera IY, Boss WF (1998) A phosphatidylinositol 4-kinase pleckstrin homology domain that binds phosphatidylinositol 4-monophosphate. J Biol Chem 273: 22761-22767.

Stevenson JM, Perera IY, Heilmann I, Persson S, Boss WF (2000) Inositol signaling and plant growth. Trends Plant Sci 5: 252-258.

Templeton GW, Moorhead GB (2005) The phosphoinositide-3-OH-kinase-related kinases of *Arabidopsis thaliana*. EMBO Rep 6: 723-728.

Toker A, Cantley LC (1997) Signalling through the lipid products of phosphoinositide-3-OH kinase. Nature 387: 673-676.

Vanhaesebroeck B, Waterfield MD (1999) Signaling by Distinct Classes of Phosphoinositide 3-Kinases. Exp Cell Res 253: 239-254.

Verma R, Oania R, Graumann J, Deshaies RJ (2004) Multiubiquitin chain receptors define a layer of substrate selectivity in the ubiquitin-proteasome system. Cell 118: 99-110.

Walters KJ, Goh AM, Wang Q, Wagner G, Howley PM (2004) Ubiquitin family proteins and their relationship to the proteasome: A structural perspective. Biochim Biophys Acta 1695: 73-87.

Wang YJ, Wang J, Sun HQ, Martinez M, Sun YX, Macia E, Kirchhausen T, Albanesi JP, Roth MG, Yin HL (2003) Phosphatidylinositol 4 phosphate regulates targeting of clathrin adaptor AP-1 complexes to the Golgi. Cell 114: 299-310.

Wei YJ, Sun HQ, Yamamoto M, Wlodarski P, Kunii K, Martinez M, Barylko B, Albanesi JP, Yin HL (2002) Type II phosphatidylinositol 4-kinase beta is a cytosolic and peripheral membrane protein that is recruited to the plasma membrane and activated by Rac-GTP. J Biol Chem 277: 46586-46593.

Welters P, Takegawa K, Emr SD, Chrispeels MJ (1994) AtVPS34, a phosphatidylinositol 3-kinase of *Arabidopsis thaliana*, is an essential protein with homology to a calcium-dependent lipid binding domain. PNAS 91: 11398-11402.

Wong K, Meyers dd R, Cantley LC (1997) Subcellular locations of phosphatidylinositol 4-kinase isoforms. J Biol Chem 272: 13236-13241.

Wu H, Yan Y, Backer JM (2007) Regulation of class IA PI3Ks. Biochem Soc Trans 35: 242-244.

Wullschleger S, Loewith R, Hall MN (2006) TOR signaling in growth and metabolism. Cell 124: 471-484.

Xu P, Lloyd CW, Staiger CJ, Drobak BK (1992) Association of Phosphatidylinositol 4-Kinase with the Plant Cytoskeleton. Plant Cell 4: 941-951.

Xue H-W, Pical C, Brearley C, Elge S, Muller-Rober B (1999) A plant 126-kDa phosphatidylinositol 4-kinase with a novel repeat structure. Cloning and functional expression in baculovirus-infected insect cells. J Biol Chem 274: 5738-5745.

Yan Y, Backer JM (2007) Regulation of class III (Vps34) PI3Ks. Biochem Soc Trans 35: 239-241.

Yang W, Burkhart W, Cavallius J, Merrick WC, Boss WF (1993) Purification and characterization of a phosphatidylinositol 4-kinase activator in carrot cells. J Biol Chem 268: 392-398.

Zhao X-H, Bondeva T, Balla T (2000) Characterization of recombinant phosphatidylinositol 4-kinase β reveals auto- and heterophosphorylation of the enzyme. J Biol Chem 275: 14642-14648.

CHAPTER 2

Characterization of a new family of protein kinases containing phosphoinositide 3/4-kinase and ubiquitin-like domains

Rafaelo M. Galvão*, Uma Kota†, Erik J. Soderblom†,
Michael B. Goshe† and Wendy F. Boss*

*Department of Plant Biology and †Department of Molecular and Structural Biochemistry North Carolina State University, Raleigh NC, 27695

Address correspondence to: Wendy F. Boss, Plant Biology Box 7649, North Carolina State University, Raleigh NC 27695-7649, Tel. 919-515-3496; Fax. 919-515-3436; E-Mail: wendy_boss@ncsu.edu

Running Title: New protein kinases from Arabidopsis

This manuscript was submitted for publication on the Biochemical Journal and has been accepted with minor revision. Uma Kota, Erik J. Soderblom, and Dr. Michael B. Goshe contributed for this manuscript with the analysis of peptides by mass spectrometry

Abstract

At least two of the genes predicted to encode type II phosphatidylinositol 4-kinase in Arabidopsis (*AtPI4Kγ4* and *γ7*), encode enzymes with catalytic properties similar to those from the PIKK family members. AtPI4Kγ4 and γ7 undergo autophosphorylation and phosphorylate Ser/Thr residues of protein substrates but have no detectable lipid kinase activity. AtPI4Kγ4 and γ7 are members of a subset of 5 putative AtPI4Ks that contain N-terminal ubiquitin-like (UBL) domains. *In vitro* analysis of AtPI4Kγ4 indicates that it interacts directly with and phosphorylates two proteins involved in the ubiquitin/proteasome system namely, UFD1 (ubiquitin fusion degradation 1) and RPN10 a non-ATPase component of the proteasome regulatory particle. Based on the data presented here, we propose that AtPI4Kγ4 and AtPI4Kγ7 should be designated UbDKγ4 and UbDKγ7 (Ubiquitin-like Domain Kinase). These UBL domain-containing AtPI4Ks correspond to a new phosphoinositide kinase-related kinase (PIKK) subfamily of protein kinases. In addition, UFD1 and RPN10 phosphorylation represents an additional mechanism by which their function can be regulated.

Introduction

Enzymes that contain the phosphoinositide 3/4- kinase (PI3/4K) domain (InterPro IPR000403) include i) phosphoinositide kinases, ii) protein kinases, and iii) kinases with dual activity that can use phosphoinositides and proteins as substrates. This diverse group of enzymes is involved in many different cellular functions including lipid- and protein-mediated signaling (Fruman et al., 1998; Abraham, 2004; Balla and Balla, 2006; Wullschleger et al., 2006).

The genome of the model plant *Arabidopsis thaliana* contains at least 18 distinct loci which encode predicted PI3/4K domain-containing proteins. Twelve of them are predicted to encode phosphatidylinositol 4-kinases (AtPI4Ks), 4 belonging to the type III group (AtPI4Kα1, α2, β1 and β2) and 8 belonging to the type II group (AtPI4Kγ1 – γ8) (Mueller-Roeber and Pical, 2002). Many of type III AtPI4Ks have been characterized (Stevenson et

al., 1998; Xue et al., 1999; Stevenson-Paulik et al., 2003; Lou et al., 2006); however, little is known about the type II PI4Ks in plants.

The type II PI4Ks in yeast and mammals have been cloned and characterized. In *Saccharomyces cerevisiae* this enzyme, named *Las* binding protein 6 (LSB6), accounts for a small percentage of the PI4K activity (Han et al., 2002; Shelton et al., 2003), while in humans, the type II PI4Ks, HsPI4KIIα and HsPI4KIIβ, contribute significantly to phosphatidylinositol-4 phosphate (PtdIns4P) production in both plasma membrane and endomembranes (for review see, (Balla and Balla, 2006)).

Five of the predicted Arabidopsis type II AtPI4Ks (γ3, γ4, γ5, γ6 and γ7) contain one or two N-terminal ubiquitin-like (UBL) domains. None of the other known PI3/4K domain-containing proteins have a predicted UBL domain. UBL domains consist of 70-100 amino acids and have significant identity with the primary sequence and structure of ubiquitin. UBL domain proteins are not like ubiquitin or the type I ubiquitin-like proteins such as SUMO (small ubiquitin-related modifier) in that UBL proteins do not covalently bind to target proteins.

UBL domains are usually found at the N-terminus and are associated with a very diverse repertoire of other protein domains (Larsen and Wang, 2002; Hartmann-Petersen and Gordon, 2004; Walters et al., 2004). In many UBL proteins the UBL domain promotes protein-protein interaction with components of the 26S proteasome (Hartmann-Petersen et al., 2003; Hartmann-Petersen and Gordon, 2004, 2004; Madura, 2004; Elsasser and Finley, 2005). Because of the presence of the UBL domain in what had been predicted originally to be type II PI4Ks (Mueller-Roeber and Pical, 2002), we asked whether these purported Arabidopsis type II PI4Ks might have other functions.

Here we show that a subset of an Arabidopsis gene family, which is predicted to encode type II PI4Ks and which contain UBL domains, encodes active protein kinases, specifically, *AtPI4Kγ4* and *γ7*. Protein-protein interaction studies reveal that AtPI4Kγ4 interacts directly with RPN10, a non-ATPase component of the 19S regulatory particle (RP) of the 26S proteasome. Furthermore, AtPI4Kγ4 interacts directly with ubiquitin fusion degradation 1 (UFD1). Both RPN10 and UFD1 bind to some form of ubiquitin and are known to facilitate substrate delivery to the 26S proteasome. AtPI4Kγ4 is a Ser/Thr kinase

that phosphorylates both RPN10 and UFD1 *in vitro*. Because of the data presented here we propose to re-annotate AtPI4Kγ4 and AtPI4Kγ7 as a new subfamily of the PIKK family of protein kinases and re-name them as UbDKγ4 and UbDKγ7 (Ubiquitin-like Domain Kinase), respectively.

Methods

cDNA cloning and construction of expression vectors

Full-length AtPI4Kγ1 (At2g40850), AtPI4Kγ4 (At2g46500), and AtPI4Kγ7 (At2g03890) coding regions were amplified via RT-PCR from total RNA of 4-day old Arabidopsis cells growing in suspension culture. The primers used were designed to contain restriction enzyme sites (Supplemental Table 1) to facilitate further cloning. AtPI4Kγ1, γ4 and γ7 coding regions were cloned into pGEM®-T Easy (Promega, Madison, WI) according to manufacturer's protocol and the clones were confirmed by sequencing. *E. coli* expression cassettes were made in pET-41 vectors (Novagen, San Diego, CA) using restriction enzymes as indicated in Supplemental Table 1. AtPI4Kγ4 sequence encoding the full-length protein and the truncations ΔUBL1, ΔUBL1/UBL2, ΔN and ΔC were PCR-amplified, cloned into the pENTR/SD/D-TOPO entry vector (Invitrogen, Carlsbad, CA) and verified by sequencing. The resulting entry clones were recombined with the *E. coli* expression vectors, pDEST15 and pDEST17 (Invitrogen, Carlsbad, CA), for production of N-terminal glutathione-S-transferase (GST)-tagged or hexa-histidine (His)-tagged fusion proteins, respectively. The AtPI4Kγ4 K284A mutant was generated by PCR using the Quick Change site-directed mutagenesis kit (Stratagene, La Jolla, CA) with the oligonucleotide primers 5'-GTGGGTGTGTTT**GCG**CCAATAGATGAGGAACCAATGGC-3' and 5'-GCCATTGGTTCCTCATCTATTGG**CGC**AAACACACCCAC-3'.

The full-length cDNA clones of the putative AtPI4Kγ-interacting proteins listed in the Table 2 were ordered from the Arabidopsis Biological Resource Center (ABRC) (Yamada et al., 2003) with the exception of Arabidopsis UFD1. AtUFD1 cDNA was amplified via RT-PCR from total RNA of Arabidopsis leaves (see Supplemental Table S1 for

primer sequences) and cloned into the pENTR/SD/D-TOPO entry vector (Invitrogen, Carlsbad, CA). The cDNA from the ABRC clones U09559, U22122, U60768 and U09430 which were supplied on pUNI51 vectors were subcloned via PCR into the pENTR/SD/D-TOPO entry vector (see Supplemental Table S1 for primer sequences). All entry clones were recombined with the *E. coli* expression vectors, pDEST15 and pDEST17 (Invitrogen, Carlsbad, CA), for production of N-terminal GST or His -tagged fusion proteins, respectively.

Recombinant protein production and purification

The various expression cassettes were transformed into *E. coli* expression strain BL21 (DE3) pLysS (Invitrogen, Carlsbad, CA). Cultures of 25 or 50 mL were grown at 37 °C in LB media containing the appropriate antibiotic until mid-logarithmic phase (A_{600} value of 0.4 - 0.6). Expression of the recombinant proteins was carried out at 28 °C for 3 - 4h after induction with 1 mM isopropyl-beta-D-thiogalactopyranoside. Bacterial cells were separated from the media by centrifugation at 5,000 *g* for 6 min at 4 °C and then frozen at -20 °C. For GST-tagged protein purifications, the bacterial pellet was thawed in the presence of 1× PBS (137 mM NaCl, 27 mM KCl, 100 mM Na_2HPO_4, 2 mM K_2HPO_4) and sonicated with a 10-s long pulse, 4 - 5 times. The crude lysate was cleared by centrifugation at 12,000 *g* for 10 min at 4 °C. Batch affinity purification was performed using Glutathione Sepharose™ 4B (Amersham Biosciences, Piscataway, NJ) according to the manufacturer's protocol. For some studies proteins were eluted with reduced glutathione elution buffer (50 mM Tris-HCl, pH 8.0, 20 mM reduced glutathione). For the His-tagged protein purifications, the bacterial pellet was thawed in the presence of Lysis buffer (50 mM sodium phosphate buffer pH 7, 150 mM NaCl, 0.1% Triton X-100, 5% glycerol). The bacterial cells were further lysed by sonication and the crude lysate was cleared by centrifugation as described above. Batch affinity purification was performed using HIS-select™ Nickel Affinity Gel (Sigma, St. Louis, MO) according to the manufacturer's protocol. The His-tagged proteins were eluted with elution buffer (50 mM sodium phosphate buffer pH 7, 150 mM NaCl, 250 mM imidazole). Protein concentrations were determined using the Bradford method (Bio-Rad, Hercules, CA) with BSA as a standard.

Protein electrophoresis and immunobloting

Protein samples were denatured by boiling in the presence SDS sample buffer 5 min prior to SDS-PAGE. For immunoblotting, proteins were transferred to PVDF membrane by electroblotting in 10 mM N-cyclohexyl-3-aminopropanesulfonic acid (CAPS) buffer pH 11 containing 10% (v/v) methanol for 1 h at 50 V. Membranes were blocked for 1 h in 5% (w/v) fat free dried milk in Tris-buffered saline (TBS, 10 mM Tris-HCl, 140 mM NaCl) solution followed by two washes in TBS with 0.2% (v/v) Tween (TBST). Tagged proteins were detected by incubating the blots with monoclonal anti-Penta·His™ (Qiagen GmbH, Hilden, Germany) antibodies at a dilution of 1:1,000 for 1 h followed by treatment with horseradish peroxidase-conjugated anti-mouse antibody as the secondary antibody at a dilution of 1:20,000 for 1 h. Immunoreactivity was visualized by incubating the blot with SuperSignal West Pico Chemiluminescence Substrate (Pierce, Rockford, IL) and subsequent exposure to x-ray film. After chemiluminescence detection, total protein was visualized by staining the blots with Amido Black (Sigma, St. Louis, MO).

In vitro phosphorylation assays

Recombinant proteins (immobilized on affinity beads or eluted) were assayed for lipid and protein kinase activity and for autophosphorylation. Protein kinase activity and autophosphorylation were assayed in buffer containing 50 mM Tris HCl (pH 7.5), 10 mM $MgCl_2$, 1 mM EGTA, 100 μM ATP (5 μCi of [γ-^{32}P]ATP per reaction) in the absence of substrate (autophosphorylation assay) or in the presence of type III-S histone (Sigma, St. Louis, MO), myelin basic protein (Sigma, St. Louis, MO) or other proteins as indicated as phosphate-acceptor substrates. Optimum Mg^{2+} concentration was analyzed and phosphorylation efficiency was indistinguishable (data not shown) at concentrations between 2.5 – 10 mM $MgCl_2$. Typically, reactions were carried out in 40-60 μL (final volume) for 10-20 min at room temperature under occasional agitation and were terminated by adding 4 × SDS sample buffer. Reaction mixtures were resolved on SDS-PAGE gel followed by autoradiography to visualize phosphate incorporation.

Phosphoinositide-kinase activity was assayed in 50 μL reactions containing 50 mM Tris HCl (pH 7.5), 10 mM $MgCl_2$, 1 mM EGTA, 0.1% (v/v) Triton X-100, 100 μM ATP (9 μCi of [γ-^{32}P]ATP per reaction) in the presence of 0.25 mg·mL^{-1} PtdIns or 0.3 mg·mL^{-1} of Type I Folch fraction I from bovine brain extract. Stock phosphatidylinositol (PtdIns) and Type I Folch fraction I (5 mg·mL^{-1}) were solubilized in 1% (v/v) Triton X-100. The reactions were incubated at room temperature for 20 min with intermittent shaking. The reactions were stopped with 1.5 ml of ice-cold $CHCl_3$:CH_3OH (1:2) and kept at 4 °C until the lipids were extracted. Lipids were extracted as described previously (Stevenson et al., 1998; Stevenson-Paulik et al., 2003). Extracted lipids were vacuum-dried, solubilized in $CHCl_3$:CH_3OH (2:1), and separated by TLC on silicagel plates (LK5D; Whatman, Clifton, NJ) using $CHCl_3$:CH_3OH:NH_4OH:H_2O (86:76:6:16) mobile phase (Stevenson et al., 1998; Stevenson-Paulik et al., 2003). [γ-^{32}P]-Labeled lipids were detected and quantified with a Bioscan System 500 Imaging Scanner and by autoradiography.

Protein pull-down assays

GST-tagged proteins immobilized in glutathione-Sepharose beads were incubated with either Arabidopsis cell extracts or *E. coli* expressed recombinant proteins containing a His-tag. Arabidopsis cell extracts were prepared from 5-day old cells growing in suspension cultures. The cells were harvested by filtration and immediately homogenized in cold TEEM buffer (50 mM Tris HCl, pH 7.5, 2 mM EGTA, 2 mM EDTA, 1 mM $MgCl_2$) supplemented with 200 mM sucrose, 1 mM phenylmethylsulfonyl fluoride and 10 μg·mL^{-1} leupeptin. Homogenation was carried in a glass Dounce homogenizer with 1% (w/v) polyvinylpolypyrrolidone to facilitate grinding. The crude extract was clarified by centrifugation at 5,000 *g* for 5 min at 4 °C. The supernatant was fractionated further (40,000 *g*, for 60 min, at 4 °C) to yield microsomal and soluble protein fractions. The microsomal pellet was solubilized in non-supplemented TEEM buffer. Microsomal and soluble fractions were pre-treated by incubating with purified GST immobilized on glutathione-Sepharose beads in a 10:1 ratio to remove non-specific binding proteins. Pre-cleared fractions were incubated with immobilized GST-AtPI4Kγ7 and GST-AtPI4Kγ4 in TEEM buffer for 2 h at

4 °C. After extensive washing the bound proteins were separated by SDS-PAGE. Selected bands revealed by Coomassie blue staining were excised from the gel and subjected to liquid chromatography-tandem mass spectrometry (LC/MS/MS) analysis for identification.

Pull-downs using recombinant proteins were performed by incubating GST-tagged proteins immobilized in glutathione-Sepharose beads with purified His-tagged proteins in the presence of binding buffer (50 mM Tris HCl, pH 7.5, 100 mM KCl, 0.05% Triton X-100). After extensive washing with binding buffer, bound proteins were added directly into 4 × SDS-PAGE sample buffer, boiled for 5 min, separated by SDS-PAGE and subjected to immunoblot analysis. GST-tagged proteins were visualized directly by Amido Black staining of the blot. Recovered His-tagged proteins were detected by immunoblot with monoclonal Penta·His™ (Qiagen GmbH, Hilden, Germany) antibody.

Protein identification by LC/MS/MS analysis

i) In-gel tryptic digestion

Selected protein bands excised from gel slices were subjected to in-gel tryptic digestion according to Wang et al. (2005). Briefly, the gel slices were first destained in acetonitrile/50 mM NH_4HCO_3, pH 8.0, (1:1, v/v), dehydrated in 75% acetonitrile/25% water, and dried in a vacuum centrifuge. The gel slices were incubated at 50 °C for 1 h in reducing solution (5 mM DTT and 50 mM NH_4HCO_3, pH 8.0), then alkylated in 25 mM NH_4CO_3 using 20 mM iodoacetamide at 37°C for 30 min. The gel slice was washed with 25 mM NH_4HCO_3 and dehydrated as before. The slice was then crushed into small pieces and rehydrated with a minimum volume of 50 mM NH_4HCO_3, pH 8.0, containing enough trypsin to provide a 1:5 trypsin-to-protein ratio, and then incubated overnight at 37 °C. After proteolysis, the peptides were extracted three times by adding 0.2 mL of 60% acetonitrile/5% formic acid (v/v) to each sample followed by sonication for 30 min in a sonicating bath. The extracts from each sample were pooled into a siliconized polypropylene Eppendorf tube, the solvent was removed via vacuum centrifugation, and the samples were stored at –80° C until LC/MS/MS analysis could be performed. The dried peptides were resuspended in 25 µL of

5% acetonitrile/0.1% formic acid, of which 8 µL was used for microcapillary reversed-phase LC/MS/MS.

ii) Microcapillary reversed-phase LC/MS/MS

Peptide samples were analyzed using an Agilent 1100 series capillary LC system (Agilent Technologies, Palo Alto, CA) coupled directly online with an LCQ Deca ion trap mass spectrometer (Thermo Finnigan, San Jose, CA, now Thermo Fisher Scientific). The instrument was equipped with an in-house manufactured electrospray interface and operated in positive ion mode with an electrospray voltage of 2.2 kV (Qian et al., 2003). The reversed-phase capillary HPLC column containing 5 µm Jupiter C_{18} stationary phase (Phenomenex, Torrance, CA) was slurry packed in house into a 150-µm i.d. × 50-cm length capillary (Polymicro Technologies, Phoenix, AZ). The mobile phase consisted of (A) 0.1% formic acid in water and (B) 0.1% formic acid in acetonitrile. After loading a sample volume of 8 µL onto the reversed-phase column, the mobile phase was held at 5% B for 20 min and the peptides were eluted using a linear gradient to 95% B for 90 min at a flow rate of 1.5 µL/min. The data acquisition sequence used for all LC/MS/MS analyses employed a full MS scan followed by four MS/MS scans, where the four most intense ions were dynamically selected from the precursor MS scan and subjected to CID using a normalized collision energy setting of 45%.

iii) Peptide identification and phosphorylation site analysis

Peptides obtained from the pull-down experiments were identified by searching the product ion spectra against the *Arabidopsis thaliana* protein database obtained from The Arabidopsis Information Resource (TAIR) website (http://www.arabidopsis.org) using TurboSEQUEST as provided in BioWorks 3.1 (Thermo Finnigan, San Jose, CA; now Thermo Fisher Scientific). Peptides obtained from the kinase experiments were identified by searching against a database containing the His-AtUFD1 protein sequence and the nonredundant *E. coli.* database obtained from the National Center for Biotechnology Information (NCBI) website (http://www.ncbi.nlm.nih.gov/). Tryptic peptides displaying a charge dependent cross-correlation score (Xcorr) of 2.0, 1.5 and 3.3, for +1, +2 and +3

charged species of the precursor ions and a delta-correlation score (ΔC_n) of 0.08 were used for identification [25]. All searches included a static carboxamidomethyl modification of 57.0 u on Cys residues due to alkylation, a differential modification of 16.0 u on Met residues due to oxidation (Met sulfoxide) and a differential phosphorylation modification of 79.96 u on Ser, Thr, and Tyr residues. The product ion spectra of all phosphopeptides were manually inspected to ensure acceptable ion coverage and phosphorylation site identification, including those ions involved in neutral losses of HPO_4 and H_3PO_4. Product ion spectra from the pull-down experiments were manually inspected in cases where a protein was identified by a single unique peptide.

Results

Phylogeny and domain organization of the putative type II AtPI4Ks

Phylogenetic analysis derived from the amino acid sequence alignment using the PI3/4K domain from human, yeast and Arabidopsis proteins (InterPro IPR000403) reveals that the PI3/4K domain-containing proteins fall into three major groups, indicated by the clusters A, B and C in the phylogenetic tree shown in the Supplemental Figure S1. Cluster A (Figure S1) grouped all the PIKK, which are high molecular weight (over 200 kDa) proteins that have Ser/Thr kinase activity. The cluster B (Figure S1) grouped the canonical PI3- and the PI4- kinases. This cluster can be separated further into PI3Ks (class I and II), type III PI4Ks and VPS-like PI3K (class III). While the type III PI4Ks and VPS-like PI3K use exclusively inositol phospholipids as substrate, some PI3K can use both lipid and protein substrates. For example, the human class Ib PI3Kγ phosphorylates phosphatidylinositol 4, 5 bisphosphate and non-muscle tropomyosin (Naga Prasad et al., 2005). Cluster C (Figure S1) grouped the human and yeast type II PI4Ks along with a group of 8 putative orthologs from Arabidopsis (AtPI4Kγ1 - γ8 according to Mueller-Roeber and Pical (2002)). The locus At1G27570 is an exception in the cluster C. Despite its similarity with the type II PI4Ks within the PI3/4K domain, the overall domain organization of the At1G27570 predicted product resembles a typical member of the PIKK group.

The cluster containing the putative type II PI4K (AtPI4Kγs) from Arabidopsis can be divided in three subgroups. This subdivision of the AtPI4Kγs extends beyond the sequence similarity within the PI3/4K domain and reflects the presence of UBL domains. AtPI4Kγ2, γ3 and γ4 have two N-terminal UBL domains and AtPI4Kγ5, γ6 and γ7 have one (Figure 1A). Both AtPI4Kγ1 and γ8 lack an UBL domain. Figure 1B and Table 1 show respectively alignments and the percentage of sequence similarity/identity between human and Arabidopsis ubiquitin and the UBL domains from AtPI4Kγ4 and γ7.

According to InterPro (http://www.ebi.ac.uk/interpro/) and protein searches based on the homology by domain architecture using the Conserved Domain Architecture Retrieval Tool-CDART (http://www.ncbi.nlm.nih.gov/Structure/lexington/lexington.cgi?cmd=rps) proteins displaying the association of the PI3/4K domain with N-terminal UBL domains are not found in metazoans, budding and fission yeast or in any prokaryotic organism. However, proteins with N-terminal UBL and C-terminal PI3/4K domains are found in Arabidopsis and other plants (dicots and monocots), algae, and protozoans (Supplemental Figure S2), indicating that this novel group of enzymes is conserved not only in the genome of plants but across genomes of several eukaryotic organisms.

Table 1. Pairwise percentage of similarity/identity of the amino acid sequence between human and Arabidopsis ubiquitin and AtPI4Kγ4 and γ7 (UbDKγ4 and γ7) UBL domains[a].

	Hs Ub	**At Ub**	**γ4 UBL1**	**γ4 UBL2**	**γ7 UBL**
Hs Ub	100/100	100/96	77/36	68/34	63/23
At Ub		100/100	78/35	68/34	62/23
γ4 UBL1			100/100	61/23	68/27
γ4 UBL2				100/100	52/25
γ7 UBL					100/100

[a]Sequence alignment performed using CLUSTALW available at http://www.genome.jp/; Hs Ub - human ubiquitin (P62988); At Ub - Arabidopsis ubiquitin (NP_568397).

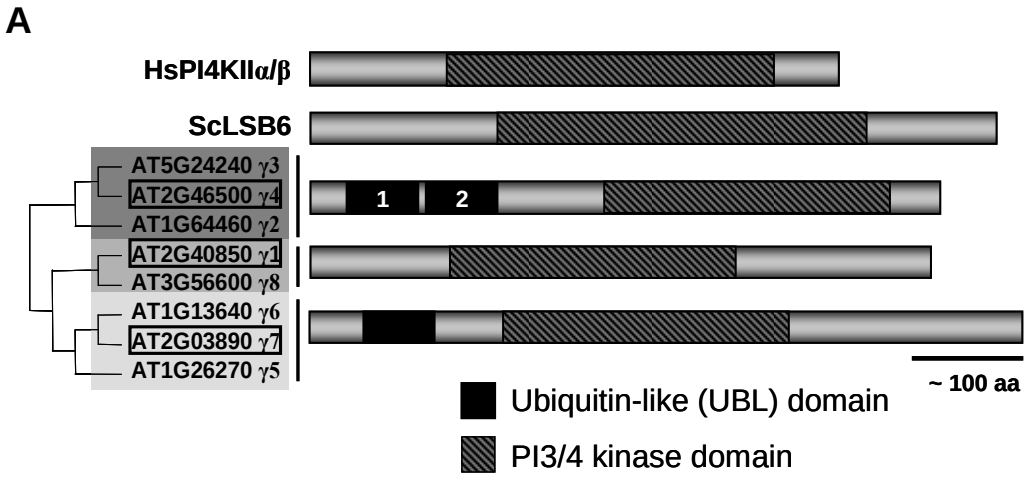

B

```
Hs_Ubiquitin          1 MQIFVKTLTGKTITLEVEPSDTIENVKAKIQDKEG--IPPDQQRLIFAGK
At_Ubiquitin          1 MQIFVKTLTGKTITLEVESSDTIDNVKAKIQDKEG--IPPDQQRLIFAGK
γ4_UBL_1             36 --MIYLTLPGSVIPMRVLESDSIESVKLRIQSYRG--FVVRNQKLVFGGR
γ4_UBL_2            112 -VLDVKTTCGKHCRFHVERGRNIGYVKKQISKKRGDFVDPDEQEILYEGE
γ7_UBL               45 RRVFVQTETGCVLGMELDRSDNVHTVKRRLQIALN--FPTEESSLTYG--
                           :   *  *    :.:  . .:  ** ::.   .  .   :. : :

Hs_Ubiquitin             QLE-DGRTLSDYNIQKESTLHLVLRLRGG 76
At_Ubiquitin             QLE-DGRTLADYNIQKESTLHLVLRLRGG 76
γ4_UBL_1                 ELARSNSNMRDYGVSEGNILHLVLKL--- 107
γ4_UBL_2                 KLE-DQSLINDICRNDDSVLHLLVRR--- 185
γ7_UBL                   ----DMVLTNDLSAVRNDSPLLLKRN--- 113
                             .     *      .   *: :
```

Figure 1. Domain organization of putative type II AtPI4Ks.
A. The PI3/4K domain is located as indicated (striped region). In Arabidopsis, two of the three subgroups of putative type II AtPI4K have N-terminal UBL domains (black). **B** Amino acid sequence alignment comparing human (Hs) and Arabidopsis (At) ubiquitin with UBL domains from AtPIKγ4 and γ7. The alignment was performed using CLUSTALW available at http://www.genome.jp/.

Activity of the AtPI4Kγs

We cloned into expression vectors the coding region of three selected isoforms, AtPI4Kγ1, γ4 and γ7, one from each of the three subgroups of the Arabidopsis type II PI4Ks (Figure 1A). Each of the three recombinant proteins was successfully produced in *E. coli* as an N-terminal GST fusion. Phosphorylation assays carried out in the presence of [γ-^{32}P] ATP in the absence of any other substrate revealed that recombinant AtPI4Kγ4 and γ7 but not γ1 would autophosphorylate (Figure 2A). None of the *E. coli*-expressed, GST-proteins showed detectable PI kinase activity in *in vitro* assays in the presence of PtdIns or Type I Folch fraction and [γ-^{32}P] ATP (data not shown).

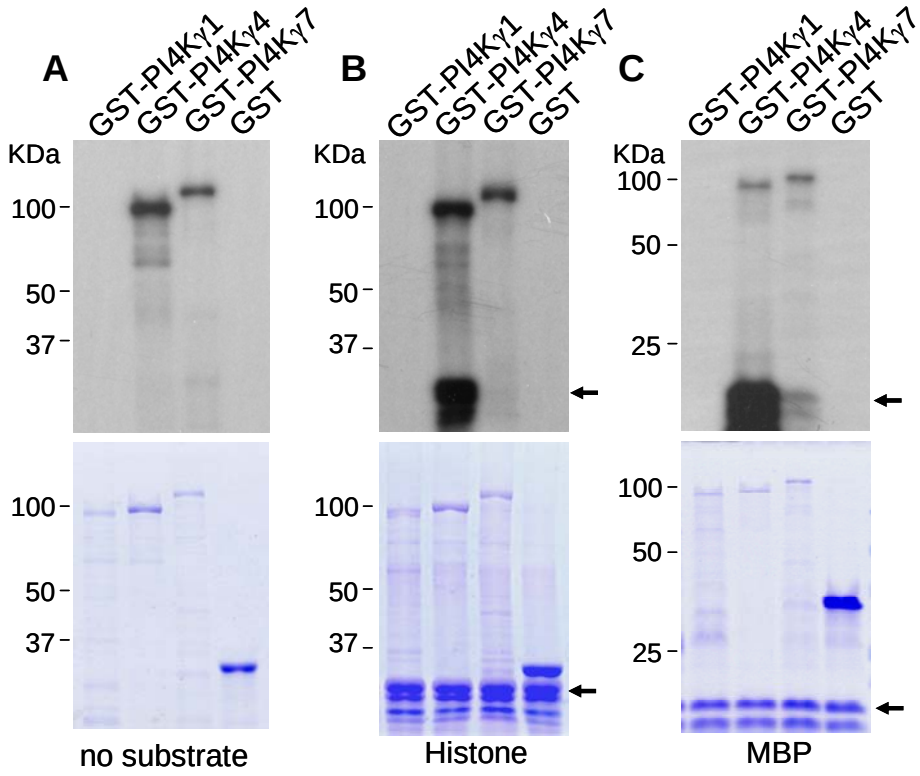

Figure 2 AtPI4Kγ4 and γ7 are protein kinases.
Recombinant GST and GST-AtPI4Kγ1, γ4 and γ7 produced in *E. coli* (1 µg) were used in protein phosphorylation reactions containing [γ-^{32}P] ATP. The reactions were conducted with (**A**) no protein substrate, (**B**) 5 µg type III Histone, or (**C**) 5 µg of myelin basic protein (MBP) as protein substrates. The products of the reactions were resolved by SDS-PAGE. The ^{32}P-labeled proteins were revealed by autoradiography (*upper panels*) and the protein amounts by Coomassie blue staining (*lower panels*). The arrows in **B** and **C** indicate the substrates used in the assays. (AtPI4Kγ4 and γ7 are henceforth denoted as UbDKγ4 and γ7).

Enzymes capable of autophosphorylation often phosphorylate other proteins. So we investigated whether the putative type II AtPI4Kγ4 and γ7 could also phosphorylate protein substrates. *In vitro* phosphorylation assays using [γ-^{32}P] ATP and protein substrates revealed that recombinant AtPI4Kγ4 and γ7, but not γ1, displayed protein kinase activity. AtPI4Kγ4 and γ7 phosphorylate type III-S histone (Figure 2B) and myelin basic protein (MBP) (Figure 2C) *in vitro*. We concluded that AtPI4Kγ4 and γ7 are protein kinases and hereafter denote them as UbDKγ4 and UbDKγ7. Due to the higher kinase activity of UbDKγ4 compared to UbDKγ7, all subsequent experiments to characterize the UbDKs were conducted using UbDKγ4.

Ca^{2+} plays an important role in stimulating protein phosphorylation by activating Ca^{2+}-regulated protein kinases (for review see, (Harper et al., 2004)). In order to determine whether the protein kinase activity of UbDKs is affected by Ca^{2+} we used the *E. coli*-expressed UbDKγ4 in a series of *in vitro* assays where autophosphorylation and phosphorylation of histone were analyzed. As shown in Supplemental Figure S3A and B, Ca^{2+} does not stimulate either UbDKγ4 autophosphorylation (Figure S3A) or type III-S histone phosphorylation (Figure S3B). If anything, the presence of 1 mM EGTA caused a slight increase in histone phosphorylation (Figure S3B, lane 2 vs. 3). Interestingly, while Ca^{2+} did not increase UbDKγ4 activity, the presence of histone, a positively charged protein, enhanced autophosphorylation (Figure S3C).

LY29400 and Wortmannin are known PI3/4K inhibitors. They not only inhibit lipid kinase activity of many PI3- and PI4- kinases but also inhibit protein kinase activity of PIKKs (Chiang and Abraham, 2004). *In vitro* assays using recombinant UbDKγ4 revealed that even at high (100 μM) concentrations, these inhibitors had no effect on autophosphorylation or phosphorylation of histone or UFD1 (data not shown).

UBL domains are not necessary for UbDKγ4 autophosphorylation

To determine the role of the different domains in the activity of UbDKs, three N-terminal truncations of UbDKγ4 were generated and produced as GST fusions in *E. coli* (Figure 3A). The absence of one (ΔUBL1) or two (ΔUBL1/UBL2) UBL domains did not

affect UbDKγ4 autophosphorylation (Figure 3B). However, no detectable autophosphorylation was observed in the absence of a 75-amino acid long interdomain region between UBL2 and the PI3/4K domain, suggesting that this region is required for autophosphorylation or its absence affects protein folding.

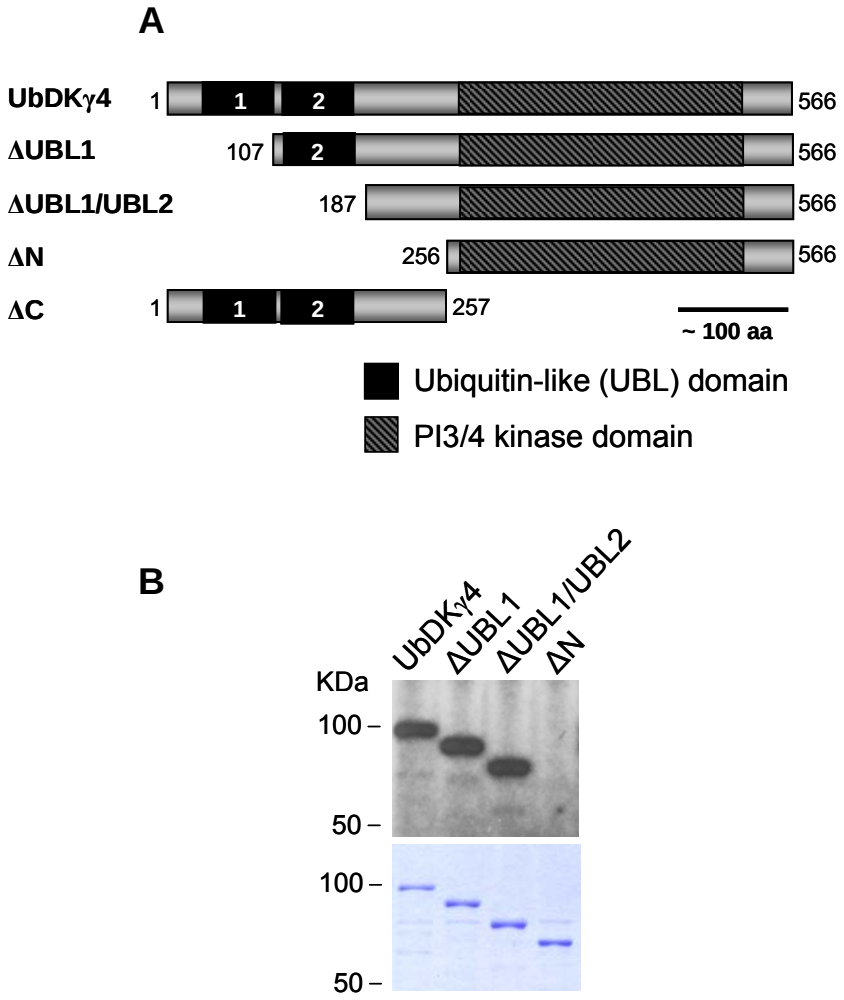

Figure 3. UBL domains are not necessary for UbDKγ4 autophosphorylation.
A. UbDKγ4 truncations constructed for expression in *E. coli*. **B.** Recombinant full-length UbDKγ4 and all N-terminal truncations (ΔUBL1, ΔUBL1/UBL2 and ΔN) fused to GST (1 µg each) were assayed for autophosphorylation by adding [γ-^{32}P] ATP as described in the Experimental Section. The products of the reactions were resolved by SDS-PAGE. The ^{32}P-labeled proteins were revealed by autoradiography (*upper panel*) and the protein amounts by Coomassie blue staining (*lower panel*).

UbDKγ4 is capable of intermolecular autophosphorylation and interaction in vitro

Phosphorylation reactions containing the full-length UbDKγ4 in combination with the inactive N- and C-terminal truncations (ΔN and ΔC, respectively (Figure 3A)) revealed that the full-length enzyme was able to phosphorylate both protein constructs (Figure 4A). The fact that ΔN protein is phosphorylated by the full-length enzyme indicates that ΔN is indeed inactive and that its inability to autophosphorylate is not due to absence of a phosphorylation site. The data in Figure 4A also indicate that UbDKγ4 has more than one potential site for phosphorylation, i.e., at least one in both the N- and C-terminus of the protein.

The ability of full-length UbDKγ4 to *trans* phosphorylate ΔN and ΔC protein constructs (Figure 4A) implies that UbDKγ4 may autophosphorylate via an intermolecular reaction. In order to further confirm the intermolecular autophosphorylation we used versions of full-length UbDKγ4 carrying different N-terminal tags (GST and His) and a kinase inactive mutant. The GST- and His-tagged UbDKγ4 can be easily distinguished by SDS-PAGE due to differences in the molecular weight (~98 kDa and ~74 kDa, respectively).

To generate a kinase inactive mutant, we identified the putative ATP-binding site from the N-terminal portion of the PI3/4K domain based on sequence alignments with the catalytic domain of the type II PI4Ks as described by Barylko et al. (2002) (data not shown). The alignment predicted that Lys 284 of UbDKγ4 was one of the key residues for ATP binding and therefore critical for the enzyme activity. Site-directed mutagenesis was used to change Lys 284 to Ala. The mutant, referred here as K284A, was successfully over-expressed in *E. coli.* Protein phosphorylation assays comparing wild type and K284A revealed that the mutation completely abolished protein kinase activity (Supplemental Figure S4).

Figure 4B shows that the kinase inactive GST-UbDKγ4 (K284A) was phosphorylated by the wild type His-UbDKγ4. K284A phosphorylation (Figure 4B) was markedly reduced compared to that observed for the ΔN and ΔC protein constructs (Figure 4A). This is probably because the phosphorylation sites of the truncated proteins are more accessible to full-length UbDKγ4. Taken together, these data indicate that UbDKγ4 utilizes an

intermolecular reaction mechanism for autophosphorylation, implying at least a transient interaction between two or more UbDKγ4 molecules.

In order to investigate whether UbDKγ4 can establish any kind of stable intermolecular interaction, we performed pull-down experiments using recombinant UbDKγ4 fused with different tags. GST-UbDKγ4 immobilized in glutathione-Sepharose beads was used to pull down His-UbDKγ4. Immobilized GST-UbDKγ4 bound to His-UbDKγ4, whereas the controls of unmodified Sepharose beads or immobilized GST elicited no detectable His-UbDKγ4 binding (Figure 4C). These data indicate that UbDKγ4 can participate in a direct intermolecular interaction.

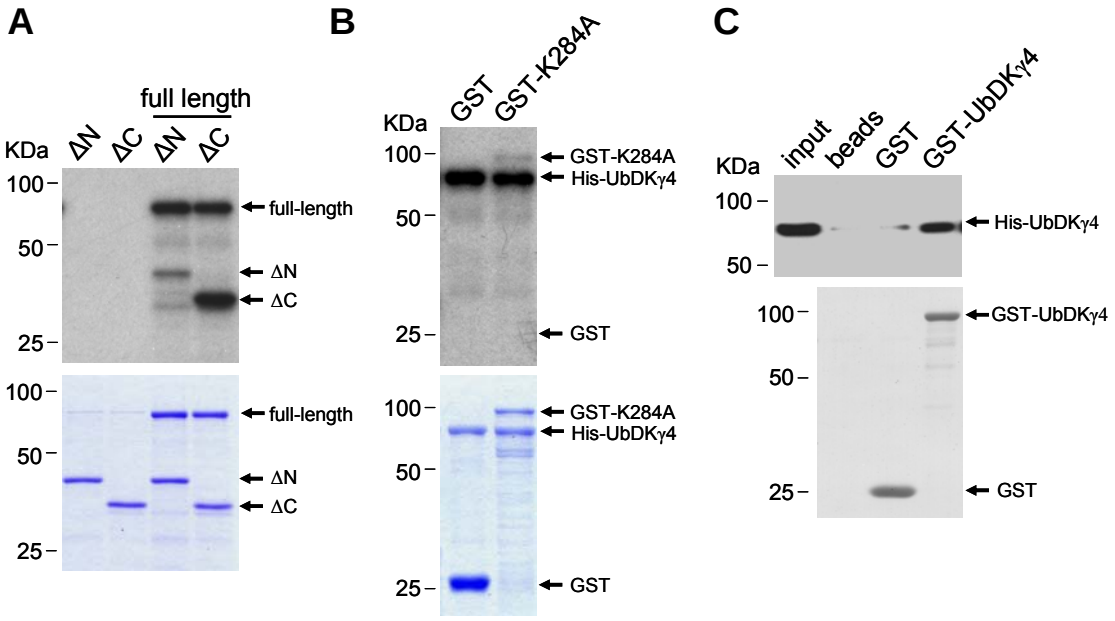

Figure 4. UbDKγ4 autophosphorylates multiple sites via intermolecular reaction and interacts with itself. **A.** Recombinant His-ΔN and -ΔC protein constructs (1 μg each) were assayed for phosphorylation in the presence or absence of 1 μg of full-length His-UbDKγ4 as indicated. **B.** Recombinant His-AtUDPKγ4 (1 μg) was assayed for phosphorylation in the presence of 1 μg of GST or GST-K284A. The products of the reactions were resolved by SDS-PAGE. The ^{32}P-labeled proteins were revealed by autoradiography (*upper panels*) and the protein amounts by Coomassie blue staining (*lower panels*). **C**. Glutathione-Sepharose beads, GST or GST-UbDKγ4 immobilized on glutathione-Sepharose beads were used as bait in pull-down assays containing His-UbDKγ4 as prey. Bound His-UbDKγ4 was detected by immunoblotting with anti His-tag antibody (*upper panel*). GST and GST- UbDKγ4 were visualized by Amido Black staining of the membrane (*lower panel*). The *input* lane corresponds to 20% of the amount of His-UbDKγ4 originally used in each binding assay.

UbDKγ4 interacts with AtRPN10 and AtUFD1, proteins of the ubiquitin/proteasome system

As a first step toward the functional characterization of the UbDKγs we attempted to identify putative interacting proteins using pull-down experiments with proteins from Arabidopsis cells growing in suspension culture. Immobilized GST-UbDKγ4 and γ7 were used to pull down putative interacting proteins. The recovered proteins were resolved by SDS-PAGE and the most intense Coomassie-stained bands were excised, subjected to in-gel trypsin digestion, and the extracted peptides identified by LC/MS/MS analysis with a list of the best identified candidates appearing in Table 2. Based on the literature regarding the function of these proteins and the availability of cDNA clones, seven of these candidates were experimentally tested for direct interaction with UbDKγ4 using recombinant proteins.

Of the seven proteins examined, both AtRPN10 and AtUFD1 demonstrated a direct interaction with UbDKγ4. In a reciprocal pull-down assay, immobilized GST-AtRPN10 and GST-AtUFD1 were incubated with His-UbDKγ4. His-UbDKγ4 was recovered bound to both GST-AtRPN10 and GST-AtUFD1 but not with GST alone (Figure 5).

In order to determine which of the UbDKγ4 domains are important for protein-protein interactions we used the UbDKγ4 truncations (Figure 3A) in binding assays with the recombinant proteins. We were particularly interested to determine which domains were responsible for the UbDKγ4 intermolecular interaction with itself and with AtRPN10 and AtUFD1. Because AtRPN10 and AtUFD1 bind different forms of ubiquitin, we anticipated that the UBL1 and UBL2 domains of UbDKγ4 would be essential for binding.

Immobilized GST-UbDKγ4 (Figure 6A), GST-AtRPN10 (Figure 6B) and GST-AtUFD1 (Figure 6C) were incubated with His-UbDKγ4, His-ΔUBL1, His-ΔN and His-ΔC. His-UbDKγ4 was recovered bound to GST-UbDKγ4, GST-AtRPN10 and GST-AtUFD1 as expected. His-ΔUBL1 was detected bound to GST-UbDKγ4 and GST-AtRPN10 but not to GST-AtUFD1 indicating that the UBL1 domain was essential for AtUFD1 binding. Furthermore, the fact that AtUFD1 bound ΔC and the full-length protein to nearly the same extent, but not ΔUBL1, confirms that AtUFD1 interaction with UbDKγ4 N-terminal domain (1-257 aa) requires the presence of the UBL1 domain (1-107). In contrast to AtUFD1,

Table 2. Putative interacting proteins of UbDKγ4 and UbDKγ7 identified from Arabidopsis using LC/MS/MS analysis.

AGI Number[a]	Protein[b]	Unique Peptides Identified[c]	Calc. $[M+H]^{+}$[d]	Meas. $[M+H]^{+}$[e]	Chg.[f]	Xcorr[g]	ΔC_n[h]	Direct Interaction[i] (cDNA ID#)
Recovered with UbDKγ4								
At4g38630	RPN10 - component of 26S proteasome regulatory particle	R.IIVFAGSPIK.Y	1045.3	1044.6	1	2.105	0.386	yes (U09430)
At3g02090	MPPβ - mitochondrial processing peptidase beta subunit precursor	K.LSSDPTTTSQLVANEPASFTGSEVR.M	2595.8	2595.6	2	3.986	0.464	inconclusive (U22122)
At3g09200	RPP0C - 60S acidic ribosomal protein P0	K.VEEKEESDEEDYGGDFGLFDEE.	2568.5	2567.6	2	4.693	0.614	not determined (U09559)
		K.FAVASVAAVSADAGGGAPAAAK.V	1860.1	1859.3	2	3.653	0.392	
At5g39740 At3g25520	RPL5B - 60S ribosomal protein L5	K.M#LEM#DDEYEGNVEATGEDFSVEPTDSR.R	3099.2	3098.1	2	5.160	0.606	no (U15332 for At3g25520)
		R.ALLDVGLIR.T	970.2	969.7	1	2.112	0.317	
At5g60390 At1g07940 At1g07930 At1g07920	eEF1A - eukaryotic elongation factor 1-alpha	K.NM#ITGTSQADCAVLIIDSTTGGFEAGISK.D	2975.2	2974.0	2	2.865	0.452	no[j]
		R.LPLQDVYK.I	976.2	976.1	2	2.597	0.327	
		R.VETGMIKPGMVVTFAPTGLTTEVK.S	2508.0	2509.1	2	2.543	0.186	
		R.VETGM#IKPGM#VVTFAPTGLTTEVK.S	2540.0	2539.3	2	2.516	0.329	
		K.IGGIGTVPVGR.V	1026.2	1026.4	2	2.394	0.278	
		K.M#TPTKPM#VVETFSEYPPLGR.F	2313.7	2312.8	2	2.214	0.253	
		R.STNLDWYK.G	1027.1	1026.9	2	2.103	0.296	
		R.STNLDWYK.G	1027.1	1026.5	1	2.066	0.182	
Recovered with UbDKγ7								
At2g21270	UFD1 - ubiquitin fusion degradation protein 1	.M#FFDGY*HYHGT*T*FEQSYR.C	2543.4	2542.9	2	2.163	0.175	yes
At3g02090	MPPβ - mitochondrial processing peptidase beta subunit precursor	K.LSSDPTTTSQLVANEPASFTGSEVR.M	2595.8	2595.8	2	4.383	0.537	inconclusive (U22122)
At2g17360	RPS4A - putative ribosomal protein S4	R.LGNVYTIGK.G	965.1	964.5	1	2.191	0.413	no (U15117)
		K.FDVGNVVM#VTGGR.N	1367.6	1367.1	2	2.270	0.323	
At5g48850	MS5 - male sterility MS5 family protein	R.CSKNSQDSLDNVLIDLYKK.C	2241.5	2241.2	2	2.151	0.086	no (U60768)
At4g35000	APX3 - L-ascorbate peroxidase	K.LSELGFNPNSSAGK.A	1421.5	1420.9	2	3.478	0.302	no (U16922)
		K.FDNSYFVELLK.G	1375.6	1375.4	2	2.433	0.181	

[a]The identified peptide sequence may not be unique to one Arabidopsis gene locus due to various protein isoforms as determined by performing a BLAST search on each peptide.

[b]Annotation according to The Arabidopsis Information Resource (TAIR) website (http://www.arabidopsis.org/).

[c]The amino acid residues appearing before and after the periods correspond to the residues proceeding and following the peptide in the protein sequence. Based on the product ion spectra, phosphoseryl, phosphothreonyl, and phosphotyrosyl residues are determined as indicated by S*, T* and Y*, respectively, and oxidized methionyl residues are denoted by M#.
[d]The average mass calculated is based upon the peptide sequence.
[e]Deconvoluted mass determined from the observed centroid mass-to-charge (*m/z*) ratio at the reported charge state.
[f]Charge state of the observed precursor ion.
[g]SEQUEST cross-correlation score (Xcorr) of the peptide is based on the degree of overlap between the product ion spectrum to the theoretical distribution of b and y ions for the peptide.
[h]SEQUEST difference of cross correlation scores (ΔC_n) is the "difference" between the top two Xcorrs for a given product ion spectrum.
[i]Direct protein interactions were determined using *in vitro* pull-down experiments using recombinant proteins as described in the Experimental Section. The interactions indicated as "inconclusive" could not be determined due to failed attempt to produce soluble recombinant protein. The indicated cDNA clones were ordered from the Arabidopsis Biological Resource Center (ABRC) at The Ohio State University, Columbus, OH as available (http://www.biosci.ohio-state.edu/~plantbio/Facilities/abrc/abrchome.htm/).
[j]Purified endogenous eEF1A from *Daucus carota* cells (Ransom et al., 1998) was used in this experiment.

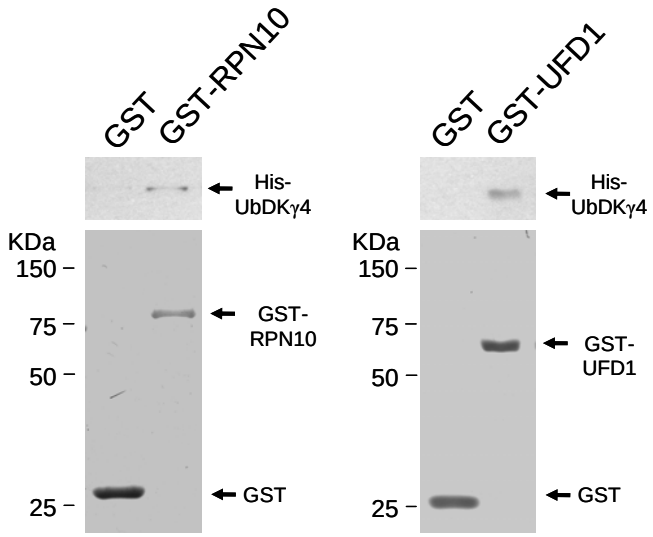

Figure 5. UbDKγ4 interacts with AtRPN10 and AtUFD1.
GST, GST-RPN10 and GST-AtUFD1 immobilized in glutathione-Sepharose beads were used as bait in pull-down assays containing His-UbDKγ4. The bound His-UbDKγ4 was visualized by immunobloting with an anti His-tag antibody (*upper panel*). GST, GST-RPN10 and GST-AtUFD1 were visualized by Amido Black staining of the membrane (*lower panel*).

AtRPN10 did not bind either ΔN or ΔC. AtRPN10 interaction was detectable with UbDKγ4 and, to a lesser extent, ΔUBL1. These observations suggest that AtRPN10 requires sequence component(s) disrupted in both ΔC and ΔN protein constructs since the absence of the UBL1 domain (ΔUBL1) did not abolish binding.

For UbDKγ4 the absence of the UBL1 domain (ΔUBL1) reduced, but did not prevent binding. Additionally, the interaction of UbDKγ4 with the ΔC protein was detectable but barely. UbDKγ4 intermolecular interaction with itself appeared to require a broader sequence region compared to AtRPN10 and AtUFD1, suggesting a more extensive self-recognition binding motif that is primarily located within the N-terminal domain.

In summary, component(s) of the UbDKγ4 within the N-terminus, including the UBL domains, were critical for the observed protein-protein interactions that were investigated (Figure 6E). More importantly, AtRPN10 and AtUFD1 bind to non-overlapping regions of UbDKγ4. His-ΔN did not bind to any of the GST fusion proteins. Interactions with the ΔUBL1/UBL2 protein, although experimentally examined, were not conclusive due to non-specific binding of the ΔUBL1/UBL2 protein to GST (Supplemental Figure S5).

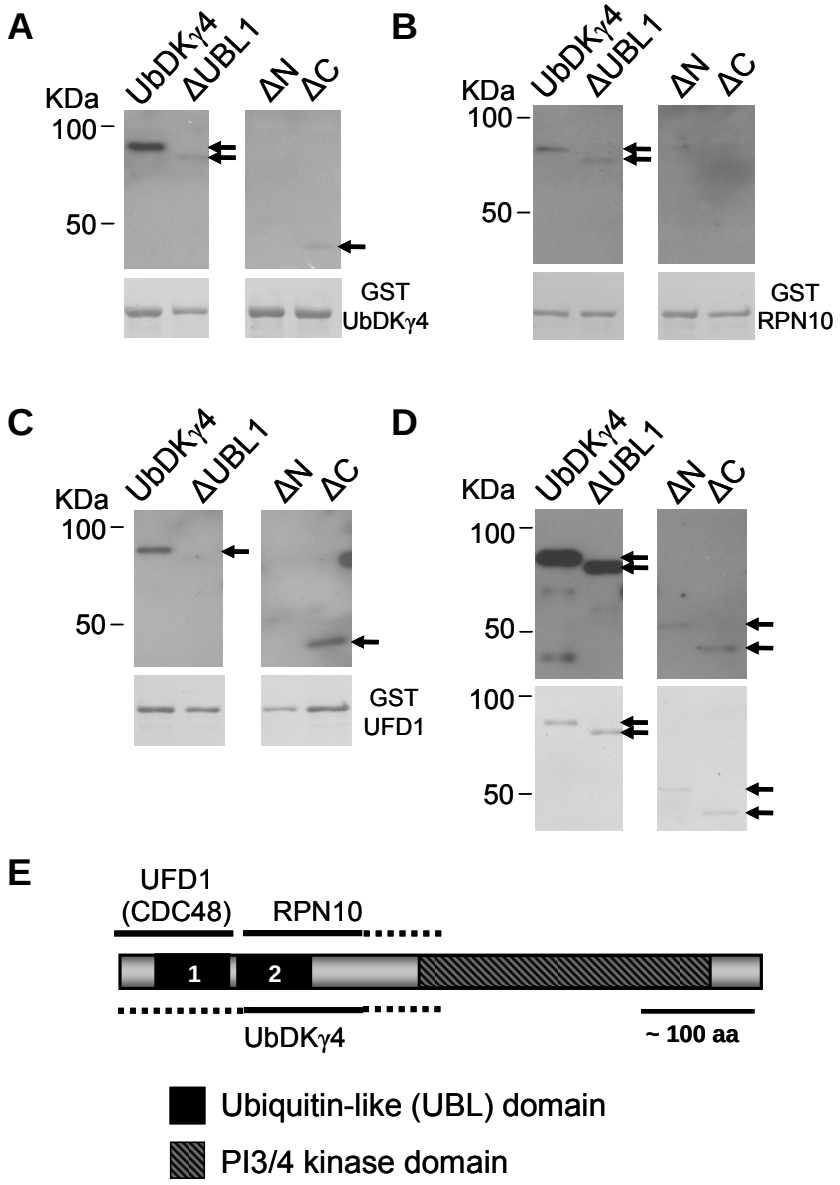

Figure 6. The N-terminus of UbDKγ4 is important for protein-protein interactions.
(**A**) GST- UbDKγ4, (**B**) GST-RPN10, and (**C**) GST-AtUFD1 immobilized on glutathione-Sepharose beads were used as bait in pull-down assays containing full-length His-UbDKγ4 and truncations ΔUBL1, ΔN, and ΔC as prey. In all binding reactions, immobilized bait and prey were incubated in a 1:2 molar ratio. The bound proteins (indicated by the arrows) were revealed by immunoblotting with anti His-tag antibody (*upper panel*). GST-tagged proteins were visualized by Amido Black staining of the membrane (*lower panel*). The panels in (**D**) correspond to 20% of the amount of all His-tagged proteins originally used in each binding assay. The diagram in **E** summarizes the mapping of the UbDKγ4 domains used in the protein-protein interactions. The two non-overlapping regions where AtRPN10 and AtUFD1/CDC48 interact and the region required for UbDKγ4 interaction with itself are indicated by the solid line. The dotted lines indicate additional regions predicted to participate in these interactions. Data for CDC48 binding are presented in Supplemental Figure S6.

In-solution protein structure analysis using NMR revealed that the N-terminal region of UFD1, which is responsible for ubiquitin and polyubiquitin binding, shares striking structural similarity with an analogous region of CDC48 (Park et al., 2005). CDC48 is an abundant AAA-ATPase that forms a homohexamer with chaperone activity, which is necessary for, among other functions, degradation of substrates of the endoplasmic reticulum-associated protein degradation (ERAD) pathway. The involvement of CDC48 in ERAD depends on the interaction with accessory proteins, such as, UFD2 and the heterodimer UFD1/NPL4 (Ye et al., 2001; Bays and Hampton, 2002; Meyer et al., 2002; Kostova and Wolf, 2003; Ye et al., 2003). To investigate further the binding properties of UbDKγ4, we performed the same binding experiment described above with Arabidopsis CDC48 (AtCDC48). GST-AtCDC48 was used as bait to pull-down His-UbDKγ4 full-length and truncations (Supplemental Figure S6). It was determined that AtCDC48, like AtUFD1, can interact with AtUDPKγ4 *in vitro* and this interaction also requires the presence of the UBL1 domain.

UbDKγ4 phosphorylates AtUFD1 and AtRPN10

To investigate whether UbDKγ4 would phosphorylate its interacting proteins revealed here, we performed phosphorylation assays in the presence of AtRPN10 and AtUFD1 with [γ-^{32}P] ATP. The results of these assays indicated that His-AtPI4Kγ4 readily phosphorylates GST-AtUFD1 (Figure 7A) but not GST-RPN10 (Figure 7B). However, AtRPN10 phosphorylation by UbDKγ4 is detected if the AtRPN10 substrate is provided as substrate as the His-fusion protein (Figure 7C). AtUFD1 phosphorylation is always detectable regardless of the combination of the substrate or enzyme tag (Supplemental Figure S7). Because AtUDF1 phosphorylation was more robust, we used AtUFD1 as a substrate to characterize the UbDKγ4 phosphorylation sites.

Protein phosphorylation reactions were performed with UbDKγ4 and AtUFD1 as the substrate using different combinations of tags. The products of each reaction were separated by SDS-PAGE and the band corresponding to AtUFD1 was excised and subjected to in-gel tryptic digestion with the resulting peptides extracted and analyzed by LC/MS/MS. With

sequence coverage of ~60%, our analysis revealed that UbDKγ4 targets Ser239/240, Thr294, and Ser311 within the C-terminus of AtUFD1 (Table 3). No detectable AtUFD1 phosphorylation was observed for the control reactions performed in the presence of the inactive UbDKγ4 (K284A) or in the absence of ATP. However, it should be noted that in addition to the identified AtUFD1 Ser/Thr phosphorylation sites, one of the detected phosphoseryl residues of the AtUFD1 construct corresponds to the linker region between the affinity tag and the AtUFD1 sequence.

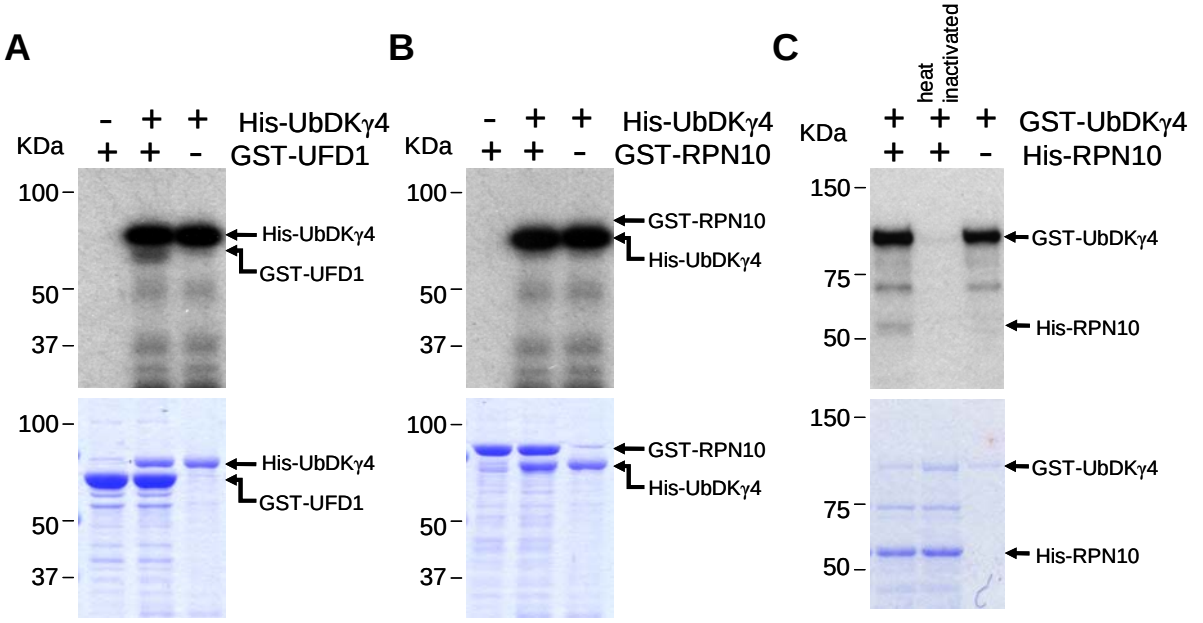

Figure 7. UbDKγ4 phosphorylates AtUFD1 and AtRPN10.
Protein phosphorylation assays were performed with 3 µg of (**A**) GST-UFD1, (**B**) GST-RPN10 and (**C**) 2 µg of His-RPN10. The reactions were carried in the presence of 2 µg of His-UbDKγ4 (**A** and **B**) or GST-UbDKγ4 (**C**). In **C** the substrate His-RPN10 was immobilized onto the nickel affinity agarose beads and GST-UbDKγ4 free in the supernatant was partially removed prior to the electrophoresis. GST-UbDKγ4 inactivation was performed by incubating the enzyme at 90 °C for 10 min. The products of the reactions were resolved by SDS-PAGE. The ^{32}P-labeled proteins were revealed by autoradiography (*upper panel*) and the protein amounts by Coomassie blue staining (*lower panel*).

Table 3 Identification of AtUFD1 *in vitro* phosphorylation sites as determined by LC/MS/MS analysis.

Peptide[a]	Calc. $[M+H]^{+}$[b]	Meas. $[M+H]^{+}$[c]	Chg.[d]	Xcorr[e]	ΔC_n[f]	Ions[g]	Phosphorylation Site[h]
K.AGS*AAALFNFK.K	1177.2	1177.7	2	3.281	0.605	24/30	Ser(-7)
R.PLAYEPAPA[SS]*SK.G	1398.4	1397.5	2	2.484	0.132	19/36	Ser 239/240
K.EAAPKVGAAKET*KKEEQEK.K	2152.3	2150.4	2	1.536	< 0.1[i]	11/54	Thr294
K.FQAFS*GKK.Y	992.9	993.0	2	2.119	0.240	14/21	Ser311

[a]The amino acid residues appearing before and after the periods correspond to the residues proceeding and following the peptide in the protein sequence. Based on the product ion spectrum, phosphoseryl and phosphothreonyl residues are determined as indicated by S* and T*, respectively. Due to the ambiguities in product ion assignment, only one of the seryl residues within the brackets is phosphorylated.

[b]The average mass calculated is based upon the peptide sequence.

[c]Deconvoluted mass determined from the observed centroid mass-to-charge (*m/z*) ratio at the reported charge state.

[d]Charge state of the observed precursor ion.

[e]SEQUEST cross-correlation score (Xcorr) of the peptide is based on the degree of overlap between the product ion spectrum to the theoretical distribution of b and y ions for the peptide.

[f]SEQUEST difference of cross correlation scores (ΔC_n) is the "difference" between the top two Xcorrs for a given product ion spectrum.

[g]The total number of b and y ions (identified/theoretical).

[h]Amino acid residues containing the phosphorylation site. Residue Ser(-7) is part of the linker region of the construct that connects the His-tag to the AtUFD1 protein and is located 7 amino acid residues upstream of the initiator Met1 residue.

[i]The ΔC_n was estimated to be less than 0.1 since the other ranked peptides for the product ion spectrum elicited lower Xcorrs and did not withstand the rigors of manual interpretation.

Discussion

Proteins containing the phosphoinositide 3/4-kinase (PI3/4K) domain include not only predicted lipid kinases such as the phosphatidylinositol 4-kinases (PI4Ks) but also protein kinases like the members of the phosphoinositide kinase-related kinase (PIKK) family. Our ongoing objective is to characterize the group of PI3/4K domain-containing proteins originally identified as putative type II PI4K in Arabidopsis (Mueller-Roeber and Pical, 2002). Here we showed that AtPI4Kγ4 and γ7, two members of this group which contain the PI3/4K and UBL domains, are protein kinases. In addition, protein-protein interactions revealed that AtPI4Kγ4 interacts with and phosphorylates *in vitro* AtRPN10 and AtUFD1, proteins involved in the ubiquitin/proteasome system. We propose that AtPI4Kγ4 and AtPI4Kγ7 are founding members of a new group of protein kinases named UbDKs that belongs to the PIKK family of atypical protein kinases (Manning et al., 2002).

Similarly to other PIKKs, UbDKγ4 and γ7 autophosphorylate, phosphorylate other proteins and display no detectable lipid kinase activity (Abraham, 2004). Autophosphorylation via an intermolecular reaction and intermolecular interaction are also common properties between members of the PIKK family and UbDKγ4. The protein kinase ataxia telangiectasia mutated (ATM) for example homodimerizes and the dissociation of the monomers is stimulated by autophosphorylation which activates ATM kinase activity (Bakkenist and Kastan, 2003). The fact that UbDKγ4 interacts with itself suggests that UbDKγ4, like ATM, may dimerize.

The presence of N-terminal UBL domains (1 or 2) in a subset of the AtPI4Kγs is the most distinctive feature of the AtPI4Kγs. Members of the class I and II PI3K have a Ras binding domain (PI3K_rbd) that falls into the ubiquitin domain superfold (Kiel and Serrano, 2006); however, in contrast to the AtPI4Kγ's UBL domain, the PI3K_rbd lacks any sequence similarity to ubiquitin. IκB kinase β (IKKβ), one of the two kinases that phosphorylate the inhibitor of the mammalian transcription factor NF-κB (IκB), is the only other known protein kinase that contains an UBL domain (May et al., 2004). The UBL domain of IKKβ, unlike the ones from some AtPI4Kγs, is located at the central portion of the protein, and it is essential for protein kinase activity (measured by phosphorylation the substrate GST-IκBα).

AtRPN10 and AtUFD1 directly interact with UbDKγ4, targeting non-overlapping regions of the UbDKγ4 N-terminus where UBL domains are located. RPN10 and UFD1 are distinct proteins, but both bind to some form of ubiquitin and are involved in controlled protein degradation via the ubiquitin/proteasome system (for review (Elsasser and Finley, 2005)). RPN10 is found in eukaryotic cells associated with the 26S proteasome and free in the cytosol. Its domain organization consists of an N-terminal von Willebrand factor-type A (vWA) domain and one (in yeast) or two (in higher eukaryotes including plants) C-terminal ubiquitin interacting motifs. RPN10 in the 26S proteasome is located more specifically at the 19S RP where it connects the base and the lid, the two subcomplexes of the 19S RP.

Arabidopsis RPN10 is encoded by a single gene that can complement yeast *Rpn10* deletion mutant and as predicted, AtRPN10 binds to polyubiquitin chains (van Nocker et al., 1996). Arabidopsis plants (*rpn10-1*) expressing an aberrant form of RPN10 due to a T-DNA insertion accumulate unusually high levels of ubiquitinated proteins indicating defective protein degradation via the 26S proteasome (Smalle et al., 2003). Specifically, *rpn10-1* plants fail to degrade the short-lived transcription factor ABA INSENSITIVE-5 (ABI5) to wild type levels. As a consequence, the *rpn10-1* plants display a range of phenotypes consistent with hypersensitivity to the plant hormone abscisic acid (ABA) (Smalle et al., 2003).

UFD1 was first identified in a yeast mutant screen for defective degradation of short-lived ubiquitin fusion proteins (Johnson et al., 1995). The best known role of UFD1 is to form a heterodimeric adaptor of CDC48 along with nuclear protein localization 4 (NPL4) (Meyer et al., 2000). The CDC48-UFD1-NPL4 complex is essential for endoplasmic reticulum-associated protein degradation (ERAD), a process that drives misfolded or short-lived proteins from ER to polyubiquitination and degradation via the 26S proteasome (Bays and Hampton, 2002; Jarosch et al., 2002). UFD1 consists of two domains, the N-terminal UT3 and the C-terminal UT6 domains. UFD1 binds to mono- and poly-ubiquitin via non-overlapping regions of its UT3 domain that has a remarkable structural similarity to the CDC48 N-terminal region (Park et al., 2005).

The Arabidopsis genome encodes three UFD1 and three CDC48 homologs but no obvious NPL4. While AtUFD1 has not been studied extensively, AtCDC48 has been implicated in membrane fusion during cytokinesis (Rancour et al., 2002). Furthermore

AtCDC48 was found to be regulated by a plant UBX domain-containing protein 1 (PUX1). PUX1 interacts directly with AtCDC48 and works as its negative regulator by inactivating AtCDC48 ATPase activity and stimulating hexamer disassembly (Rancour et al., 2004; Park et al., 2007).

The simplest explanation for UbDKγ4 interaction with proteins involved in 26S proteasome substrate delivery is that UbDKγ4 itself is a 26S proteasome substrate and is directed to degradation. For example, Parkin, a protein responsible for early age Parkinson's onset, is an E3 ligase that contains an N-terminal UBL domain. Parkin is a short-lived protein compared to its ΔUBL mutants (Finney et al., 2003). However, the idea that UbDKγ4 interacts with two proteins that facilitate substrate presentation to the 26S proteasome with the sole purpose of UbDKγ4 degradation is conceivable but not very likely due to the fact that it would be rather counterproductive and incompatible with UFD1 function. UFD1 as substrate delivery mediator seems to operate exclusively in ER-derived 26S proteasome substrates and there is no evidence based on amino acid sequence that indicates that UbDKγ4 is an ER-associated or ER-resident protein.

An alternative and more attractive explanation is that UbDKγ4 uses AtRPN10 as a docking site in the proteasome and assists AtUFD1 to deliver polyubiquitinated proteins targeted for degradation. This scenario is supported by the notion that AtRPN10 and AtUFD1 have non-overlapping interaction sites within UbDKγ4. Both AtRPN10 and AtUFD1 appeared to bind UbDKγ4 via its N-terminus where the UBL1 and 2 are located. However, while the N-terminal 107 amino acid region of UbDKγ4 which includes the UBL1 is necessary for AtUFD1 interaction, AtRPN10 targets a broader region and the absence of UBL1 does not prevent AtRPN10:UbDKγ4 interaction.

As part of a substrate delivery mechanism, UbDKγ4 might facilitate protein degradation via the 26S proteasome in a similar manner as the ubiquitin associated (UBA)/UBL-domain-containing proteins, except that the UbDKγ4 interaction with polyubiquitinated proteins would be indirect via AtUFD1 alone or possibly in complex with CDC48. Another, non-exclusive, possibility is that UbDKγ4 plays a regulatory role by phosphorylating AtUFD1 and AtRPN10 and affects their binding properties and functions.

Phosphorylation of the C-terminus of AtUFD1 most likely affects its affinity for other interacting proteins and not for polyubiquitinated proteins.

In summary, we have identified a new family of protein kinases and show that they may participate in substrate delivery to the 26S proteasome via direct interaction with AtRPN10 and AtUFD1. In addition, we show that AtUFD1 and AtRPN10 can be phosphorylated by UbDKγ4 and have identified *in vitro* phosphorylation sites on AtUFD1.

Acknowledgements

We would like to thank Dr. Norma L. Houston for the assistance with the phylogenetic analysis. This work was funded in part by The National Council for Scientific and Technological Development CNPq - Brazilian government (scholarship to RMG), by the National Science Foundation grant # MCB-0315869 (WFB) and MCB-0419819 (MBG), and by the North Carolina Agricultural Research Service.

References

Abraham RT (2004) PI 3-kinase related kinases: 'big' players in stress-induced signaling pathways. DNA Repair (Amst) 3: 883-887.

Bakkenist CJ, Kastan MB (2003) DNA damage activates ATM through intermolecular autophosphorylation and dimer dissociation. Nature 421: 499-506.

Balla A, Balla T (2006) Phosphatidylinositol 4-kinases: old enzymes with emerging functions. Trends Cell Biol 16: 351-361.

Barylko B, Wlodarski P, Binns DD, Gerber SH, Earnest S, Sudhof TC, Grichine N, Albanesi JP (2002) Analysis of the catalytic domain of phosphatidylinositol 4-kinase type II. J Biol Chem 277: 44366-44375.

Bays NW, Hampton RY (2002) Cdc48-Ufd1-Npl4: stuck in the middle with Ub. Curr Biol 12: R366-371.

Chiang GG, Abraham RT (2004) Determination of the catalytic activities of mTOR and other members of the phosphoinositide-3-kinase-related kinase family. Methods Mol Biol 281: 125-141.

Elsasser S, Finley D (2005) Delivery of ubiquitinated substrates to protein-unfolding machines. Nat Cell Biol 7: 742-749.

Finney N, Walther F, Mantel PY, Stauffer D, Rovelli G, Dev KK (2003) The cellular protein level of parkin is regulated by its ubiquitin-like domain. J Biol Chem 278: 16054-16058.

Fruman DA, Meyers RE, Cantley LC (1998) Phosphoinositide Kinases. Ann Rev Biochem 67: 481-507.

Han GS, Audhya A, Markley DJ, Emr SD, Carman GM (2002) The *Saccharomyces cerevisiae* LSB6 gene encodes phosphatidylinositol 4-kinase activity. J Biol Chem 277: 47709-47718.

Harper JF, Breton G, Harmon A (2004) Decoding Ca^{2+} signals through plant protein kinases. Annu Rev Plant Biol 55: 263-288.

Hartmann-Petersen R, Gordon C (2004) Integral UBL domain proteins: a family of proteasome interacting proteins. Semin Cell Dev Biol 15: 247-259.

Hartmann-Petersen R, Gordon C (2004) Proteins interacting with the 26S proteasome. Cell Mol Life Sci 61: 1589-1595.

Hartmann-Petersen R, Seeger M, Gordon C (2003) Transferring substrates to the 26S proteasome. Trends Biochem Sci 28: 26-31.

Jarosch E, Taxis C, Volkwein C, Bordallo J, Finley D, Wolf DH, Sommer T (2002) Protein dislocation from the ER requires polyubiquitination and the AAA-ATPase Cdc48. Nat Cell Biol 4: 134-139.

Johnson ES, Ma PCM, Ota IM, Varshavsky A (1995) A proteolytic pathway that recognizes ubiquitin as a degradation signal. J Biol Chem 270: 17442-17456.

Kiel C, Serrano L (2006) The ubiquitin domain superfold: structure-based sequence alignments and characterization of binding epitopes. J Mol Biol 355: 821-844.

Kostova Z, Wolf DH (2003) For whom the bell tolls: protein quality control of the endoplasmic reticulum and the ubiquitin-proteasome connection. EMBO J 22: 2309-2317.

Larsen CN, Wang H (2002) The ubiquitin superfamily: Members, features, and phylogenies. J Proteome Res 1: 411-419.

Lou Y, Ma H, Lin W-H, Chu Z-Q, Mueller-Roeber B, Xu Z-H, Xue H-W (2006) The highly charged region of plant β-type phosphatidylinositol 4-kinase is involved in membrane targeting and phospholipid binding. Plant Mol Biol 60: 729-746.

Madura K (2004) Rad23 and Rpn10: perennial wallflowers join the melee. Trends Biochem Sci 29: 637-640.

Manning G, Whyte DB, Martinez R, Hunter T, Sudarsanam S (2002) The protein kinase complement of the human genome. Science 298: 1912-1934.

May MJ, Larsen SE, Shim JH, Madge LA, Ghosh S (2004) A novel ubiquitin-like domain in IκB kinase β is required for functional activity of the kinase. J Biol Chem 279: 45528-45539.

Meyer HH, Shorter JG, Seemann J, Pappin D, Warren G (2000) A complex of mammalian Ufd1 and Npl4 links the AAA-ATPase, p97, to ubiquitin and nuclear transport pathways. EMBO J 19: 2181-2192.

Meyer HH, Wang Y, Warren G (2002) Direct binding of ubiquitin conjugates by the mammalian p97 adaptor complexes, p47 and Ufd1-Npl4. EMBO J 21: 5645-5652.

Mueller-Roeber B, Pical C (2002) Inositol phospholipid metabolism in Arabidopsis. Characterized and putative isoforms of inositol phospholipid kinase and phosphoinositide-specific phospholipase C. Plant Physiol. 130: 22-46.

Naga Prasad SV, Jayatilleke A, Madamanchi A, Rockman HA (2005) Protein kinase activity of phosphoinositide 3-kinase regulates beta-adrenergic receptor endocytosis. Nat Cell Biol 7: 785-796.

Park S, Isaacson R, Kim HT, Silver PA, Wagner G (2005) Ufd1 exhibits the AAA-ATPase fold with two distinct ubiquitin interaction sites. Structure 13: 995-1005.

Park S, Rancour DM, Bednarek SY (2007) Protein domain-domain interactions and requirements for the negative regulation of arabidopsis CDC48/p97 by the plant ubiquitin regulatory X (UBX) domain-containing protein, PUX1. J Biol Chem 282: 5217-5224.

Qian WJ, Goshe MB, Camp DG, 2nd, Yu LR, Tang K, Smith RD (2003) Phosphoprotein isotope-coded solid-phase tag approach for enrichment and quantitative analysis of phosphopeptides from complex mixtures. Anal Chem 75: 5441-5450.

Rancour DM, Dickey CE, Park S, Bednarek SY (2002) Characterization of AtCDC48. Evidence for multiple membrane fusion mechanisms at the plane of cell division in plants. Plant Physiol 130: 1241-1253.

Rancour DM, Park S, Knight SD, Bednarek SY (2004) Plant UBX domain-containing protein 1, PUX1, regulates the oligomeric structure and activity of Arabidopsis CDC48. J Biol Chem 279: 54264-54274.

Ransom WD, Lao P-C, Gage DA, Boss WF (1998) Phosphoglycerylethanolamine posttranslational modification of plant eukaryotic elongation factor 1α. Plant Physiol 117: 949-960.

Shelton SN, Barylko B, Binns DD, Horazdovsky BF, Albanesi JP, Goodman JM (2003) *Saccharomyces cerevisiae* contains a Type II phosphoinositide 4-kinase. Biochem J 371: 533-540.

Smalle J, Kurepa J, Yang P, Emborg TJ, Babiychuk E, Kushnir S, Vierstra RD (2003) The pleiotropic role of the 26S proteasome subunit RPN10 in Arabidopsis growth and development supports a substrate-specific function in abscisic acid signaling. Plant Cell 15: 965-980.

Stevenson-Paulik J, Love J, Boss WF (2003) Differential regulation of two Arabidopsis type III phosphatidylinositol 4-kinase isoforms. A regulatory role for the pleckstrin homology domain. Plant Physiol 132: 1053-1064.

Stevenson JM, Perera IY, Boss WF (1998) A phosphatidylinositol 4-kinase pleckstrin homology domain that binds phosphatidylinositol 4-monophosphate. J Biol Chem 273: 22761-22767.

van Nocker S, Deveraux Q, Rechsteiner M, Vierstra RD (1996) Arabidopsis MBP1 gene encodes a conserved ubiquitin recognition component of the 26S proteasome. PNAS 93: 856-860.

Walters KJ, Goh AM, Wang Q, Wagner G, Howley PM (2004) Ubiquitin family proteins and their relationship to the proteasome: A structural perspective. Biochim Biophys Acta 1695: 73-87.

Wang X, Goshe MB, Soderblom EJ, Phinney BS, Kuchar JA, Li J, Asami T, Yoshida S, Huber SC, Clouse SD (2005) Identification and functional analysis of *in vivo* phosphorylation sites of the Arabidopsis BRASSINOSTEROID-INSENSITIVE1 receptor kinase. Plant Cell 17: 1685-1703.

Wullschleger S, Loewith R, Hall MN (2006) TOR signaling in growth and metabolism. Cell 124: 471-484.

Xue H-W, Pical C, Brearley C, Elge S, Muller-Rober B (1999) A plant 126-kDa phosphatidylinositol 4-kinase with a novel repeat structure. Cloning and functional expression in baculovirus-infected insect cells. J Biol Chem 274: 5738-5745.

Yamada K, Lim J, Dale JM, Chen H, Shinn P, Palm CJ, Southwick AM, Wu HC, Kim C, Nguyen M, Pham P, Cheuk R, Karlin-Newmann G, Liu SX, Lam B, Sakano H, Wu T, Yu G, Miranda M, Quach HL, Tripp M, Chang CH, Lee JM, Toriumi M, Chan MMH, Tang CC, Onodera CS, Deng JM, Akiyama K, Ansari Y, Arakawa T, Banh J, Banno F, Bowser L, Brooks S, Carninci P, Chao Q, Choy N, Enju A, Goldsmith AD, Gurjal M, Hansen NF, Hayashizaki Y, Johnson-Hopson C, Hsuan VW, Iida K, Karnes M, Khan S, Koesema E, Ishida J, Jiang PX, Jones T, Kawai J, Kamiya A, Meyers C, Nakajima M, Narusaka M, Seki M, Sakurai T, Satou M, Tamse R, Vaysberg M, Wallender EK, Wong C, Yamamura Y, Yuan S, Shinozaki K, Davis RW, Theologis A, Ecker JR (2003) Empirical analysis of transcriptional activity in the Arabidopsis genome. Science 302: 842-846.

Ye Y, Meyer HH, Rapoport TA (2001) The AAA ATPase Cdc48/p97 and its partners transport proteins from the ER into the cytosol. Nature 414: 652-656.

Ye Y, Meyer HH, Rapoport TA (2003) Function of the p97-Ufd1-Npl4 complex in retrotranslocation from the ER to the cytosol: Dual recognition of non-ubiquitinated polypeptide segments and polyubiquitin chains. J Cell Biol 162: 71-84.

Supplemental data

Supplemental Figure S1. Phylogeny of the PI3/4K domain.
All PI3/4K domain-containing proteins identified in Arabidopsis (AT), Humans (Hs) and Yeast (Sc) were selected for the present analysis. The PI3/4K domain sequence according to the InterPro (IPR000403) and pfam (PF004540) database was extracted from the complete amino acid sequence of each protein and the redundant entries were eliminated. The present tree represents the consensus phylogenetic tree resulting from Bayesian analysis of PI3/4K domain sequences using MrBayes 3.0. Posterior probability values (>50%) indicate nodal support and are shown above internodes. The different entries are identified by the locus (Arabidopsis), gene product name or protein accession number according to UniProt/Swiss-Prot (http://www.pir.uniprot.org/index.shtml) (Human and Yeast).The observed clustering pattern sorted the three major groups of PI3/4K domain-containing enzymes (labeled as **A**, **B** and **C**). Cluster **A** (*top*): PI kinase-like kinases (PIKK), Cluster **B** (*middle*): PI3K (class I and II), type III PI4K and VPS-like PI3K (class III). Cluster **C** (*bottom*): human and yeast type II PI4Ks along with the putative homologues from Arabidopsis. The accession for the sequences identified by the gene product name are: *Saccharomyces cerevisiae* - P38110 (Sc TEL1), P38111 (Sc MEC1), P22543 (Sc VPS34), P38811 (Sc TRA1), P39104 (Sc PIK1), P37297 (Sc STT4), P35169 (Sc TOR1), P32600 (Sc TOR2) and P42951 (Sc LSB6); *Homo sapiens* - P42356 (Hs PI4KA), P78527 (Hs PRKDC), Q13315 (Hs ATM), Q13535 (Hs ATR), Q9Y4A5 (Hs TRRAP), P48736 (Hs PK3CG), P42338 (Hs PK3CB), P42345 (Hs FRAP), P42336 (Hs PK3CA), Q9UBF8 (Hs PI4KB), Q8TCG2 (Hs PI4KIIB), Q9BTU6 (Hs PI4KIIA), O75747 (Hs PK3C2G), O00329 (Hs PK3CD), Q9Y4A5 (Hs TRRAP) and O00750 (Hs PK3C2B)

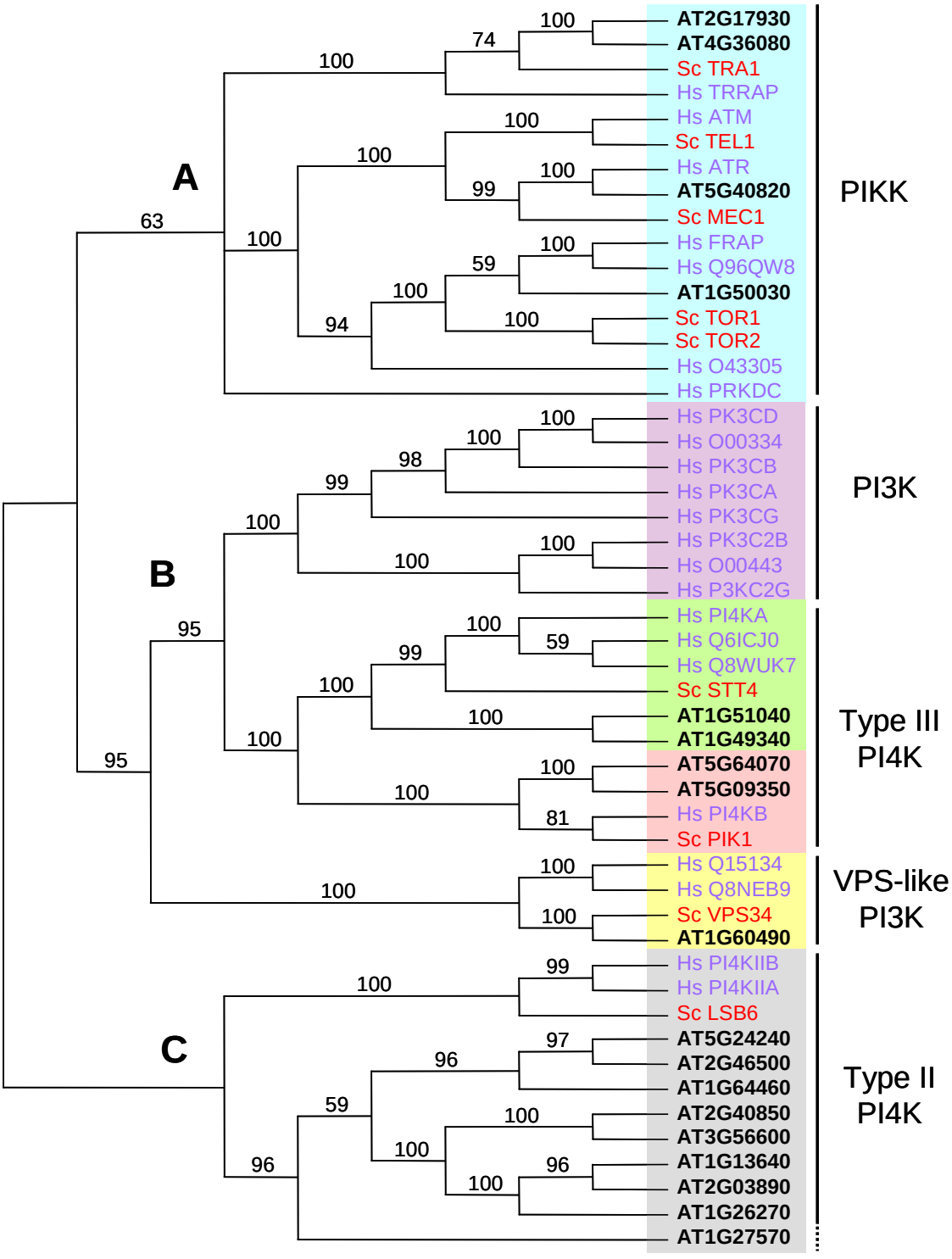
A
B
C
AT2G17930
AT4G36080
Sc TRA1
Hs TRRAP
Hs ATM
Sc TEL1
Hs ATR
AT5G40820
Sc MEC1
Hs FRAP
Hs Q96QW8
AT1G50030
Sc TOR1
Sc TOR2
Hs O43305
Hs PRKDC
PIKK
Hs PK3CD
Hs O00334
Hs PK3CB
Hs PK3CA
Hs PK3CG
Hs PK3C2B
Hs O00443
Hs P3KC2G
PI3K
Hs PI4KA
Hs Q6ICJ0
Hs Q8WUK7
Sc STT4
AT1G51040
AT1G49340
AT5G64070
AT5G09350
Hs PI4KB
Sc PIK1
Type III
PI4K
Hs Q15134
Hs Q8NEB9
Sc VPS34
AT1G60490
VPS-like
PI3K
Hs PI4KIIB
Hs PI4KIIA
Sc LSB6
AT5G24240
AT2G46500
AT1G64460
AT2G40850
AT3G56600
AT1G13640
AT2G03890
AT1G26270
AT1G27570
Type II
PI4K

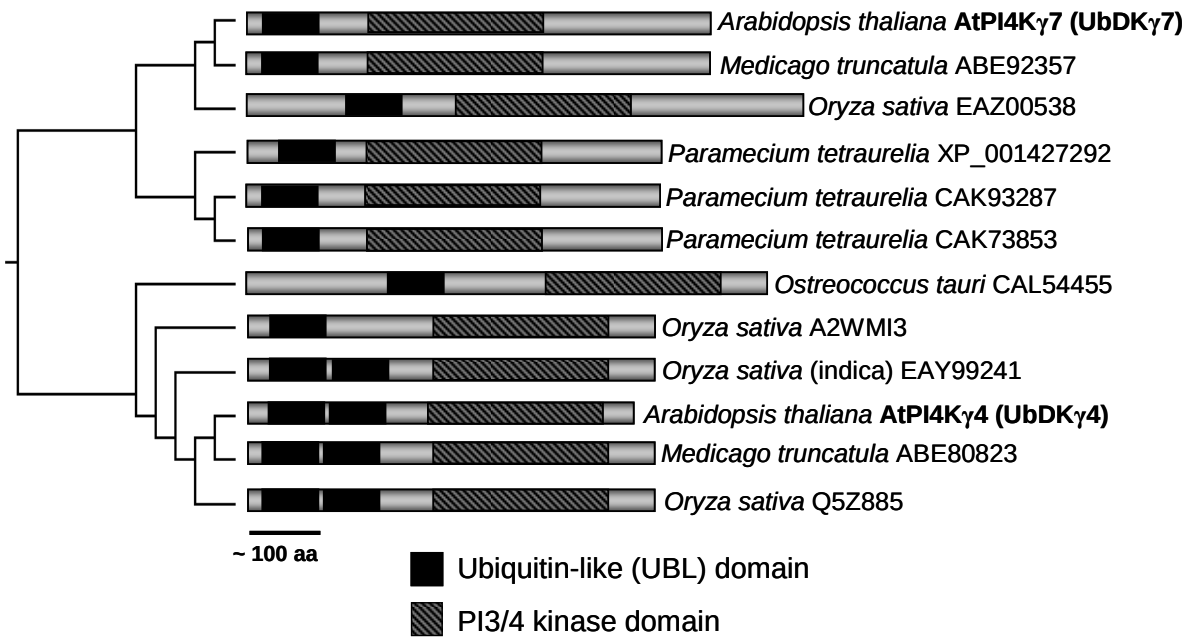

Supplemental Figure S2. PI3/4K domain proteins that contains N-terminal UBL-domains.
Proteins containing PI3/4K (InterPro IPR000403) domain in combination with N-terminal UBL domains (supfam SSF54236 / InterPro IPR000626) are present in other species of plants, including dicots, monocots and green algae, and protozoans. The dendrogram is based on multiple sequence alignments performed with full-length amino acid sequence of AtPI4Kγ4 and γ7 (UbDKγ4 and γ7) and similar proteins from rice (*Oryza sativa*), alfafa (*Medicago truncatula*) and the unicellular green algae *Ostreococcus tauri*, and the unicellular ciliate protozoa *Paramecium tetraurelia*. The alignment and the dendrogram were generated using CLUSTALW at http://www.genome.jp.

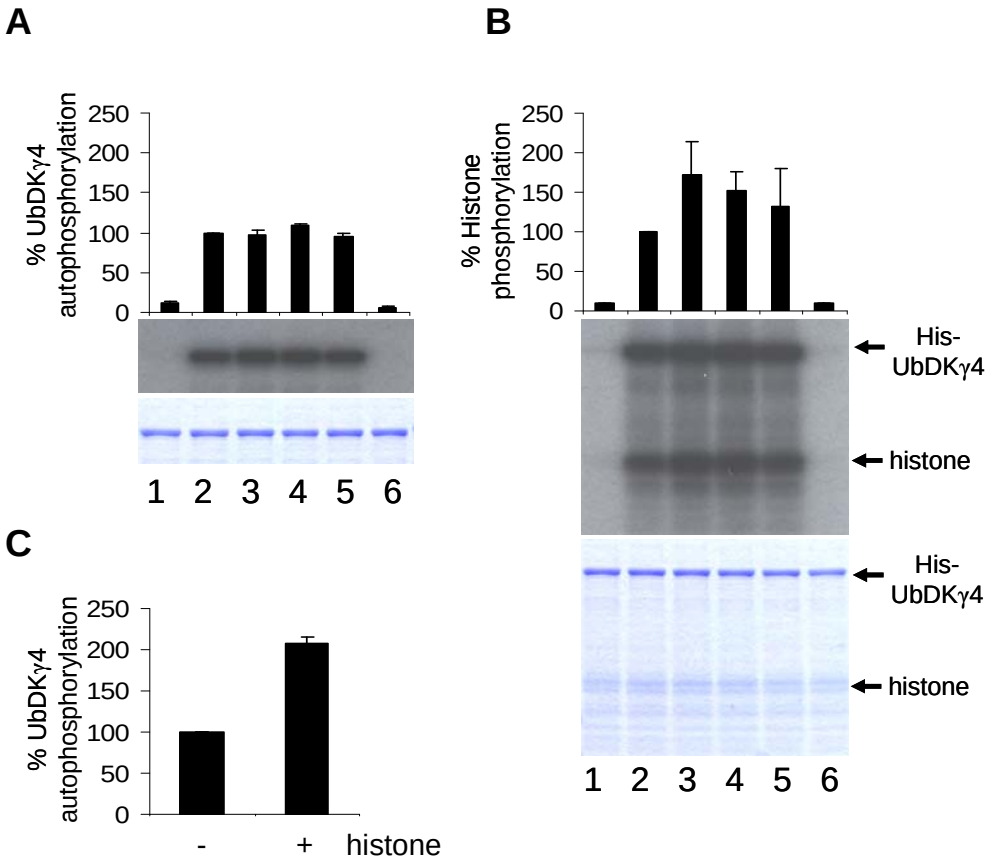

Supplemental Figure S3. UbDKγ4 activity is Ca^{+2}-independent and stimulated by type III histones.
Recombinant His-UbDKγ4 produced in *E. coli* (1 μg) was used in protein phosphorylation reactions containing [γ-^{32}P] ATP in the absence (**A**) or presence (**B**) of 2.5 μg of type III histones as protein substrates. In both *A* and *B* the reaction conditions were: *lane 1*: 30 mM Tris HCl pH 7.5; *lane 2* - 30 mM Tris HCl pH 7.5 and 10 mM $MgCl_2$; *lane 3*: 30 mM Tris HCl pH7.5, 10 mM $MgCl_2$ and 1 mM EGTA; *lane 4* : 30 mM Tris HCl pH 7.5, 10 mM $MgCl_2$, 1 mM EGTA and 1.01 mM $CaCl_2$; *lane 5*: 30 mM Tris HCl pH 7.5, 10 mM $MgCl_2$, 1 mM EGTA and 1.1 mM $CaCl_2$; and *lane 6*: 30 mM Tris HCl pH 7.5, 1 mM EGTA and 1.1 mM $CaCl_2$. The products of the reactions were resolved by SDS-PAGE. The gel was stained with Coomassie blue and dried (*lower panels*). The radiolabeled proteins were revealed by autoradiography (*upper panels*) and quantified by scintillation. The bar graphs representing (**A**) UbDKγ4 autophosphorylation and (**B**) histone phosphorylation were plotted as percentage activity compared to the reaction in *lane 2* (100%) within each assay. The graph in (**C**) represents the percentage activity comparing UbDKγ4 autophosphorylation in the absence (100%) or presence of 2.5 μg of type III histone in the reaction condition as in *lanes 2* (**A** and **B**). The gel and the autoradiogram images are representative results from two replicates and the bar graphs show average percentages with standard deviation of values from the two replicated experiments.

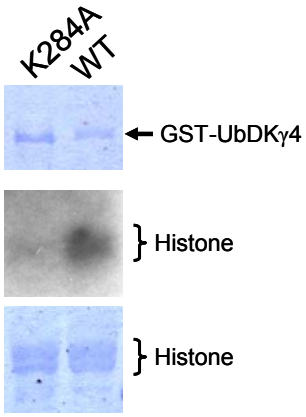

Supplemental Figure S4. Mutating Lys 284 to Ala (K284A) in the ATP-binding site abolishes UbDKγ4 activity.
Protein phosphorylation assays containing 1 µg of wild type and mutated enzyme (K284A) were carried with [γ-^{32}P] ATP in the presence of 2.5 µg of type III Histone. The products of the reactions were resolved by SDS-PAGE. The ^{32}P-labeled proteins were revealed by autoradiography (*upper panels*) and the protein amounts by Coomassie blue staining (*lower panels*).

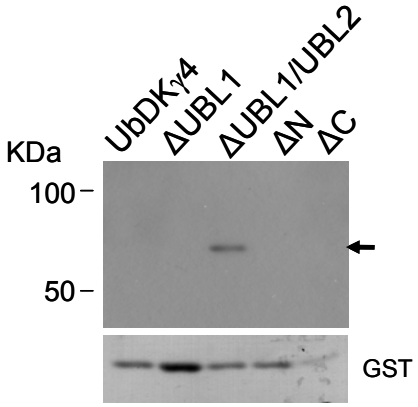

Supplemental Figure S5. Full-length His-UbDKγ4 and all truncations except ΔUBL1/UBL2 do not interact with GST.
GST immobilized on glutathione-Sepharose beads was used as bait in pull-down assays containing full-length His-UbDKγ4 and truncations ΔUBL1, ΔUBL1/UBL2, ΔN, and ΔC as prey. In all binding reactions, immobilized GST and prey were incubated in an approximate 1:2 molar ratio. The bound proteins (indicated by the arrows) were revealed by immunoblotting with anti His-tag antibody (*upper panel*). GST-tagged proteins were visualized by Amido Black staining of the membrane (*lower panel*).

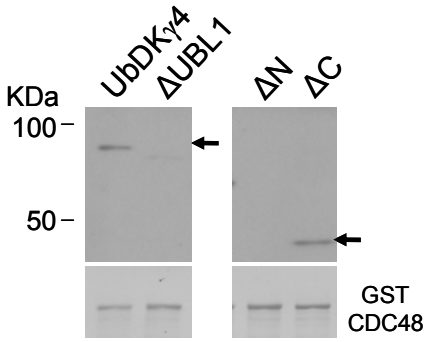

Supplemental Figure S6. AtCDC48 and AtUFD1 share similar binding properties toward UbDKγ4.
GST-CDC48 immobilized on glutathione-Sepharose beads was used as bait in pull-down assays containing His-UbDKγ4 full-length or the truncations, ΔUBL1, ΔUBL1/UBL2, ΔN and ΔC as prey. In all binding reactions immobilized bait and prey were incubated in a 1:2 molar ratio. The bound proteins were revealed by immunobloting with anti His-tag antibody (*upper panel*). Proteins were visualized by Amido Black staining of the membrane (*lower panel*). The *input* of the His-tagged proteins used in the binding assay was the same as indicated in Figure 6D.

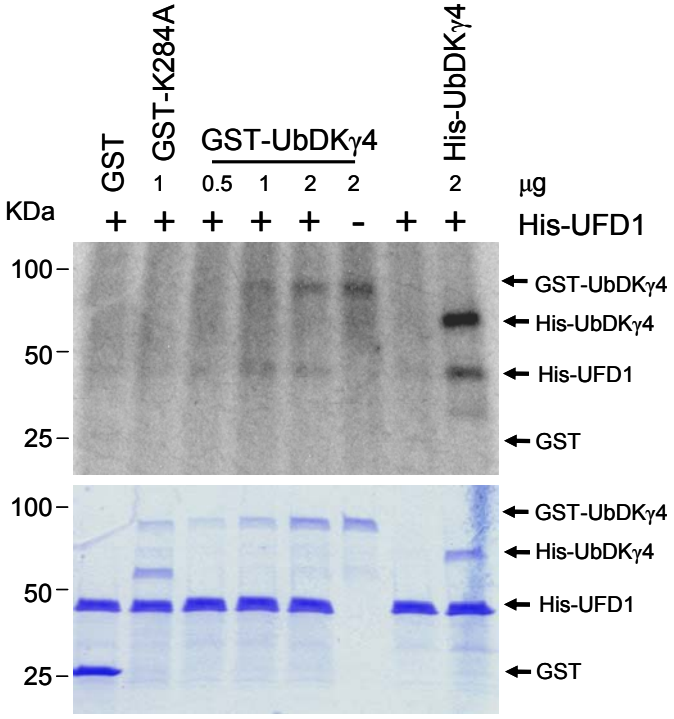

Supplemental Figure S7. AtUFD1 is phosphorylated by both GST- and His-tagged UbDKγ4.
Protein phosphorylation assays were performed with different amounts of GST-UbDKγ4 as indicated using 3 μg of His-AtUFD1 as substrate. His-AtUFD1 phosphorylation was detected only in the presence of functional UbDKγ4 (both as the GST- and His-tag fusion protein). The products of the reactions were resolved by SDS-PAGE. The ^{32}P-labeled proteins were revealed by autoradiography (*upper panel*) and the protein amounts by Coomassie blue staining (*lower panel*).

Suplemental Table S1 List of the DNA fragments for the expression of recombinant proteins and the primers used in the PCR amplifications and cloning.

DNA fragment	Locus (clone ID[a])	Forward primer (5' → 3')	Reverse primer (5' → 3')
pGEM®-T Easy cloning[b]			
AtPI4Kγ1	At2g40850	CGGGATCCATGAATTGCTTGGCTACGACCATA	CGGGATCCTCAAATTTCGCAGGAGCATCCTAA
AtPI4Kγ4	At2g46500	CGGGATCCATGTCATCAGCTGGTGTTGCGTTA	CGGGATCCTTAGTGTTCCTGAGAGTGATCGAGAT
AtPI4Kγ7	At2g03890	AAA*CTGCAG*ATGTCGAGGAACTTAGA	AAACTGCAGTCTCAAAACTGGCATGAA
pENTR/SD/D-TOPO cloning			
AtPI4Kγ4	At2g46500	CACCATGTCATCAGCTGGTGTTGC	TTAGTGTTCCTGAGAGTG
UFD1	At2g21270	CACCATGTTTTTCGATGGATACCATTATC	TCAACCCCTCAATGAATACTTC
RPN10	At4g38630 (U09430)	CACCATGGTTCTCGAGGCGACTATG	TTATTGAGACTCTCAGATCC
MPPβ	At3g02090 (U22122)	CACCATGGCGATGAAGAATCTACTG	TTAGTACCGGTTCCAGTAGGTTC
MS5	At5g48850 (U60768)	CACCATGGAGAGAAGCTTGAAGAAG	CTAGCAAACTAATGTATTTC
RPP0C	At3g09200 (U09559)	CACCATGGTGAAAGCAACTAAGGC	CTACTCTTCATCGAACAAAC
AtPI4Kγ4 ΔUBL1	-	CACCATGCTCTCTGATCTTCAGGTTC	TTAGTGTTCCTGAGAGTG
AtPI4Kγ4 ΔUBL1/UBL2	-	CACCATGGCTAAAGTTCGAGTTAAGCC	TTAGTGTTCCTGAGAGTG
AtPI4Kγ4 ΔN	-	CACCATGAATTCTCCGGTCAGGTC	TTAGTGTTCCTGAGAGTG
AtPI4Kγ4 ΔC	-	CACCATGTCATCAGCTGGTGTTGC	TTAAGAATTCCCACTTTTAAGTCCAT

[a] Full-length cDNA clones ordered from ABRC made in pUNI51.

[b] The primers for pGEM®-T Easy cloning were designed to contain restriction enzyme sites shown underlined in the primer sequence (AtPI4Kγ1and γ4 – *Bam*HI and AtPI4Kγ7 – *Pst*I)

CHAPTER 3

Characterization of transgenic NT1 tobacco cells and Arabidopsis plants over-expressing *UbDKγ4*-derived polypeptides

Abstract

Ubiquitin-like domain kinase γ4 (*UbDKγ4*) is one of many genes up-regulated during the unfolded protein response (UPR) in *Arabidopsis thaliana*. *UbDKγ4* encodes a protein (Ser/Thr) kinase originally identified as a putative type II phosphatidylinositol 4-kinase. *In vitro*, UbDKγ4 interacts with and phosphorylates proteins involved in controlled protein degradation namely, UFD1 (ubiquitin fusion degradation protein 1) and RPN10 a non-ATPase component of the proteasome regulatory particle. To investigate the role of UbDKγ4 *in vivo*, we generated transgenic NT1 tobacco cell lines and *Arabdopsis thaliana* plants that over-express *UbDKγ4*-derived polypeptides. Here we report the initial characterization of both transgenic cells and plants. Under normal growth conditions, cells and plants over-producing *UbDKγ4*-derived polypeptides display no obvious phenotype, indicating the absence of pleiotropic effects. However, over-expression of GFP fused UbDKγ4 ΔC truncation (GFP-γ4ΔC) or UbDKγ4 inactive mutant (GFP-γ4KD) in transgenic plants results in hypersensitivity to treatment with tunicamycin, an antibiotic that induces UPR. Our working model is that producing either the γ4ΔC or γ4KD peptides disrupts the normal substrate delivery system that drives ER-associated protein degradation substrates to degradation via 26S proteasome.

Introduction

Ubiquitin-like domain kinases (UbDKs) are protein kinases found in Arabidopsis that belong to the family of the phosphoinositide kinase-related kinases (PIKKs). UbDKs are characterized by the presence of one or two N-terminal ubiquitin-like domains. UbDKγ4, the best studied UbDK, interacts with and phosphorylates both ubiquitin fusion degradation protein (UFD1) and RPN10, a non ATPase component of the 19S regulatory particle of the 26S proteasome *in vitro* (**Chapter 2**). Both UFD1 (Meyer et al., 2002; Ye et al., 2003; Park et al., 2005) and RPN10 (van Nocker et al., 1996; van Nocker et al., 1996; Fu et al., 1998) bind to different forms of ubiquitin and are involved in the delivery of ubiquitinated proteins to the proteasome for degradation.

The interaction of UbDKγ4 with UFD1 and RPN10 suggests that UbDKγ4 is involved in regulating protein degradation via the ubiquitin/proteasome system. Our working hypothesis is that UbDKγ4 regulates degradation of proteins derived from the endoplasmic reticulum (ER)-associated protein degradation (ERAD) pathway. The ERAD pathway is part of a quality control system that prevents unfolded or misfolded proteins that are translocated into the ER from progressing further into the secretory pathway. For example, many ERAD targets are translocated to the cytosol ("retrotranslocation"), ubiquitinated and degraded by the 26S proteasome (for review [Tsai et al., 2002]).

Two lines of evidence support our hypothesis: *i*) UFD1, a UbDKγ4 interacting partner and substrate, has been directly implicated in ERAD (Jarosch et al., 2002; Verma et al., 2004). More specifically, UFD1 participates in the retrotranslocation of ERAD-substrates as part of a heterodimeric (UFD1/NPL4) adaptor of CDC48, an AAA-ATPase that forms a homohexamer with chaperone activity. *ii*) *UbDKγ4* is one of many genes up-regulated during the unfolded protein response (UPR) in Arabidopsis. *UbDKγ4* transcript increased 5.4 and 11.5 fold in seedlings after 5 h treatment with tunicamycin (Tm) and dithiothreitol (DTT), respectively (Martinez and Chrispeels, 2003). Tm and DTT promote protein misfolding and trigger UPR which presumably activates ERAD. Tm in particular causes protein misfolding by inhibiting glycosylation of asparagine and preventing the production of (N)-linked glycoproteins synthesized in the ER.

To begin testing our hypothesis *in vivo*, we first validated UbDKγ4 gene expression data by Martinez and Chrispeels (2003) using Real Time RT-PCR. Second, we generated plant binary vectors containing different constructs derived from UbDKγ4 and used them to transform NT1 tobacco cells and Arabidopsis plants. Although we could not overproduce the full-length protein, we predicted that over-expressing *UbDKγ4*-derived polypeptides would affect the UPR at the level of protein degradation.

We were able to stably transform tobacco cells and Arabidopsis plants with a construct carrying the UbDKγ4 N-terminus (referred here as γ4ΔC). γ4ΔC contains the UBL domain 1 (UBL1) required for the UbDKγ4-UFD1 interaction but lacks the C-terminal catalytic domain (the phosphoinositide 3/4-kinase [PI3/4K] domain) (**Chapter 2**). We also obtained transformed Arabidopsis over-expressing a kinase inactive UbDKγ4 (referred here

as γ4KD for kinase dead). γ4KD is a full-length UbDKγ4 with a mutation (K284A) in the ATP binding site (**Chapter 2**). We anticipated that both γ4ΔC and γ4KD peptides would act as dominant negatives for UFD1 function. Here we show that over-expression of *γ4ΔC* and *γ4KD* in transgenic Arabidopsis causes hypersensitivity to Tm. Our results suggest that UbDKγ4 is involved in the UPR in plants, possibly in concert with UFD1 via ERAD regulation.

Methods

Cloning

The cDNA encoding the UbDKγ4 WT (At2g46500), K284A mutant and the UbDKγ4 truncations ΔC and ΔN cloned into the pENTR/SD/D-TOPO (Invitrogen) vectors (**Chapter 2**) were recombined into pK7WGF2 binary plasmids (Functional Genomics Division of the Department of Plant Systems Biology, Gent, Belgium) for production of GFP fusion proteins under the control of a cauliflower mosaic virus 35S promoter. The orientation of the resulting plasmids was verified by PCR and DNA sequencing.

NT1 Tobacco cells: maintenance, transformation and selection

Tobacco cell culture, transformation and growth analysis were performed according to Im et al. (2007). Briefly, tobacco cells (*Nicotiana tabacum* NT-1 cells) were maintained in 25 mL of liquid culture medium (Perera et al., 2002) in 125-mL Erlenmeyer flasks at 125 rpm and 27°C and subcultured weekly with a 6% (v/v) inoculum. To monitor cell growth, two replicate 25-mL cultures were harvested at 2, 4, 6, 8 and 10 d after transfer. The cells were collected by low-speed centrifugation (~500*g* for 3 min), the supernatant removed by pipetting, and the cells' fresh weight was measured.

The recombinant binary plasmids (pK7WGF2 γ4ΔC, pK7WGF2 γ4ΔN, pK7WGF2 γ4KD, and pK7WGF2 γ4WT) were transformed into *Agrobacterium tumefaciens* EHA105 by the freeze-thaw method (Chen et al., 1994). NT-1 cells were transformed using

Agrobacterium-mediated gene transfer as described (Perera et al., 2002). Selected kanamycin-resistant microcalli were used to establish suspension cultures that were maintained by weekly subculture in NT-1 medium containing 50 μg mL^{-1} kanamycin.

Arabidopsis plants: maintenance, transformation and selection

Arabidopsis (*Arabidopsis thaliana* Columbia-0 (Col-0)) plants were grown to maturity under long-day conditions until primary inflorescence stems had emerged. Plants were transformed by the floral dip method with *Agrobacterium* containing the appropriate plasmid as described by Clough and Bent (1998). Selection of transformed plants was done according to Perera et al. (2006). Briefly, plants were grown until seed set. Seeds were harvested and dried and stored at –20°C. For selection, surface-sterilized seeds were plated on plates containing 1× MS salts, 1% sucrose, MES buffer, pH 5.7, 0.8% type M agar (Sigma, Saint Louis, MO), and 50 μg·mL^{-1} kanamycin. Plants were grown for 2 weeks, and kanamycin-resistant seedlings (from lines segregating 3:1 for kanamycin resistance) were transferred to soil, grown to maturity, and allowed to self-fertilize to produce T_2 generation seed. Homozygous transformant lines were selected in T_3 generation and stable expression of the transgene was determined by RT-PCR and by immunoblotting as described below.

Tunicamycin treatment

Tunicamycin (Sigma, Saint Louis, MO) was prepared in dimethyl sulfoxide (DMSO) at 10 mg·mL^{-1}. For the gene expression analysis the Tm treatment was performed according to Martínez and Chrispeels (2003). Arabidopsis Col-0 surface-sterilized seeds were germinated and grown in 1× MS salts, 1% sucrose, MES buffer, pH 5.7. The seedlings (~25/flask) were cultivated for 6 days in 13 mL of liquid medium in 50 mL flasks on a rotary shaker (85 rpm) under a short day cycle (8 h light and 16 h dark). Seedlings were then treated with 6.5 μL of DMSO or DMSO plus Tm, added to a final concentration of 5 μg·mL^{-1}. The seedlings were harvested at 0, 2.5, 5, and 10 h after treatment, immediately frozen in liquid N_2, ground to a fine powder and stored at – 80 ºC until use.

Tm tolerance assay was performed according to Wang et al. (2007). Surface-sterilized Arabidopsis Col-0 seeds were sown on plates containing 1× MS salts, 1% sucrose, MES buffer, pH 5.7, 0.8% type M agar (Sigma, Saint Louis, MO) supplemented with 0.03 $\mu L \cdot mL^{-1}$ of DMSO or DMSO plus Tm, added to a final concentration of 0.1 $\mu g \cdot mL^{-1}$. After 6 days the treated seedlings were transferred to plates containing fresh non-supplemented medium. The plates were photographed 3 and 7 days after transferring. During germination in supplemented medium and recovery on non-supplemented medium the plants were kept under a short day cycle (8 h light and 16 h dark). The experiment was terminated after18 days, when the seedlings were harvested for analysis of chlorophyll content.

Pigments were extracted using 80 % acetone for 2 h. The chorophyll content was estimated from the absorbance measurement at λ 663 nm. Data were normalized based on number of seedlings/mL of extraction solution. The comparison between DMSO or DMSO plus Tm treatment was expressed as % reduction of chlorophyll content.

RNA extraction and RT-PCR

Total RNA isolation from seedlings and reverse transcription (RT) was performed as described in the Appendix 2, except that here Omniscript Reverse transcriptase (Qiagen, Hilden, Germany) was used for cDNA synthesis. Real time RT-PCR and data analysis were done also as described in the Appendix 2, except that here the DNA polymerase/Syber green dye reaction mix used was from Stratagene (La Jolla, CA). The semi-quantitative RT-PCRs (Figure 6) were performed with 100 ng cDNA equivalents and 10 pmol of each primer and with Hot-Start Taq ^{TM} (Denville Scientific, Metuchen, NJ). Real time and semi-quantitative RT-PCR primer sets are described in Table 1.

Protein isolation, pull-downs, electrophoresis and immunoblotting

Extraction and fractionation of proteins from NT1 cells were performed as described by Perera et al.(2002). Recombinant GST-fused proteins used in the pull-downs were produced in *E. coli* and affinity purified as described in **Chapter 2**. Pull-downs assays

Table 1. List of primers used in the semi-quantitative RT-PCR.

Target sequence	Forward primer (5' → 3')	Reverse primer (5' → 3')
GFP-UbDKγ4[a]	TGACCCTGAAGTTCATCTGCACCA	ACTCAAAGTTCTTCTCCACCGGCT
UbDKγ4 [b]	GCTTTCTTTGGAGCCGGTAGTT	TTGACCTGACCGGAGAATTCC
UbDKγ7 [b]	AAAGCGCAAACGAACAGCTT	CCGGTCCAAGTAACTCTTGGAA
Actin 2/8[a]	ACCTTGCTGGACGTGACCTTACTGAT	GTTGTCTCGTGGATTCCAGCAGCTT
Actin 2/8[c]	GGTAACATTGTGCTCAGTGGTGG	AACGACCTTAATCTTCATGCTGC

[a] Primer sets used in the semi-quantitative RT-PCR.
[b] Primer sets used in both Real time and semi-quantitative RT-PCR.
[c] Primer sets used in the Real Time RT-PCR.

were also done according to **Chapter 2** except that the NT1 cells were homogenized in 3 volumes of cold buffer containing 50 mM Tris pH 7.5, 100 mM KCl, 0.05 % Triton X100, supplemented with 1 mM phenylmethylsulfonyl fluoride and 10 $\mu g \cdot mL^{-1}$ leupeptin.

Protein extraction from Arabidopsis seedlings for immunoblotting was performed as follows. Frozen seedlings ground in liquid N_2 were mixed with extraction buffer (50 mM Tris acetate pH 7.9, 100 mM potassium acetate, 1 mM ethylenediamine tetraacetic acid (EDTA), 1 mM dithiothreitol and 20 % glycerol) supplemented with 1 mM phenylmethylsulfonyl fluoride and 10 $\mu g \cdot mL^{-1}$ leupeptin. Ground tissue and extraction buffer were combined at a ratio of 0.2 mL per 100 mg of tissue e, vortexed vigorously and centrifuged at 12,000 *g*, 10 min at 4 ºC. Supernatant was quantified (Bradford method) and used for immunoblotting.

Protein electrophoresis and immunoblotting were performed as described in **Chapter 2**. Monoclonal anti-GFP (Clontech, Mountain View, CA) and polyclonal anti-γ4 (Figure 2) antibodies were used at 1:1,000 dilution and polyclonal anti-ubiquitin (Sigma, Saint Louis, MO) antibody at 1:100 dilution. Immunoblotting using antibody against BiP (ID9; Stressgen, Victoria, British Columbia, Canada) was performed according to Im et al. (2007).

Microscopy

Confocal fluorescence images were acquired as per Im et al.(2007).

Results

Up-regulation of UbDKγ4 gene expression

To validate the observation that *UbDKγ4* transcript levels increase in response to UPR-inducing treatments (Martinez and Chrispeels, 2003), we replicated the experiment described by Martinez and Chrispeels (2003) and performed Real Time RT-PCR analysis of gene expression. We used primer sets designed for *UbDKγ4*, *UbDKγ7* and *Actin 2/8*, the chosen reference gene. The *UbDKγ4* transcript went up in DMSO + Tm treated seedlings by

2.5 h after treatment (~4.5-fold) and was sustained at similar level at 5 h. At 10 h after treatment the *UbDKγ4* transcript was still significantly higher (3.75-fold increase) compared to the 0 h reference sample (Figure 1A). Negligible changes in the transcript levels of *UbDKγ7* were observed in response to DMSO + Tm treatment or in the transcript levels of both *UbDKγ4* and *UbDKγ7* in response to the control treatment (DMSO) (Figure 1A and B). The results reported here confirm that *UbDKγ4* but not *UbDKγ7* is up-regulated in response to an acute Tm treatment. It is noteworthy that *UbDKγ4* does not have any obvious *cis*-acting regulatory element such as an ER stress response element (ERSE) in its promoter (Urade, 2007).

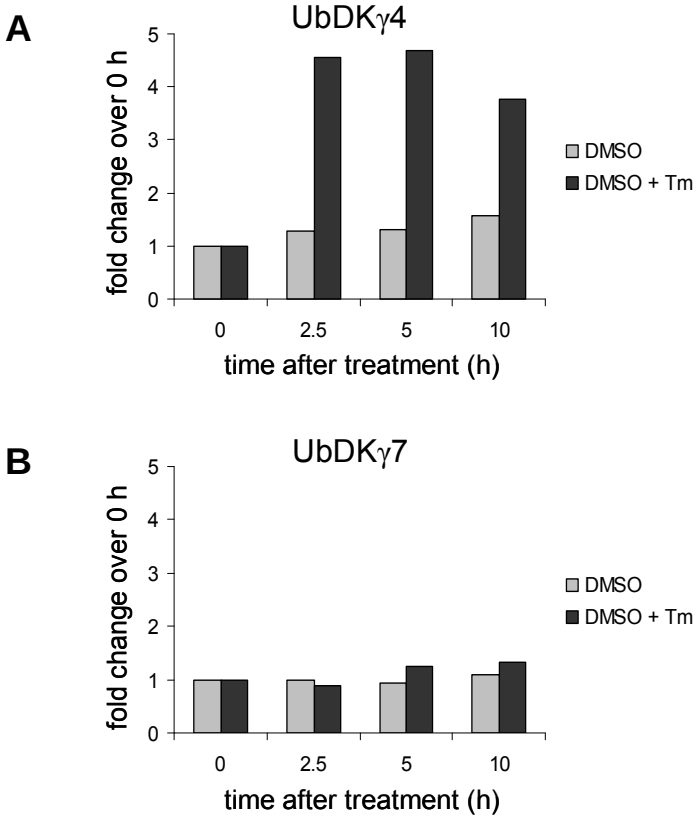

Figure 1. Up-regulation of UbDKγ4 gene expression in response to Tm treatment.
Real Time RT-PCR analysis of *UbDKγ4* (**A**) and *UbDKγ7* (**B**) expression in response to Tm treatment. Raw C_T values were normalized with actin transcript levels and calculated to fold change in comparison to the reference sample ($2^{-\Delta\Delta Ct}$ method (Livak and Schmittgen, 2001)). The bars represent the fold change (average of duplicated reactions) in transcript abundance 2.5, 5 and 10 h after treatment (DMSO or DMSO + Tm) relative to the transcript level at 0 h (reference sample).

Characterization of Tobacco cells overexpressing GFP-γ4ΔC

Four different constructs derived from the UbDKγ4 sequence and the green fluorescent protein (GFP) were made for plant transformation (Figure 2). In order to test the efficacy of the constructs, we performed *Agrobacterium*-mediated transformation of *Nicotiana tabacum* (NT1) cells. After two attempts, 11 independent, kanamycin-resistant calli were selected from the transformation of NT1 cells using the γ4ΔC construct. All 11 calli were confirmed by immunoblotting to overproduce GFP-γ4ΔC protein (data not shown); however, no transformation events were obtained using GFP-γ4ΔN, GFP-γ4KD or GFP-γ4WT. Two independent calli were used to start suspension cultures, designated NTγ4ΔC-1 and NTγ4ΔC-5 (Figure 3A).

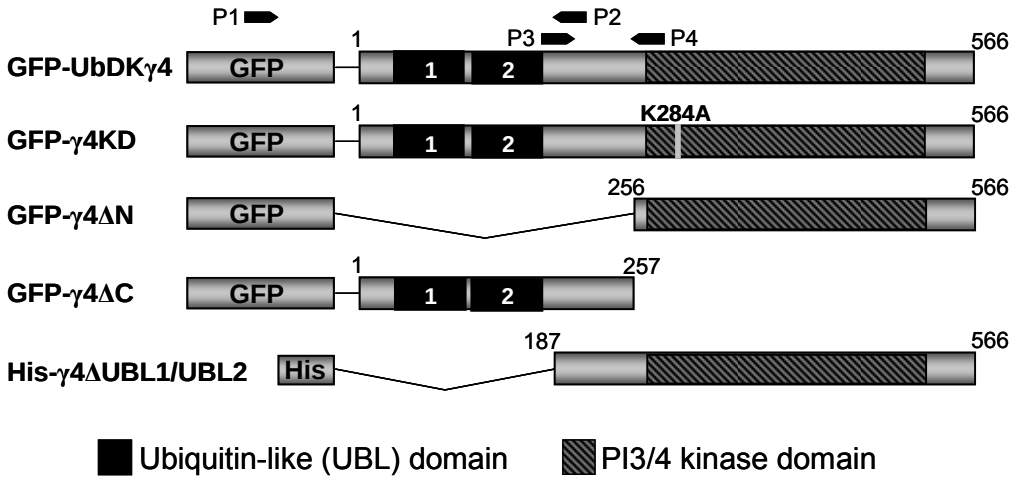

Figure 2. Expression cassettes derived from UbDKγ4.
Wild type UbDKγ4 (GFP-UbDKγ4), UbDKγ4 K284A mutant (GFP-γ4KD) and UbDKγ4 ΔN and ΔC truncations (GFP-γ4ΔN and GFP-γ4ΔC, respectively) were cloned into the expression cassettes generated for plant transformation. They were constructed in pK7WGF2 plasmids which are designed to express N-terminal GFP fusion proteins under control of the 35S CaMV promoter. The construct His-γ4ΔUBL1/UBL2 was cloned in a pET 41 plasmid for production of recombinant (6×His-tagged) protein in *E. coli*. Affinity purified His-γ4ΔUBL1/UBL2 was used to produce polyclonal antibodies against UbDKγ4. P1-P2, and P3-P4 were primer sets used to detect *UbDKγ4*-derived transcripts via RT-PCR (Table 1). The GFP and 6×His-tag representations in the diagram are not in proportion with the linear representations of the proteins.

NTγ4ΔC-1 and NTγ4ΔC-5 suspension culture lines showed no obvious morphological phenotype. However, the growth of both cell lines was slightly slower compared to the wild type (Figure 3B). During a 10-d culture cycle the largest difference in fresh weight was observed at d 6. Despite their slower rate of growth, by d 10 the differences in fresh weight were not statistically significant.

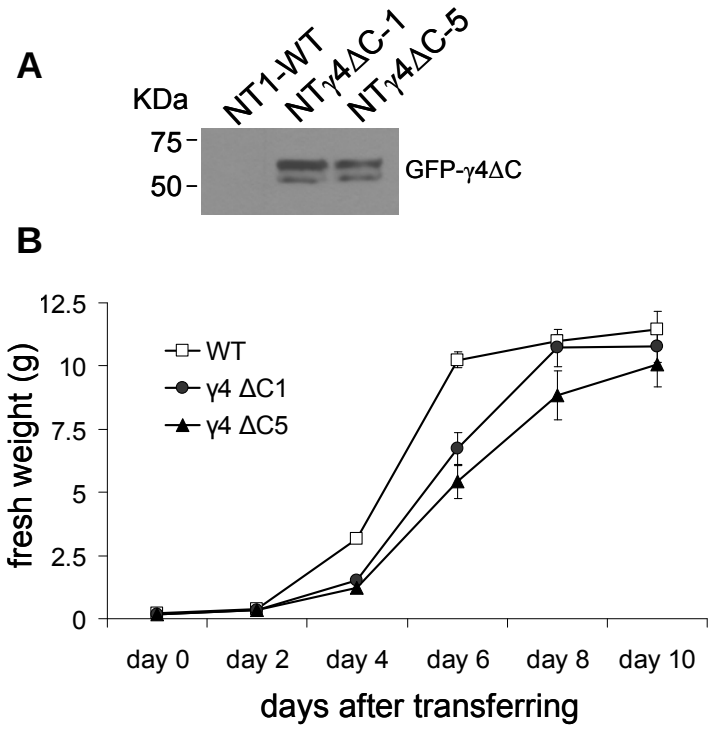

Figure 3. NTγ4ΔC cells grow slightly slower than wild type NT1 cells.
A. Extracts (45 µg) from wild type (NT1-WT) and transgenic (NTγ4ΔC) cells were analyzed by SDS-PAGE followed by immunoblotting with monoclonal anti-GFP antibodies. **B.** Wild type (WT) and transgenic (γ4ΔC) cells were cultivated side-by-side for 10 d and the growth curve was determined by measurement of fresh weight on the indicated d. The data plotted are the mean +/- std deviation of duplicate values from 2 independent experiments. NTγ4ΔC-1 and NTγ4ΔC-5 are two independent transgenic cell lines.

To further investigate the effect of GFP-γ4ΔC over-expression in NT1 cells, we analyzed the levels of ubiquitin monomers, oligomers and ubiquitinated proteins in the extracts of transgenic cell lines versus the wild type. Total protein extracts were resolved by SDS-PAGE, blotted and probed with an anti-ubiquitin antibody (Figure 4). No obvious

difference was detected. We also analyzed the levels of ubiquitinated protein capable of interacting with RPN10 and UFD1 in GST pull down assays (Figure 5). As expected, GST-RPN10 and GST-UFD1 pulled down high molecular weight ubiquitinated protein from wild type extract. Again, no obvious difference was detected when the amount of ubiquitinated protein recovered by these proteins in the extracts from the transgenic cell lines was compared to that recovered from the wild type lines. Of interest, both GST-RPN10 and GST-UFD1 bound preferentially to ubiquitinated protein (high molecular weight, > 150 kDa) relative to short ubiquitin chains (2, 3, 4, 5×Ub) or monomeric ubiquitin. In addition, this is the first report of interaction of a plant UDF1 homolog with ubiquitinated proteins.

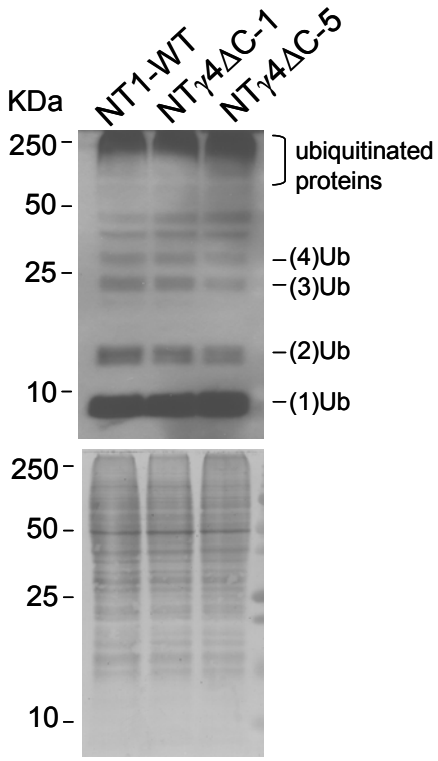

Figure 4. NTγ4ΔC cells accumulate wild type levels of ubiquitin.
Total lysate (15 μg) from wild type (NT1-WT) and transgenic (NTγ4ΔC) cells were analyzed by SDS-PAGE followed by immunoblotting with polyclonal anti-Ubiquitin antibody (*upper panel*). Protein was visualized by Amido Black staining of the blot (*lower panel*).

Levels of the chaperone BiP, an ER resident protein up-regulated during UPR, were also analyzed. Membrane fractions from transgenic and wild type cells harvested at 4 and 6 d after transferring were probed with an anti-BiP antibody. The relative abundance of BiP in the extract was indistinguishable in the different lines (Figure 6). Taken together, the data described above indicate that the NT1 cells expressing GFP-γ4ΔC do not display detectable pleiotropic effects associated with levels of ubiquitin and BiP under normal growth conditions.

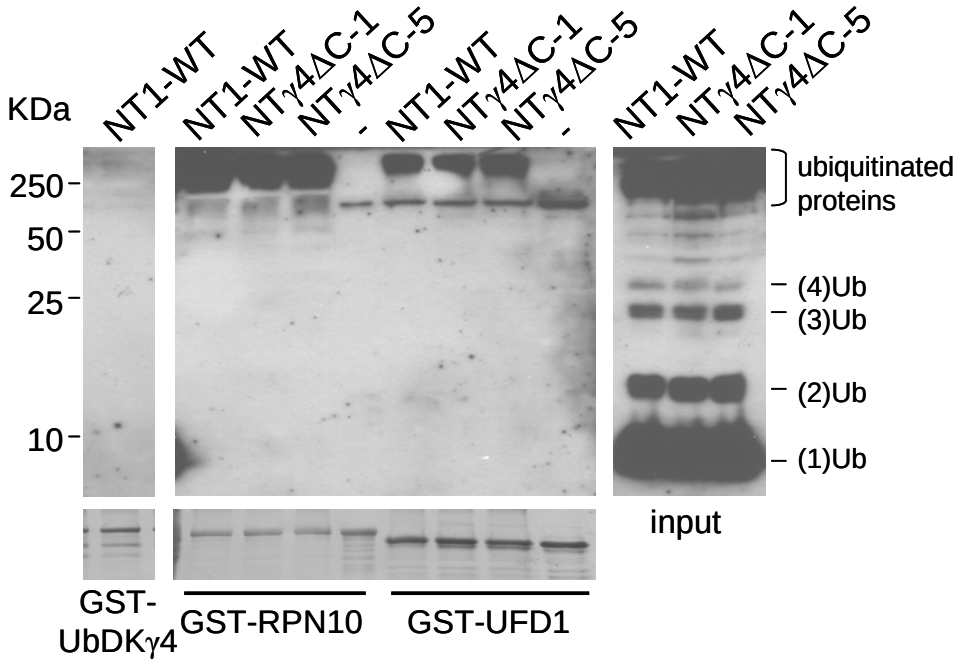

Figure 5. RPN10- and UFD1-GST pull downs recovered comparable amounts of ubiquitinated proteins from NT1-WT and NTγ4ΔC cells extracts.
GST-RPN10 and GST-UFD1 immobilized on glutathione-Sepharose beads were used as bait in pull-down assays containing extracts from wild type (NT1-WT) and transgenic (NTγ4ΔC) cells. The bound proteins were probed by immunoblotting with polyclonal anti-Ubiquitin antibodies (*upper panel*). Proteins were visualized by Amido Black staining of the membrane (*lower panel*). GST-UbDKγ4 pull downs with wild type (NT1-WT) cell extract and pull downs with no extract (-) are shown as controls. The *input* panel in the right corresponds to 20% of the amount of extract originally used in each binding assay. NTγ4ΔC-1 and NTγ4ΔC-5 are two independent transgenic cell lines

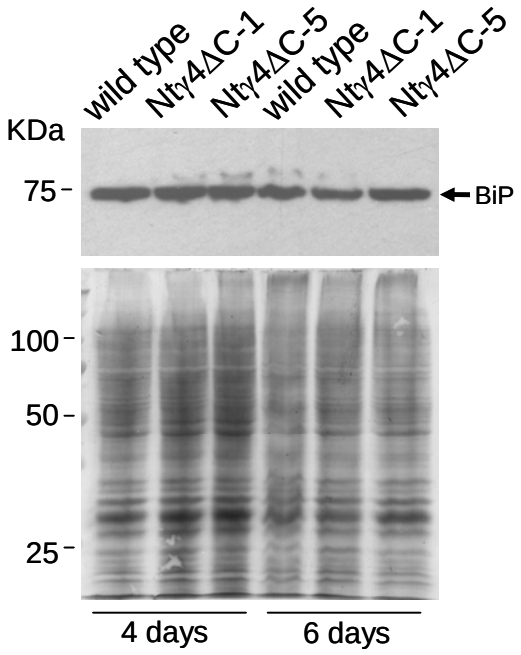

Figure 6. NTγ4ΔC accumulates wild type levels of BiP.
Microsomal fraction (30 μg) from 4- and 6-d old wild type (NT1-WT) and transgenic (NTγ4ΔC) cells were analyzed by SDS-PAGE followed by immunoblotting with polyclonal anti-BiP antibodies (*upper panel*). Proteins were visualized by Amido Black staining of the blot (*lower panel*).

GFP-γ4ΔC subcellular localization

Next, we asked where the GFP-γ4ΔC peptide was localized in the cell. Although UbDKγ4 has no obvious targeting motif like an ER retention- or nuclear-localization signal, many proteins containing UBL domains have distinct localization patterns. For example, the UBL domain-containing protein HHR23, the human homolog of Rad23, is localized to the nucleus where it plays a role in nucleotide excision repair (van der Spek et al., 1996).

Confocal microscopy revealed that GFP-γ4ΔC localizes differently compared to GFP alone. While GFP was found in the cytosol and in the nucleus of the NT1 cells, GFP-γ4ΔC localized in the cytosol but was excluded from the nucleus (Figure 7A). GFP-γ4ΔC appeared to demonstrate some punctate distribution in the cytosol which would suggest potential endomembrane association; however, the majority of the fluorescence appeared evenly dispersed throughout the cytosol and the majority of GFP-γ4ΔC was found in the soluble fraction of NTγ4ΔC cells following membrane isolation.

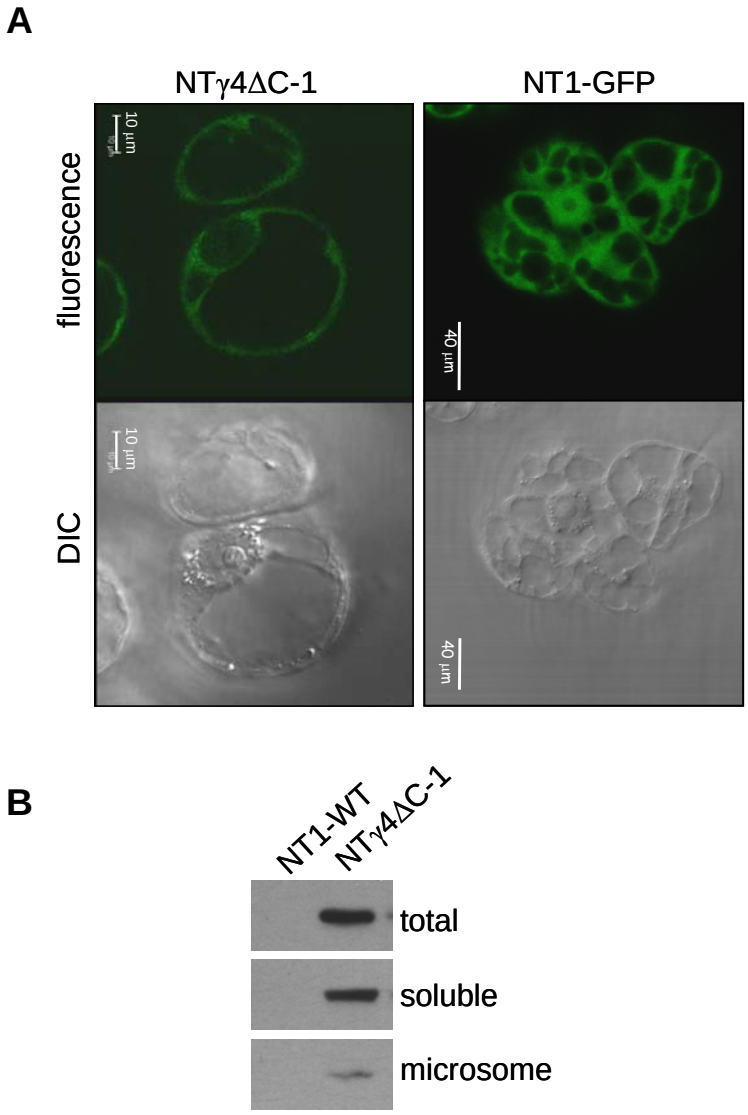

Figure 7. GFP-γ4ΔC is a soluble protein localized in the cytosol of NTγ4ΔC cells.
A. NTγ4ΔC-1 and NT1-GFP cells were imaged using a confocal microscope. Top panels show fluorescence, and bottom panels show differential interference contrast (DIC) images. NT1-GFP cell images from Im et al. (2007). **B.** Total lysate, soluble and microsomal fractions (30 μg) from wild type (NT1-WT) and transgenic NTγ4ΔC-1 cells were analyzed by SDS-PAGE followed by immunoblotting with monoclonal anti-GFP antibody.

Over-production of UbDKγ4-derived peptides in Arabidopsis plants

Agrobacterium-mediated transformation of Arabidopsis plants using the UbDKγ4-derived constructs shown in Figure 2 resulted in the generation of six independent kanamycin-resistant plant lines, 4 carrying GFP-γ4ΔC (referred as Atγ4ΔC-1, -2, -3 and -4) and 2 GFP-γ4KD (referred as Atγ4KD-1 and -2). Segregation of kanamycin-resistance indicated that Atγ4ΔC-1, -3, -4 and Atγ4KD-2 have a single T-DNA locus. The Atγ4KD-1 line could not complete its life cycle and died due to the lack of root system development.

RT-PCR from total RNA of homozygous T3 plants allowed the detection of the transcript from the GFP-fused expression cassette in the Atγ4ΔC-1, -4 and Atγ4KD-2 plants (Figure 8). The transcript accumulation from the endogenous *UbDKγ4* in the transgenic plants was undistinguishable from that of wild type and GFP plants, except in the Atγ4KD-2 line (Figure 8). In the Atγ4KD-2 line the RT-PCR product for *UbDKγ4* was more abundant compared to the other lines. The reason for such an observation is that the primer set used to detect the *UbDKγ4* transcript does not distinguish the transcript of the endogenous *UbDKγ4* from the GFP-γ4KD (Figure 1, P3 and P4 primer set). Over-expression of *GFP-γ4ΔC* and *GFP-γ4KD* did not affect transcript accumulation of *UbDKγ7*, another UbDK (Figure 8).

GFP-fusion proteins were readily detected in Atγ4ΔC-1, -4, Atγ4KD-2 and GFP control lines by immunoblot using anti-GFP antibody (Figure 9). GFP-KD protein in the Atγ4KD-2 line was also detected using a specific antibody raised against recombinant His-UbDKγ4 ΔUBL1/UBL2 produced in *E. coli* (Figure 9).

Similar to the transgenic NT1 cells, the transgenic Arabidopsis plants over-producing GFP-γ4ΔC and GFP-γ4KD had no obvious phenotype and were able to set seed and complete their life cycle. Also, no apparent pleiotropic effects were observed as a result of expression of the *UbDKγ4*-derived peptides in Arabidopsis plants.

Atγ4ΔC and Atγ4KD plants are hypersensitive to tunicamycin

In order to investigate whether UbDKγ4 is involved in ERAD, we tested the tolerance of the transgenic plants to chronic exposure to the antibiotic Tm. Tm is known to trigger

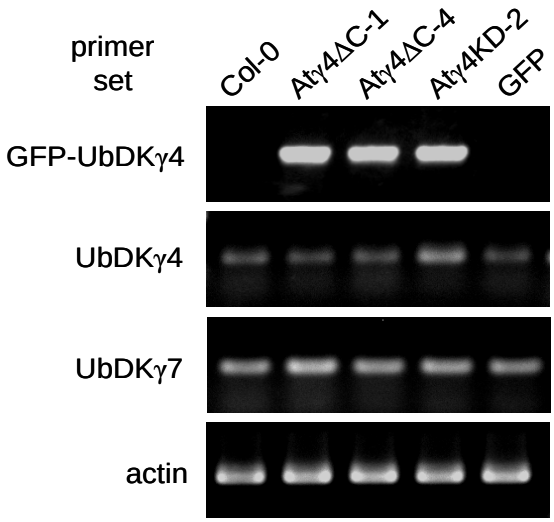

Figure 8. RT-PCR analysis of the expression of GFP-γ4ΔC and GFP-γ4KD in transgenic Arabidopsis plants.
RNA was isolated from 2-week old wild-type and T3 transgenic Arabidopsis seedlings. Equal amounts of RNA from each sample were reverse transcribed and subjected to RT-PCR. The *GFP-UbDKγ4* transcripts from Atγ4ΔC and Atγ4KD plants were identified with a combination of GFP forward and the selective *UbDKγ4* reverse primers (see Figure 2 - primers P1 and P2). Endogenous *UbDKγ4* transcript was detected by a primer set that can also detect the transcript from *GFP-γ4KD* but not from *GFP-γ4ΔC* (Figure 2 - primers P3 and P4). Amplification of *UbDKγ7* and *actin* transcripts was detected with a gene specific primer sets. Amplification of actin is shown as a loading control. Col-0 (wild type); GFP (GFP vector control); Atγ4ΔC-1, Atγ4ΔC-4 and Atγ4KD-2 (three independent transgenic lines producing GFP fused *UbDKγ4*-derived polypeptides). PCR targeting UbDKγ4, UbDKγ7 and actin were performed with a limited number (28) of cycles.

UPR via ER stress which presumably activates ERAD (Tsai et al., 2002; Urade, 2007). Atγ4ΔC-4, Atγ4KD-2, GFP and wild type (Col-0) seeds were sown on MS agar medium supplemented with DMSO or DMSO + 0.1 $\mu g \cdot mL^{-1}$ tunicamycin (DMSO + Tm). After d 6, visual inspection of the germinated seedlings revealed that all lines including the controls were affected by the treatment – seeds germinated in the presence of DMSO + Tm were slightly smaller than the ones germinated in DMSO alone. No obvious differences were observed between the various genetic backgrounds at this point (data not shown). The 6-d old seedlings were then transferred to non-supplemented MS agar medium and left to recover. The seedlings were inspected daily. After only 3 d on normal medium, differences in growth were readily evident. The Atγ4ΔC-4 and Atγ4KD-2 seedlings were not able to recover as well as the GFP and wild type (Figure 10A, B, C and D). The cotyledonary

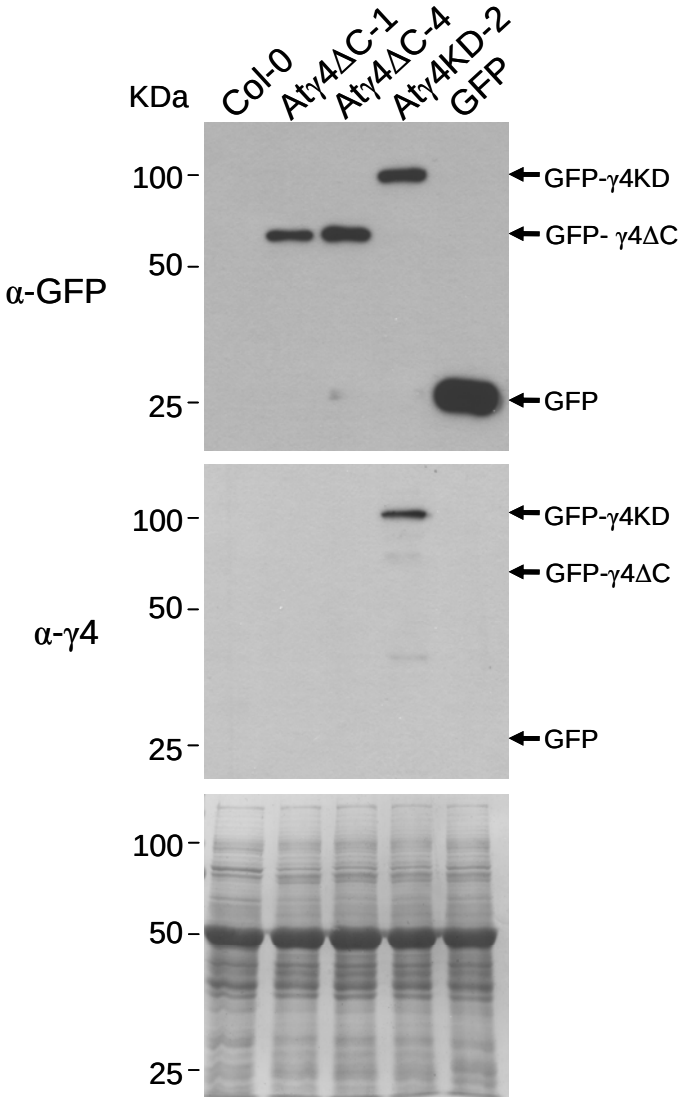

Figure 9. Transgenic Arabidopsis plants produce the predicted GFP, GFP-γ4ΔC and GFP-γ4KD proteins. Extracts (50 μg) from wild type (Col-0) and transgenic (Atγ4ΔC, Atγ4KD and GFP) plants were analyzed by SDS-PAGE followed by immunoblotting with monoclonal anti-GFP antibody (*upper panel*) and polyclonal anti-γ4 ΔUBL1/UBL2 antibody (*middle panel*). Proteins were visualized by Amido Black staining of the blot (*lower panel*).

Figure 10. Atγ4ΔC-4 and Atγ4KD-2 plants are hypersensitive to Tm.
Seeds from wild type (Col-0) and transgenic (Atγ4ΔC-4, Atγ4KD-2 and GFP) plants were sown on medium supplemented with DMSO (**A** and **C**) or DMSO with 0.1 $\mu g \cdot mL^{-1}$ tunicamycin (DMSO + Tm) (**B** and **D**). After 6 d, germinated seedlings were transferred to non-supplemented medium. The seedlings from the most representative plate (from duplicated experiments) were photographed 3 d (**A** and **B**) and 7 d (**C** and **D**) after transferring. **E.** Comparison of chlorophyll content between DMSO and DMSO + Tm treated seedlings 18 d after transferring to non-supplemented medium. Bars represent % reduction in the average chlorophyll content (from duplicate experiments) in the Tm treated plants compared to their controls (DMSO) treatment.

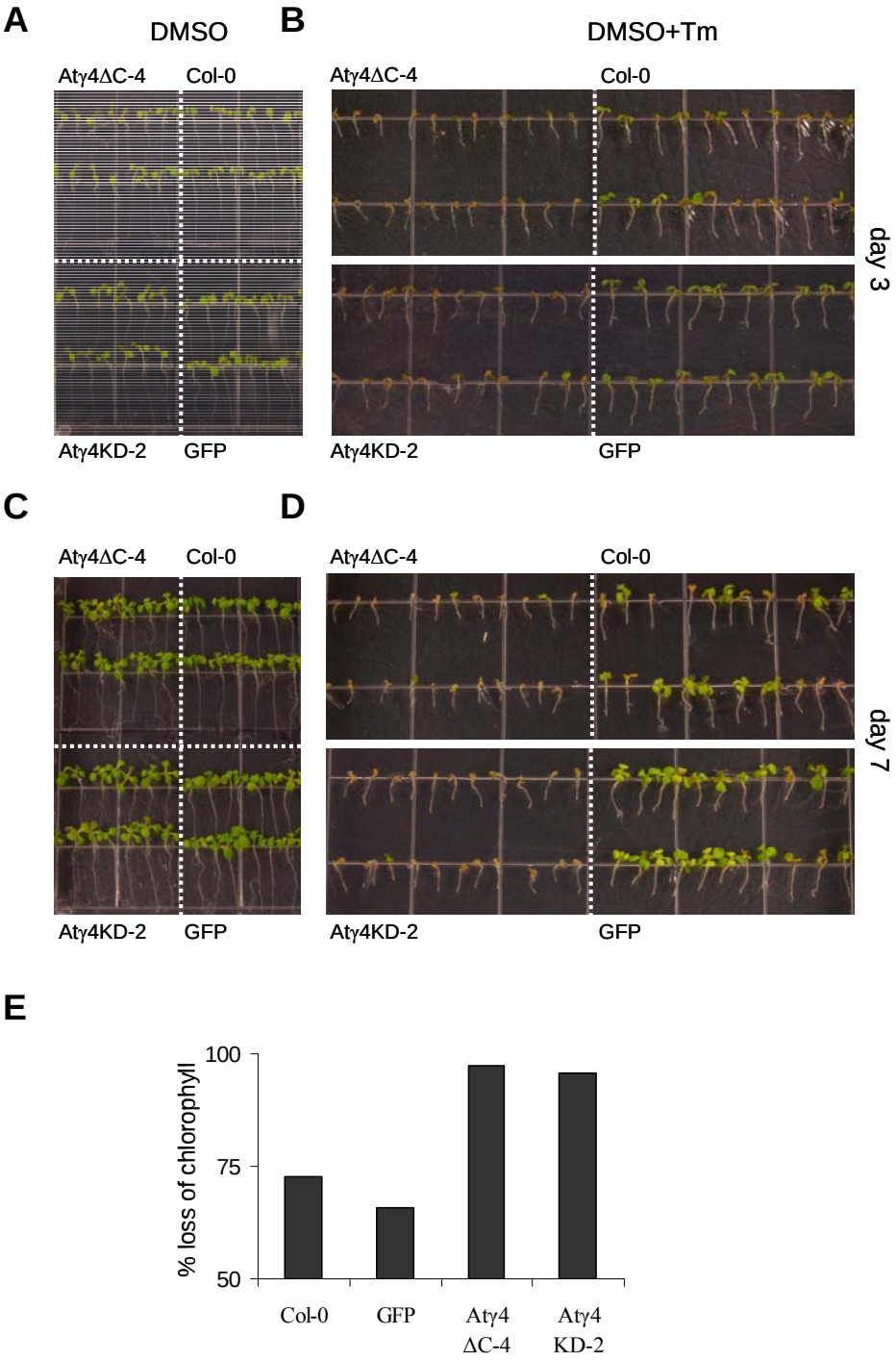
A
DMSO
B
DMSO+Tm
Atγ4ΔC-4
Col-0
Atγ4KD-2
GFP
day 3
C
D
day 7
E
% loss of chlorophyll
100
75
50
Col-0
GFP
Atγ4 ΔC-4
Atγ4 KD-2

leaves of Atγ4ΔC-4 and Atγ4KD-2 plants turned brown while in the control seedlings they remained green. After 17 d, the experiment was terminated and the chlorophyll content of treated and control seedlings was analyzed. Tm treatment caused a reduction of chlorophyll in the control plants (72 and 65 % in Col-0 and GFP seedlings, respectively). However, in the Atγ4ΔC-4 and Atγ4KD-2 seedlings the reduction was a lot more drastic, 97 and 95 %, respectively (Figure 10E).

Discussion

Tm-resistant plants have been characterized (Koizumi et al., 1999; Wang et al., 2007); however, to our knowledge, Atγ4ΔC and Atγ4KD are the first reported transgenic Arabidopsis lines with enhanced sensitivity to Tm. Tm-sensitive yeast strains include the classical mutants, e.g. IRE1 (Cox et al., 1993) and HAC1 (Nikawa et al., 1996), as well as many others found in a large scale screen (Chen et al., 2005). The fact that UbDKγ4 interacts with UFD1, a protein directly involved in the retrotranslocation and consequent degradation of ERAD-substrates (Jarosch et al., 2002; Ye et al., 2003; Verma et al., 2004), suggests that the over-expression of UbDKγ4-derived peptides enhances Tm-sensitivity by disturbing UFD1 (and possibly CDC48) function and affecting ERAD.

In our hypothetical model (Figure 11), we envision that wild type UbDKγ4 will assist degradation of ERAD-substrates by facilitating its delivery to the proteasome. The rationale for this hypothesis is that UbDKγ4 can bind to both UFD1 (possibly in the context of CDC48/UFD1 complex) and to RPN10, a component of the proteasome. UbDKγ4 may help UFD1 (or CDC48/UFD1) to "hand over" ubiquitinated proteins to the proteasome via RPN10 interaction. Alternatively, UbDKγ4 may control the formation and stability of the CDC48/UFD1 complex via phosphorylation. UFD1 phosphorylation sites (**Chapter 2**) are located in its C-terminus, presumably the region by which UFD1 interacts with CDC48 (Park et al., 2005).

In Atγ4ΔC and Atγ4KD plants (Figure 12) the accumulation of *UbDKγ4*-derived polypeptides can potentially affect UFD1 (or CDC48/UFD1) in many ways. An excess of *UbDKγ4*-derived polypeptides might *i*) prevent the formation of CDC48/UFD1 complex by

sequestering UFD1; *ii*) compete with emerging ERAD-substrate in the cytosol, preventing its recognition by CDC48/UFD1 complex; and *iii*) prevent UbDKγ4 function in the substrate delivery process by intermolecular interaction between the endogenous UbDKγ4 with the recombinant *UbDKγ4*-derived polypeptides.

While these data suggest a putative role for UbDKγ4 in regulating ERAD, further investigation is needed to determine whether there is a direct role for UbDKγ4 in the ERAD response under normal conditions and to understand the exact mechanism by which *UbDKγ4*-derived polypeptides affect plant tolerance to Tm-treatment.

Figure 11. Hypothetical model of UbDKγ4 function during ERAD and the effect of UbDKγ4-derived peptides in transgenic cells.
A. In wild type cells UFD1 and CDC48 form a complex (1) which is recruited (2) to the surface of ER to recognize and assist in the retrotranslocation (3) of ERAD substrates. The CDC48/UFD1 complex escorts (4) and delivers (5) the ubiquitinated ERAD substrate to the proteasome where it is degraded. The proposed function of UbDKγ4 is that it will either regulate the formation of the CDC48/UFD1 complex (1) by phosphorylation or assist CDC48/UFD1 complex in delivering the ubiquitinated ERAD substrate to the proteasome via UbDKγ4 – RPN10 interaction, or both. **B.** In the transgenic cells the accumulation of *UbDKγ4*-derived polypeptide (represented in the cartoon by γ4ΔC), potentially affects CDC48/UFD1 complex function by preventing the complex formation (1') and recruitment to the ER surface (2') or by disrupting delivery of ERAD substrate to the proteasome (5').

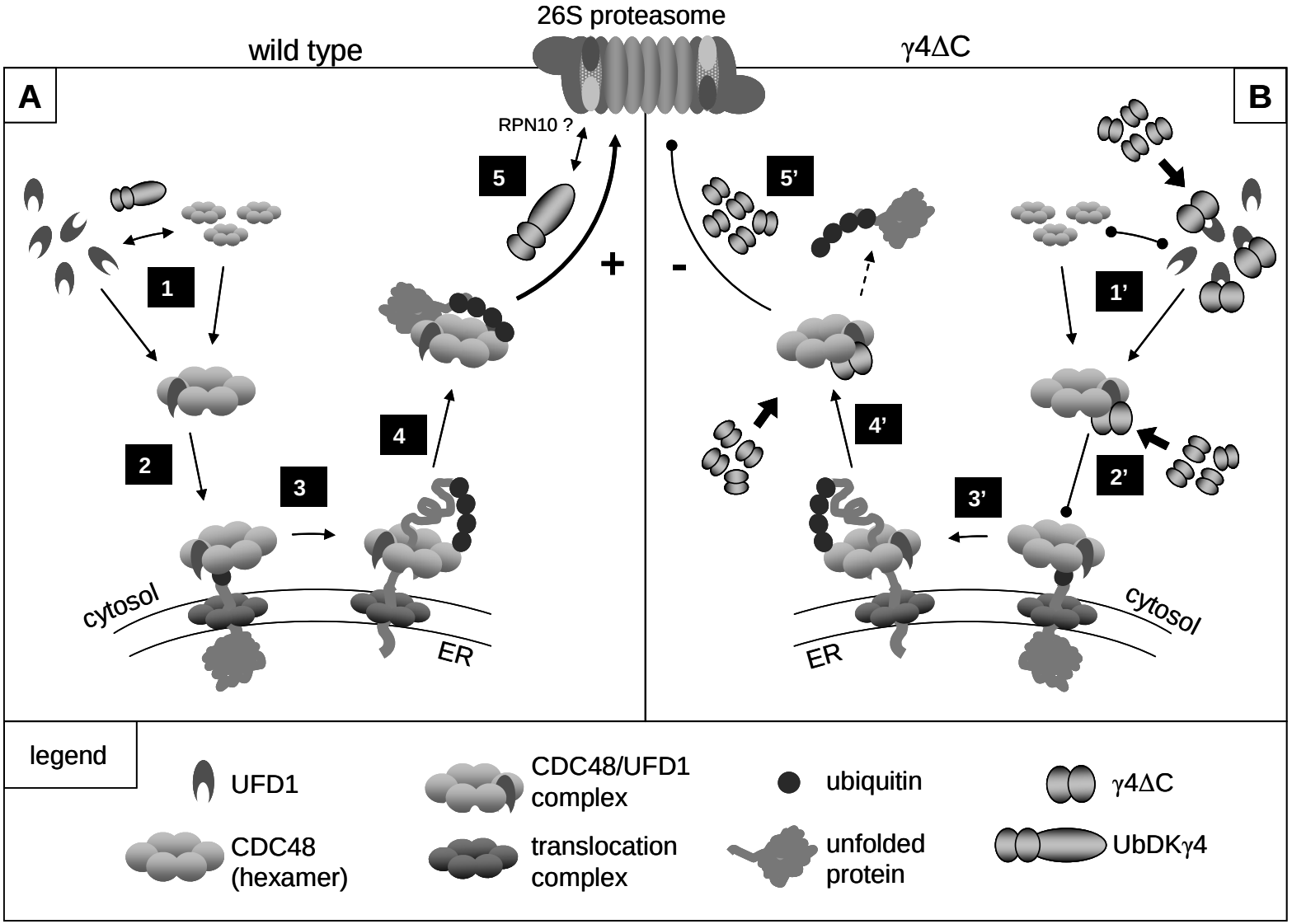
26S proteasome
wild type
γ4ΔC
A
B
RPN10 ?
5
5'
+
-
1
1'
2
2'
3
3'
4
4'
cytosol
ER
cytosol
ER
legend
UFD1
CDC48/UFD1 complex
ubiquitin
γ4ΔC
CDC48 (hexamer)
translocation complex
unfolded protein
UbDKγ4

References

Chen H, Nelson RS, Sherwood JL (1994) Enhanced recovery of transformants of *Agrobacterium tumefaciens* after freeze-thaw transformation and drug selection. Biotechniques 16: 664-668, 670.

Chen Y, Feldman DE, Deng C, Brown JA, De Giacomo AF, Gaw AF, Shi G, Le QT, Brown JM, Koong AC (2005) Identification of mitogen-activated protein kinase signaling pathways that confer resistance to endoplasmic reticulum stress in *saccharomyces cerevisiae*. Mol Cancer Res 3: 669-677.

Clough SJ, Bent AF (1998) Floral dip: a simplified method for Agrobacterium-mediated transformation of Arabidopsis thaliana. Plant J 16: 735-743.

Cox JS, Shamu CE, Walter P (1993) Transcriptional induction of genes encoding endoplasmic reticulum resident proteins requires a transmembrane protein kinase. Cell 73: 1197-1206.

Fu H, Sadis S, Rubin DM, Glickman M, van Nocker S, Finley D, Vierstra RD (1998) Multiubiquitin chain binding and protein degradation are mediated by distinct domains within the 26 S proteasome subunit Mcb1. J Biol Chem 273: 1970-1981.

Im YJ, Perera IY, Brglez I, Davis AJ, Stevenson-Paulik J, Phillippy BQ, Johannes E, Allen NS, Boss WF (2007) Increasing plasma membrane phosphatidylinositol(4,5)bisphosphate biosynthesis increases phosphoinositide metabolism in *Nicotiana tabacum*. Plant Cell 19: 1603-1616.

Jarosch E, Taxis C, Volkwein C, Bordallo J, Finley D, Wolf DH, Sommer T (2002) Protein dislocation from the ER requires polyubiquitination and the AAA-ATPase Cdc48. Nat Cell Biol 4: 134-139.

Koizumi N, Ujino T, Sano H, Chrispeels MJ (1999) Overexpression of a gene that encodes the first enzyme in the biosynthesis of asparagine-linked glycans makes plants resistant to tunicamycin and obviates the tunicamycin-induced unfolded protein response. Plant Physiol. 121: 353-362.

Livak KJ, Schmittgen TD (2001) Analysis of relative gene expression data using real-time quantitative PCR and the $2^{-\Delta\Delta CT}$ method. Methods 25: 402-408.

Martinez IM, Chrispeels MJ (2003) Genomic analysis of the unfolded protein response in Arabidopsis shows its connection to important cellular processes. Plant Cell 15: 561-576.

Meyer HH, Wang Y, Warren G (2002) Direct binding of ubiquitin conjugates by the mammalian p97 adaptor complexes, p47 and Ufd1-Npl4. EMBO J 21: 5645-5652.

Nikawa J, Akiyoshi M, Hirata S, Fukuda T (1996) Saccharomyces cerevisiae IRE2/HAC1 is involved in IRE1-mediated KAR2 expression. Nucl Acids Res 24: 4222-4226.

Park S, Isaacson R, Kim HT, Silver PA, Wagner G (2005) Ufd1 exhibits the AAA-ATPase fold with two distinct ubiquitin interaction sites. Structure 13: 995-1005.

Perera IY, Hung CY, Brady S, Muday GK, Boss WF (2006) A universal role for inositol 1,4,5-trisphosphate-mediated signaling in plant gravitropism. Plant Physiol 140: 746-760.

Perera IY, Love J, Heilmann I, Thompson WF, Boss WF (2002) Up-regulation of phosphoinositide metabolism in tobacco cells constitutively expressing the human type I inositol polyphosphate 5-phosphatase. Plant Physiol 129: 1795-1806.

Tsai B, Ye Y, Rapoport TA (2002) Retro-translocation of proteins from the endoplasmic reticulum into the cytosol. Nat Rev Mol Cell Biol 3: 246-255.

Urade R (2007) Cellular response to unfolded proteins in the endoplasmic reticulum of plants. FEBS J 274: 1152-1171.

van der Spek PJ, Eker A, Rademakers S, Visser C, Sugasawa K, Masutani C, Hanaoka F, Bootsma D, Hoeijmakers JH (1996) XPC and human homologs of RAD23: intracellular localization and relationship to other nucleotide excision repair complexes. Nucl Acids Res 24: 2551-2559.

van Nocker S, Deveraux Q, Rechsteiner M, Vierstra RD (1996) Arabidopsis MBP1 gene encodes a conserved ubiquitin recognition component of the 26S proteasome. PNAS 93: 856-860.

van Nocker S, Sadis S, Rubin DM, Glickman M, Fu H, Coux O, Wefes I, Finley D, Vierstra RD (1996) The multiubiquitin-chain-binding protein Mcb1 is a component of the 26S proteasome in Saccharomyces cerevisiae and plays a nonessential, substrate-specific role in protein turnover. Mol Cell Biol 16: 6020-6028.

Verma R, Oania R, Graumann J, Deshaies RJ (2004) Multiubiquitin chain receptors define a layer of substrate selectivity in the ubiquitin-proteasome system. Cell 118: 99-110.

Wang S, Narendra S, Fedoroff N (2007) Heterotrimeric G protein signaling in the Arabidopsis unfolded protein response. PNAS 104: 3817-3822.

Ye Y, Meyer HH, Rapoport TA (2003) Function of the p97-Ufd1-Npl4 complex in retrotranslocation from the ER to the cytosol: Dual recognition of non-ubiquitinated polypeptide segments and polyubiquitin chains. J Cell Biol 162: 71-84.

APPENDICES

APPENDIX 1

Characterization of UbDKγ7

Abstract

UbDKγ4 and UbDKγ7 are closely related protein kinases containing phosphoinositide 3/4- kinase (PI3/4K) and N-terminal ubiquitin like (UBL) domains. Both UbDKγ4 and UbDKγ7 autophosphorylate and phosphorylate protein substrates. UbDKγ4 interacts with itself and can autophosphorylate via an intermolecular reaction. Data from studies of protein-protein interaction, transcriptional regulation and plant transformation suggest that UbDKγ4 is involved in the ubiquitin/proteasome system and may affect degradation of proteasome substrates from the ER-associated protein degradation (ERAD) pathway. Here we show that UbDKγ7, in contrast to UbDKγ4, cannot autophosphorylate via an intermolecular reaction. In addition, protein pull-downs followed by protein phosphorylation assays revealed that UbDKγ7 interacts with a protein kinase that can phosphorylate UbDKγ7. We speculate that UbDKγ7 may be functionally involved in a phosphorylation cascade activated in response to hyperosmotic stress.

Introduction

UbDKγ4 and γ7 are the founding members of a new subfamily of protein kinases belonging to the phosphoinositide kinase-related kinase family (**Chapter 2**). UbDKγ4 and γ7 have a catalytic phosphoinositide 3/4- kinase (PI3/4K) domain and N-terminal ubiquitin like (UBL) domains. Both phosphorylate artificial protein kinase substrates, type IIIS histone and myelin basic protein and have no detectable lipid kinase activity. In addition, UbDKγ4, the isoform chosen for in depth characterization by Galvão et al. (**Chapter 2**), autophosphorylates via an intermolecular reaction and interacts and phosphorylates an Arabidopsis UFD1 (ubiquitin fusion degradation protein 1) (Johnson et al., 1995; Bays and Hampton, 2002) homolog and RPN10 (van Nocker et al., 1996; Glickman et al., 1998; Fu et al., 1999), a non-ATPase component of the proteasome regulatory particle *in vitro*.

In spite of their similarities, UbDKγ4 and γ7 differ in domain organization, and when assayed side by side for activity, UbDKγ4 always displays higher levels of

autophosphorylation and phosphorylation of protein substrates. The reason for these differences is not known.

Here we report a preliminary characterization of UbDKγ7. Both UbDKγ4 and UbDKγ7 undergo autophosphorylation. However, UbDKγ7 appears to autophosphorylate via an intramolecular reaction, in contrast to UbDKγ4 which uses an intermolecular reaction. Pull-down assays followed by phosphorylation reactions revealed that UbDKγ7 interacts with a protein kinase present in a soluble fraction of Arabidopsis cells that can phosphorylate the UbDKγ7 inactive mutant (K194A). UbDKγ7 K194A phosphorylation by this unknown kinase was enhanced by pretreatment of the cells with hyperosmotic stress. Together our results indicate that UbDKγ4 and γ7 have differences in how they are regulated by phosphorylation and suggest that the UbDKγ7 may be involved in a signaling cascade stimulated by hyperosmotic stress.

Methods

Cloning

Cloning of the full-length UbDKγ7 (At2g03890) coding region is described in **Chapter 2**. The UbDKγ7 truncations ΔN and ΔC and ΔN/ΔC were PCR-amplified (for primer sequence see Table 1), cloned into pGEM®-T Easy vector (Promega, Madison, WI) according to manufacturer's protocol and the clones were confirmed by sequencing. *E. coli* expression cassettes were made in pET-41 vectors (Novagen, San Diego, CA) using restriction enzymes as indicated in Table 1. The UbDKγ7 K194A mutant was generated by PCR using the Quick Change site-directed mutagenesis kit (Stratagene, La Jolla, CA) with the oligonucleotide primers 5'- GTGTTGCCATTGTCGCGCCGACGGATGAAGAGCC-3' and 5'- GGCTCTTCATCCGTCGGCGCGACAATGGCAACAC -3'.

Recombinant protein production and purification

Table 1. List of the UbDKγ7 fragments for the expression of recombinant proteins and the primers used in the PCR amplifications and cloning.

UbDKγ7 fragment	Forward primer (5' → 3')[a]	Reverse primer (5' → 3')[a]
full length	AAACTGCAGATGTCGAGGAACTTAGA	AAACTGCAGTCTCAAAACTGGCATGAA
ΔN/ΔC	AAACTGCAGTTGTCTTTCGCCTACTGGGA	AAACTGCAGCAGTGACTGATCTCTTGGCTTC
ΔN	AAACTGCAGTTGTCTTTCGCCTACTGGGA	AAACTGCAGTCTCAAAACTGGCATGAA
ΔC	AAACTGCAGATGTCGAGGAACTTAGA	AAACTGCAGCAGTGACTGATCTCTTGGCTTC

[a] The primers were designed to contain *Pst*I restriction sites (shown underlined in the primer sequence) flanked by AAA at the 5' end.

The production of recombinant protein in *E. coli* and affinity purification was performed as described in **Chapter 2**.

Protein electrophoresis and immunobloting

Protein electrophoresis and immunoblotting were performed as described in Chapter 2. Monoclonal anti-GST (BD Biosciences, San Jose, CA), anti-phosphoSer and anti-phosphoThr (Sigma, Saint Louis, MO) antibodies were used at 1:5,000, 1:500 and 1:50 dilutions, respectively.

Arabidopsis cell suspension culture maintenance and treatment

Arabidopsis cell cultures were initiated from hypocotyls of wild type Col-0 seedlings. The cultures were maintained at 23 ºC under 100 rpm shaking in 25 mL of ½ strength culture medium described by Chen and Boss (1990). The culture is maintained by transferring ~20 % of the total amount of cells from a 7-day old culture to fresh medium. For the hyperosmotic stress the osmolality of the medium of 4-d old culture was increased 10 fold (0.04 to 0.4 osmolal) by adding a concentrated sorbitol solution made in conditioned medium. In the hyposmotic stress the osmolality of the medium was decreased 4 fold by adding distilled water to the culture medium. The heat stress was imposed by incubating the cell culture at 40°C. The stressed cells were collected at different time points after each treatment as indicated.

Protein pull-down assays

Protein pull-down using GST-UbDKγ7 was performed as described in **Chapter 2**, except that bound protein was submitted to protein phosphorylation reactions in the presence of [γ-^{32}P]ATP prior to electrophoresis.

Protein phosphorylation assay

Recombinant protein or bound protein from pull-downs was assayed for protein kinase activity and autophosphorylation in buffer containing 50 mM Tris HCl (pH 7.5), 10 mM $MgCl_2$, 1 mM EGTA, 100 μM ATP (10 μCi for pull-downs and 5 μCi elsewhere of [γ-^{32}P]ATP per reaction. Typically, reactions were carried out in 40-60 μL (final volume) for 10-20 min at room temperature under occasional agitation and were terminated by adding 4 × SDS sample buffer. Reaction mixtures were resolved on SDS-PAGE gel followed by autoradiography or immunoblotting.

Results and Discussion

Both UbDKγ4 and γ7 have the catalytic phosphoinositide 3/4- kinase (PI3/4K) domain and N-terminal ubiquitin like (UBL) domains. However, while UbDKγ4 has two UBL domains, UbDKγ7 has only one (Figure 1A). In addition UbDKγ7 has an extended C-terminal sequence that contains a Glu-enriched region (Figure1A). The overall amino acid identity between UbDKγ4 and γ7 is 31%. Inside the catalytic PI3/4K domain the sequence identity increases to 48%.

Sequence alignment and published data (Barylko et al., 2002) were used in the identification of key amino acids potentially required for ATP binding and activity of UbDKγ4. A Lys284→Ala (K284A) mutation resulted in an inactive form of UbDKγ4 (**Chapter 2**). Similarly, we located an UbDKγ7 Lys (Lys194) analogous to Lys284 of UbDKγ4 (Figure 2A). Site directed mutagenesis was used to produce the Lys194→Ala (K194A) mutation. As expected, the UbDKγ7 K194A mutation abolished autophosphorylation (Figure 2B) and protein kinase activity toward MBP (data not shown).

To determine the impact of the UBL domain and the C-terminal extension containing the Glu-enriched motif on the UbDKγ7 activity, N-, C- and N-/C-terminal truncations of UbDKγ7 (Figure 1B) were introduced in *E. coli* expression cassettes for production of GST-tagged recombinant protein. For undetermined reasons, the UbDKγ7 ΔC truncation could not be produced in *E. coli*. Both ΔN and ΔN/ΔC UbDKγ7 truncations had no detectable

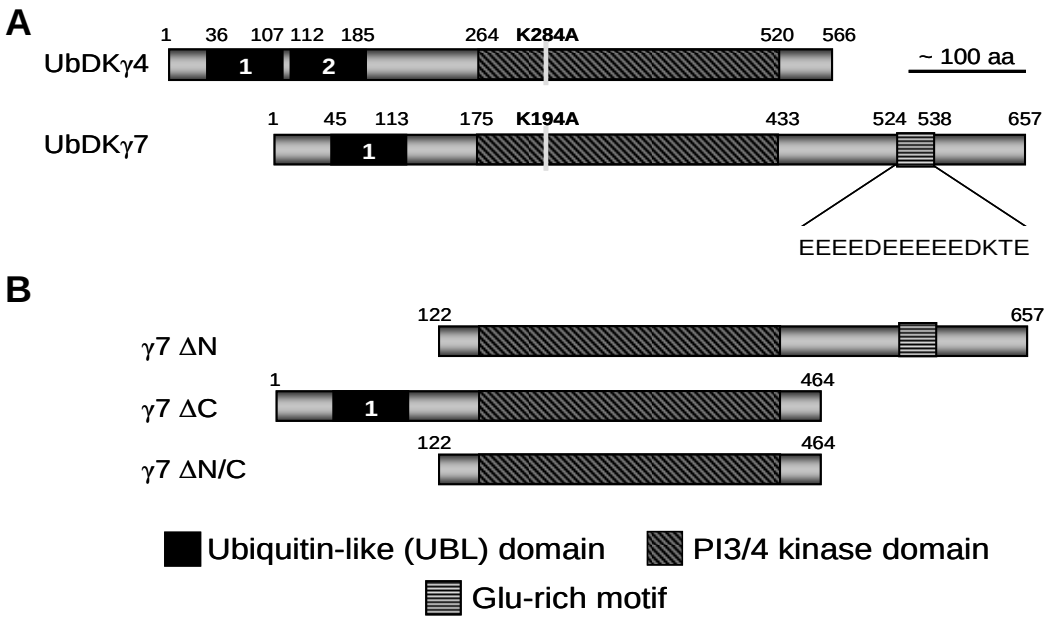

Figure 1. Detailed domain organization of UbDKγ4 and UbDKγ7 and UbDKγ7 truncations.
A. Domain organization of UbDKγ4 and UbDKγ7. The boundaries of each functional domain are indicated on top of both UbDKγ4 and UbDKγ7 diagrams. K284A and K194A are analogous mutations targeting a putative ATP binding sites in UbDKγ4 and UbDKγ7, respectively. **B.** UbDKγ7 truncations cloned into *E. coli* expression vectors for production of N-terminal GST-tagged recombinant proteins.

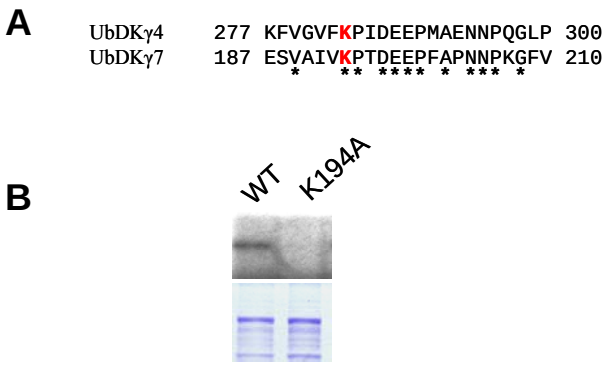

Figure 2. Identification of the UbDKγ7 ATP binding site.
A. Alignment of an N-terminal portion of the PI3/4K domain of UbDKγ4 and UbDKγ7. The Lys284 of UbDKγ4 and the correspondent Lys (Lys194) in the UbDKγ7 sequence is highlighted in red. The stars represent the identical residues between the aligned sequences. **B.** The GST-UbDKγ7 K194A mutant was produced in *E. coli* and assayed for protein kinase activity side by side with the GST-UbDKγ7 wild type protein. The products of the reactions were resolved by SDS-PAGE. The ^{32}P-labeled proteins were revealed by autoradiography (*upper panel*). The proteins were visualized by Coomassie blue staining of the gel (*lower panel*).

autophosphorylation (Figure 3A), suggesting that the N-terminal (aa 1-122) was necessary for autophosphorylation.

In order to investigate whether UbDKγ7 and UbDKγ4 use a similar mechanism for autophosphorylation, we asked whether the UbDKγ7 truncations described above could be phosphorylated by the full-length UbDKγ7. Phosphorylation reactions containing the full-length UbDKγ7 in combination with the inactive ΔN and ΔN/ΔC UbDKγ7 truncations revealed that the full-length enzyme was not able to phosphorylate either protein construct (Figure 3A).

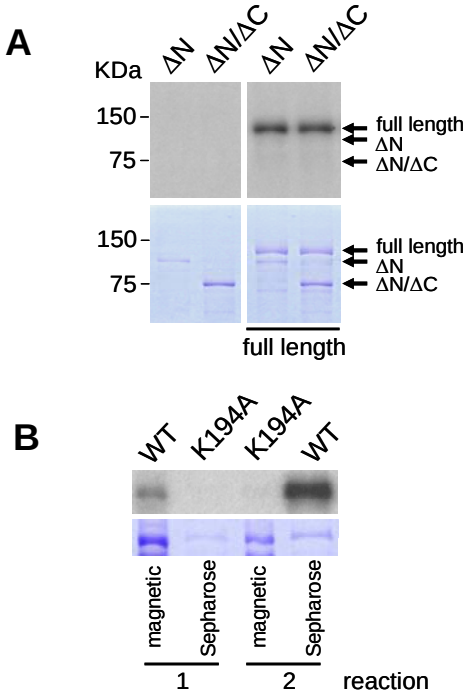

Figure 3. UbDKγ7 is phosphorylated by an intramolecular reaction.
A. Recombinant full-length UbDKγ7 and the truncations ΔN and ΔN/ΔC fused to GST (1 μg each) were assayed for autophosphorylation by adding [γ-^{32}P] ATP as described in the Experimental Section. The products of the reactions were resolved by SDS-PAGE. The ^{32}P-labeled proteins were revealed by autoradiography (*upper panel*) and the proteins were visualized by Coomassie blue staining (*lower panel*). **B.** Bound GST-UbDKγ7 wild type and GST-K194A mutant proteins were assayed together in the presence of [γ-^{32}P] ATP in two independent reactions. In reaction 1 wild type GST-UbDKγ7 was immobilized in magnetic beads while the GST-K194A mutant was immobilized on Sepharose beads. In reaction 2, recombinant GST-UbDKγ7 and GST-K194A were immobilized on the reciprocal combination of beads as indicated. After 15 min incubation at room temperature with intermittent mixing, magnetic and Sepharose beads were separated with a magnet and the products of the reactions were resolved separately by SDS-PAGE. The ^{32}P-labeled proteins were revealed by autoradiography (*upper panel*) and the proteins were visualized by Coomassie blue staining (*lower panel*).

In order to further investigate whether UbDKγ7 autophosphorylation occurs via an intramolecular reaction, we used wild type and kinase inactive (K194A) versions of UbDKγ7. Both GST-UbDKγ7 versions were bound to either Sepharose or magnetic glutathione beads and then mixed in reciprocal reactions (reactions 1 and 2 Figure 3B) containing [γ-^{32}P]-ATP. The respective wild type or K194A UbDKγ7 proteins were recovered with a magnet and [γ-^{32}P]-labeled proteins were detected by SDS-PAGE followed by autoradiography. No detectable phosphorylation of K194A UbDKγ7 was observed indicating that under the conditions used, UbDKγ7 did not autophosphorylate via an intermolecular reaction. The mechanism by which UbDKγ7 autophosphorylates maybe more similar to the one used by mammalian phosphatidylinositol 4-kinase (PI4K) IIIβ (Zhao et al., 2000), than the one used by UbDKγ4.

Based on LC/MS/MS analysis, UbDKγ4 targeted Ser and Thr phosphorylation sites of AtUFD1, (**Chapter 2**). In addition, preliminary unpublished results indicated that UbDKγ4 autophosphorylates Ser and Thr sites in its own sequence (**Appendix 3**). In order to investigate whether UbDKγ7 targets Ser or Thr or both residues for phosphorylation we used specific anti-phospho-amino acid antibodies to probe the full length UbDKγ7 and the inactive truncation ΔN/ΔC. Both recombinant proteins were assayed side by side in reactions containing ATP. Active, full-length UbDKγ7 was readily detected by both anti-phosphoSer and anti-phosphoThr antibodies; whereas, the ΔN/ΔC UbDKγ7 truncation was barely detectable (Figure 4). This result suggests that UbDKγ7, like UbDKγ4, targets Ser and Thr residues and that UbDKγ7 may have at least two autophosphorylation sites (one Ser and one Thr).

To investigate whether GST-UbDKγ7 could be phosphorylated by other Arabidopsis protein kinases, we performed side by side pull-downs with microsomes and soluble Arabidopsis fractions using GST-UbDKγ7 (wild type) and K194A in the presence of [γ-^{32}P]-ATP. The recovered UbDKγ7 (wild type) was phosphorylated to a greater extent than the kinase dead K194A mutant. Phosphorylation of K194A was exclusively detected when the pull-down reactions were performed with thesoluble fraction and not with a microsomal fraction. These results indicate that UbDKγ7 interacts with and is phosphorylated by an

unknown protein kinase which is either absent or inactive in the microsomal fraction (Figure 5A).

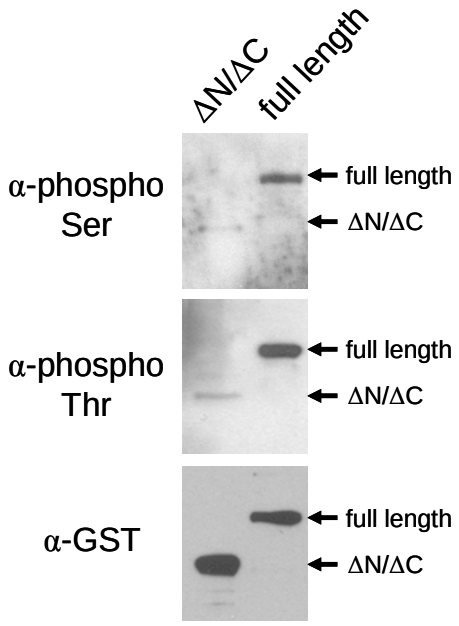

Figure 4. UbDKγ7 autophosphorylation targets Ser and Thr residues.
The full length and ΔN/ΔC truncation of recombinant GST-UbDKγ7 were assayed for autophosphorylation in the presence of ATP. The products of each reaction were resolved by SDS-PAGE. The proteins were revealed by immunoblotting with the indicated phosphopeptide antibodies. The immunoblotting with anti-GST antibody is shown as a loading control.

Next, we asked whether the protein kinase that can phosphorylate UbDKγ7 responded to stimuli. A GST-UbDKγ7 K194A pull-down reaction followed by protein phosphorylation assay was performed using soluble fractions of Arabidopsis cells that were pre-stimulated with hyperosmotic and hyposmotic stress and with heat (40 ºC) shock. The results shown in Figure 5B revealed that the UbDKγ7 K194A phosphorylation increased after the cells were exposed to hyperosmotic stress and decreased after the cells were heat shocked. No significant change was observed when the cells were exposed to hyposomotic stress. These results together suggest that UbDKγ7 is a substrate of one (or more) of the many protein kinases that respond to hyperosmotic stress, e.g. members of the families of mitogen-activated protein kinases (MAPK), calcium-dependent kinases (CDPK) or Suc non-

fermenting-related kinases (SnRK) (Boudsocq and Lauriere, 2005). We speculate that UbDKγ7 may function as part of a phosphorylation cascade modulated in response to environmental stimuli.

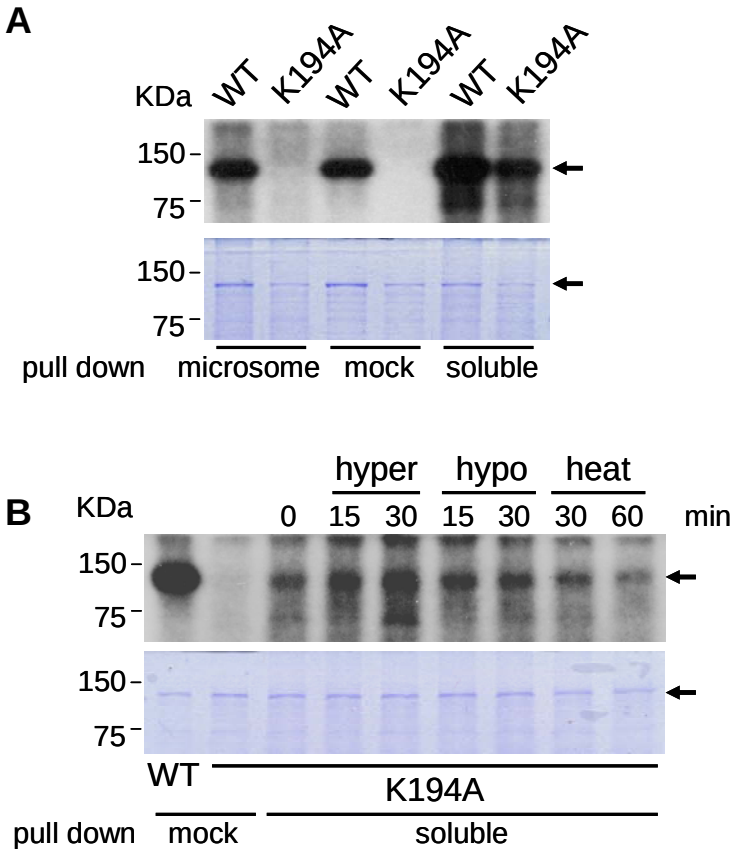

Figure 5 UbDKγ7 is phosphorylated by an interacting protein kinase which is stimulated by hyperosmotic stress.

A. Pull-down reactions using GST-UbDKγ7 wild type and the GST-K194A mutant were performed with microsomal, soluble or mock (buffer) extract from Arabidopsis cells grown in suspension culture. Bound proteins were assayed for protein phosphorylation by adding [γ-^{32}P] ATP as indicated in the Experimental Section. **B.** Pull-down reactions using GST-UbDKγ7 wild type and the GST-K194A mutant were performed with soluble or mock (buffer) extract from Arabidopsis cells that had been stimulated with hyperosmotic (10-fold higher osmolality than the culture medium) or hyposmotic (a 4-fold dilution with water) stress or heat shocked (40 ºC). The cells were collected after stimulation at the times indicated. Bound proteins were assayed for protein phosphorylation with [γ-^{32}P] ATP as described in the Experimental Section. In both **A** and **B** the products of the reactions were resolved by SDS-PAGE. The ^{32}P-labeled proteins were revealed by autoradiography (*upper panel*) and proteins were visualized by Coomassie blue staining (*lower panel*).

APPENDIX 2

Expression analysis of phosphoinositide pathway genes – A Real Time tool box

Abstract

Changes in the concentration of inositol phospholipids and inositol (*poly*)phosphates occur as result of changes in the activity of the enzymes involved in synthesis and turnover of these signaling molecules. Changes in the activity of these enzymes can happen from activation or inhibition of enzyme activities, changes in their subcellular localization or changes in their abundance within the plant cell. Changes in abundance can happen as a result of changes in the enzyme turnover rates (translation/degradation) or changes at the level of gene expression. In the present study we report the design of Real Time RT-PCR primer sets targeting phosphoinositide kinases and lipases directly involved in $InsP_3$ biosynthesis in Arabidopsis. We experimentally tested the effectiveness of these primers and used Arabidopsis cells grown in suspension culture as a model system for analysis of gene expression.

Introduction

The phosphoinositide (PI) pathway, which include inositol phospholipids and species of inpositol (poly)phosphate, produces the signaling molecules, inositol (1,4,5) trisphosphate ($InsP_3$) and diacylglycerol (DAG). The polyphosphorylated inositol phospholipids are also signaling molecules themselves. They interact directly with cytoskeletal proteins, enzymes, channels and pumps, altering their subcellular localization and regulating their activity. Thus, changes in PI metabolism will affect vesicle trafficking, cytoskeleton organization, membrane biogenesis and membrane-associated signal transduction (Carpenter and Cantley, 1996; Toker and Cantley, 1997; Fruman et al., 1998; Stevenson et al., 2000; Cantrell, 2001; Cockcroft and De Matteis, 2001; Cantley, 2002; Roth, 2004; Boss et al., 2006).

Changes in the concentration of $InsP_3$ and others PIs occur in plant cells in response to a diverse range of stimuli (Mikami et al., 1998; Perera et al., 1999; Drobak and Watkins, 2000; DeWald et al., 2001; Klusener et al., 2002). These changes in metabolite concentrations are driven by the activity of enzymes involved in their synthesis and turnover. Our hypothesis was that changes in the concentration of $InsP_3$ and other PIs are, at least in

part, a result of differential regulation of key genes of the PI pathway (phosphatidylinositol 4-kinases [PI4K], phosphatidylinositol phosphate 5-kinases [PIP5K] and phospholipases C [PLC]) at the level of transcription. Here we report the design of Real Time RT-PCR primer sets targeting Arabidopsis PI4Ks, PIP5Ks and PLCs. In addition, we characterized Arabidopsis cells grown in suspension culture as a potential experimental system to undertake future gene expression analysis. We used hyperosmotic stress as a stimulus for testing the efficacy of the tools we developed.

Methods

Arabidopsis cell suspension culture maintenance, growth curve and treatment

Arabidopsis cell cultures were maintained as described in **Chapter 4**. Cell growth was monitored and recorded using two replicate 25-mL cultures harvested daily from 3 to 9 days after transferring. Cells and medium were separated and collected by low-speed centrifugation (~500*g* for 3 min). The cells fresh weight and the pH of the medium were measured. Cells from 3, 5, 7 and 9 days were frozen using liquid N_2 and stored at -80 ºC until use.

For the hyperosmotic stress treatment we used 4-day old cells. Cultures from multiple flasks were mixed and proportionally aliquoted back into 10-mL of conditioned medium. The cells were allowed to recover from handling for 1 h and then either conditioned medium or conditioned medium supplemented with sorbitol was added. The sorbitol final concentration was 360 mM. Treated and control cells were harvested 0, 20, 60 and 120 minutes after treatment. The cells were immediately frozen using liquid N_2 and stored at -80 ºC until use.

RNA isolation and reverse transcription

Total RNA was isolated from the Arabidopsis cells previously ground in liquid N_2 using RNeasy Plant Mini Kit (Qiagen, Hilden, Germany). Genomic DNA contamination was removed by *on column* DNAse treatment (RNase-Free DNase Set – Qiagen) according to

manufacturer's protocol. RNA quantities and quality was analyzed by spectrophotometry and agarose gel electrophoresis, respectively. cDNA synthesis was performed from 2 μg of total RNA with random primers using High Capacity cDNA Archive Kit (Applied Biosystems, Foster City, CA). cDNA samples were aliquoted and stored at -20 ºC.

Primer design and PCR

Gene-specific primer sets were designed using Primer Express software (Applied Biosystems) for cDNA coding sequences of the PI pathway genes. Sequence mining was performed from The Arabidopsis Information Resource (TAIR) database (http://www.arabidopsis.org/). Amplicon size varied from 80 to 150 bp. Primer Tm was 58 +/- 2 ºC (Tm in 50 mM NaCl according to primer synthesis specifications by Integrated DNA Technologies (IDT - Coralville, IA)).

The PCR step was performed typically in 30 μL using 5 to 20 pmoles of each primer/reaction containing 20 ng of cDNA equivalent unless otherwise indicated. Reaction mix including DNA polymerase and dyes for real time amplification detection was provided by SYBR® Green PCR Master Mix (Applied Biosystems). All reactions were pipetted on ice into MicroAmp® Optical 96-Well Reaction Plates and sealed with ABI PRISM™ Optical Caps (Applied Biosystems). PCRs were run on ABI 7000 Sequence Detection System (Applied Biosystems) with the following 2-step cycling program: 95 ºC, 10 min (initial denaturing) plus 40 cycles of 95 ºC, 15 s (denature) and 60 ºC, 1 min (anneal/extend).

Data analysis

Resulting amplification plots and melting curves were individually inspected and the threshold fluorescence level was manually adjusted for each primer set. C_T values were exported to Excel spread sheets and analyzed. Primer efficiency was experimentally determined with at least 4 to 5 template concentrations (typically from 0.5 to 40 ng of cDNA equivalent). Differences in gene expression were assessed from two triplicated reactions, each one from an independent biological replica of the experiment. We used the $2^{-\Delta\Delta Ct}$

method (Livak and Schmittgen, 2001) to calculate relative fold differences in gene expression compared to a reference sample.

Results and Discussion

In order to characterize the Arabidopsis cell line used in this study, we investigated its growth pattern over a 9-day period. Compared to the tobacco NT1 cell line (**Chapter 3** – Figure 3) the Arabidopsis cells grow more slowly. Whereas the NT1 cells fresh weight increases ~ 50-fold in an 8-day period, the Arabidopsis cells display less than a 5-fold increase in fresh weight in the same period (Figure 6A). Growth arrest occurs at day 7 in NT1 cells and at day 8 in Arabidopsis cells. Medium pH, which presumably correlates with cellular metabolism, was monitored in the same cultures used for the growth study. Noteworthy, the cells maintain the acidity of the medium during the period where their growth rate is the highest. A sharp alkalinization of the medium (days 7 and 8) precedes growth arrest (Figure 6B).

Real Time RT-PCR primers were designed for 12 genes encoding PI4K, 10 genes encoding PIP5K, 6 genes encoding PLC and 3 reference genes (Tables 2, 3, 4 and 5). No primer was designed for AtPIP5K5 that met the parameters of gene specificity. cDNA synthesized from total RNA of 4-day old cells was used for testing the conditions (primer and template concentration) in which a single amplicon was detected with the highest signal (fluorescence)/ng of template and no primer dimer. A PCR product of correct size was not detected for AtPI4Kα2, β2 and γ8; AtPIP5K11; AtPLC3 and 6 indicating that the transcript for those genes was not present in that biological sample or the primer set designed for them was not effective.

Primer efficiency was verified for all primer sets targeting PI4Ks and reference genes and some selected PIP5Ks (Tables 2, 3, and 5). Primer efficiency was calculated using the slope of the equation that best fits the linear correlation between C_T value variation over a range of the template concentration ($\log_{10}$ scale) in the reaction (Figure 7). Ideally, all primer sets should have efficiency within 90% to 110%. Only 3 out of 15 primer sets had efficiency out of that range (Tables 2, 3, and 5).

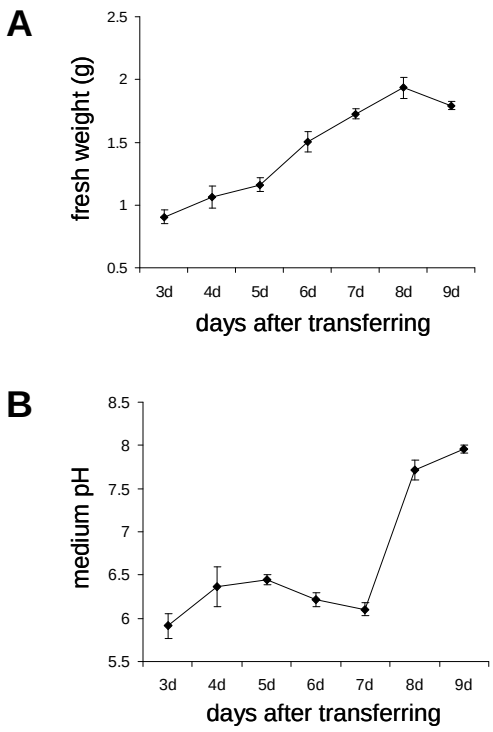

Figure 6. Growth and medium pH of Arabidopsis cells grown in suspension culture.
A. Growth of cells recorded as change in fresh weight over time. **B.** Changes in medium pH of the same cultures used in **A**. In **A** and **B** the data presented are the average of 4 measurements/time point (two culture flasks for each of two independent biological replicates). The error bars represent standard deviation.

In order to test the primers and the Arabidopsis culture as a system to analyze patterns of gene expression we designed two experiments. First, we collected cells over time during the culture cycle. We specifically, analyzed changes in expression of PI4K genes in Arabidopsis cells 3, 5, 7 and 9 d after transferring. In the second experiment we analyzed expression of PI4K genes in Arabidopsis cells challenged with hyperosmotic stress. We collected cells that were treated either with conditioned medium or with conditioned medium supplemented with sorbitol over a time course (0, 20, 60, and 120 min). The osmolality of the medium initially was 0.04 and after sorbitol addition was 0.4 (10-fold increase).

The data analysis was based on a relative comparison with a reference sample within the experiment. For example, the expression of a gene in the first experiment was compared to its level at d 3, the reference sample in that experiment. In the hyperosmotic stress experiment the expression of a gene was compared to its level at 0 min after treatment, the

Table 2. AtPI4K primers.

PI4K Type	Name	Locus	Amplicon size (bp)	Efficiency[a] (%)	Forward 5'→3'	Reverse 5'→3'
II	AtPI4Kγ1	At2g40850	128	100.1	CACGGCTACTTCGGTTCATAGG	CAGCGGTCCCAAGTCGATTAT
	AtPI4Kγ2	At1g64460	106	94.5	TGCGCTTCTGCAACTCCAT	TGGCGTCAGGTTTCTCTCAAC
	AtPI4Kγ3	At5g24240	95	96.3	CCCTGTCGATCAGGTTCACAA	CCATCTTTTCCATCTCGGCTAA
	UbDKγ4[b]	At2g46500	116	93.2	GCTTTCTTTGGAGCCGGTAGTT	TTGACCTGACCGGAGAATTCC
	AtPI4Kγ5	At1g26270	104	88.8	GAACAGATCCCATCAAGCACAA	ATGGCTGGATAAAGCAGCTCTT
	AtPI4Kγ6	At1g13640	115	nd	TGACGAAGAGGAGGCAAAACTT	TTGGTTGTCTTTCGGAGGTTTC
	UbDKγ7[b]	At2g03890	111	100.1	AAAGCGCAAACGAACAGCTT	CCGGTCCAAGTAACTCTTGGAA
	AtPI4Kγ8	At3g56600	105	nd	GCTGCCAATCTATCTGCTCTCA	GCTCCTCACGATACTCCGATCT
III	AtPI4Kα1	At1g49340	109	110.5	GCAGCAGAACTCGGCTAACTCT	ATCGCCAGGACTAGCCATTTC
	AtPI4Kα2	At1g51040	101	nd	GCTTCCTTGGATATGCCAACAA	GAGTCACGGCTAAGATCGCATT
	AtPI4Kβ1	At5g64070	108	111.3	GTAACGGCTGACCCAGGACTTA	CCTAACTTCCTCCATGGCAACA
	AtPI4Kβ2	At5g09350	168	nd	CTGGTGTCCTGAGGACTGGTTT	CAGCAGCCCTTACTTCCTCGTA

[a] The equation for primer efficiency was calculated using the equation $[(10^{-1/slope})-1] \times 100$. nd – not determined.
[b] UbDKγ4 and UbDKγ7 were originally called AtPI4Kγ4 and AtPI4Kγ7.

Table 3. AtPIP5K primers

PIP5K Type	Name	Locus	Amplicon size (bp)	Efficiency (%)	Forward 5'→3'	Reverse 5'→3'
I/II A	AtPIPK10	At1g01460	104	101.0	AGGTTCTCCGAAAGGTCGATCT	TCGCCAAAGGATCAACGTAGA
	AtPIPK11	At4g01190	87	nd	ATGCACTCCCAGCAGAATTGA	GCGTTGGTTTGTGCTGGACTA
I/II B	AtPIP5K1	At1g21980	132	99.2	AGGAGGAGCCAGTTATCCATCA	GGATCGGCTTGCAGTGACTTAT
	AtPIP5K2	At1g77740	88	100.3	TTTCAGCGGTGAGGCTAAGAA	AATTCCATGCTGCAGGTTGAG
	AtPIP5K3	At2g26420	98	106.2	CACATGGCCGTACTATCGACAA	TGAGGTCTCGAGTCGAAACACA
	AtPIP5K4	At3g56960	92	nd	AAACAAGCTCCGGTTGTGTCTC	TTGGTTCCTTCTGGTGGAAATC
	AtPIP5K6	At3g07960	92	nd	CACTCCATCCATAGGCGGTTT	AGCGTCGTGTTTGGATCGAT
	AtPIP5K7	At1g10900	128	nd	TCGCAGTGCATCGGTAAATG	CTGGCCCATGACATGTAAAGTC
	AtPIP5K8	At1g60890	95	nd	CAACAAGCGGACTGACAAGAAC	TGAAGGCCCATGATGCATAA
	AtPIP5K9	At3g09920	89	nd	CCTTGACGTACGAGGAGCAGTT	TGTTTAGCGCCGATAGGATCTC

[a] The equation for primer efficiency was calculated using the equation $[(10^{-1/slope})-1] \times 100$. nd – not determined.

Table 4. AtPLC primers.

Name	Locus	Amplicon size (bp)	Forward 5'→3'	Reverse 5'→3'
AtPLC1	At5g58670	104	GTCGGAGGTAAGGCCAGGTATT	AACGAGGCTCCAAGACAAACC
AtPLC2	At3g08510	125	GGCCCTGCTACGATTAGAAGTG	TCCGGCTATGTAAAGGAAATGC
AtPLC3	At4g38530	108	GCAGAAATGTCTAACCGCCATT	GCAACTTGCGCTTGAAGCTT
AtPLC4	At5g58700	109	TTCATGAGCACGACGTGAATG	CCCTTGCGATTAAAGAGTGGAA
AtPLC5	At5g58690	115	AGGTGCAGGACGAGACTGAAGT	TCATCGAGGTTCAGCGTATGC
AtPLC6	At2g40116	108	TGATCAAAGCCTTGCAACGA	CAGGCGTTGTAAGCGTTCTTC
AtPLC7	At3g55940	144	CCGAAAGGCGGAATAACTGA	AACCCGTAGCAAATTCCTCTGA

Table 5. Primers for control genes

Name	Locus	Amplicon size (bp)	Efficiency (%)	Forward 5'→3'	Reverse 5'→3'
18S rRNA	18S RRNA	81	99.7	AGTCATCAGCTCGCGTTGACT	CTTCACCGGATCATTCAATCG
Ubq10	AT4G05320	136	102.7	GGTGGTTTCTAAATCTCGTCTCTGTTA	AACAGGAACGGAAACATAGTAGAACAC
Act 2/8	AT3G18780(2) AT1G49240(8)	108	104.7	GGTAACATTGTGCTCAGTGGTGG	AACGACCTTAATCTTCATGCTGC

[a] The equation for primer efficiency was calculated using the equation $[(10^{-1/slope})-1] \times 100$.

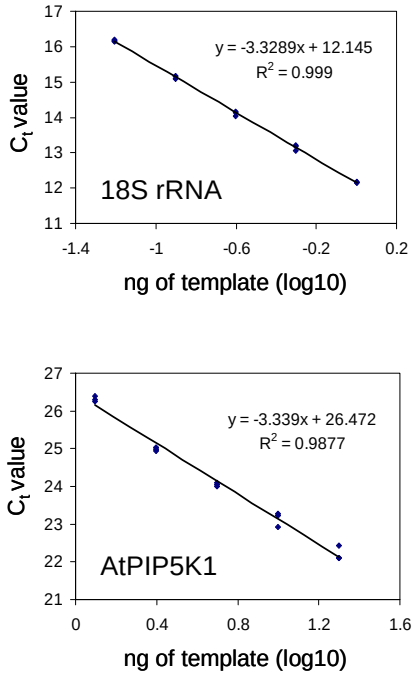

Figure 7. Linear correlation between C_T value variations over template concentrations.
Scatter plot of C_T values over ng of cDNA equivalent (log10 scale) in triplicate reactions with the 18S rRNA (*top*) and AtPIP5K (*bottom*) primer sets. The insets display the best fit linear equation. For 18S rRNA plot template concentrations were 0.065, 0.125, 0.250, 0.5 and 1 ng. For AtPIP5K plot template concentrations were 1.25, 2.5, 5, 10 and 20 ng.

reference sample in that experiment. In both experiments transcript accumulation of PI4K genes were first normalized with transcript level of reference genes (Table 5). We selected 3 "housekeeping" genes as reference genes, 18S rRNA, ubiquitin 10 (*Ubq10*) and actin 2/Actin 8 (*Act2/8*). As part of our analysis we investigated the behavior of these genes in the course of the two experiments. We sought to determine whether the transcript level of these reference genes would change. We found that all 3 genes had negligible variation in their C_T values in all samples collected in both experiments confirming that 18S rRNA, Ubq10 and Act2/8 are indeed good reference genes for Arabidopsis cells and for hyperosmotic treatments (Figure 8).

The analysis of the expression of PI4K genes indicated that under the conditions tested here these genes are not significantly regulated at the level of transcription. We found that PI4K genes do not change dramatically over the transfer cycle of the Arabidopsis cell culture (Figure 9). If anything a slight drop in the transcript levels occurred at d 7.

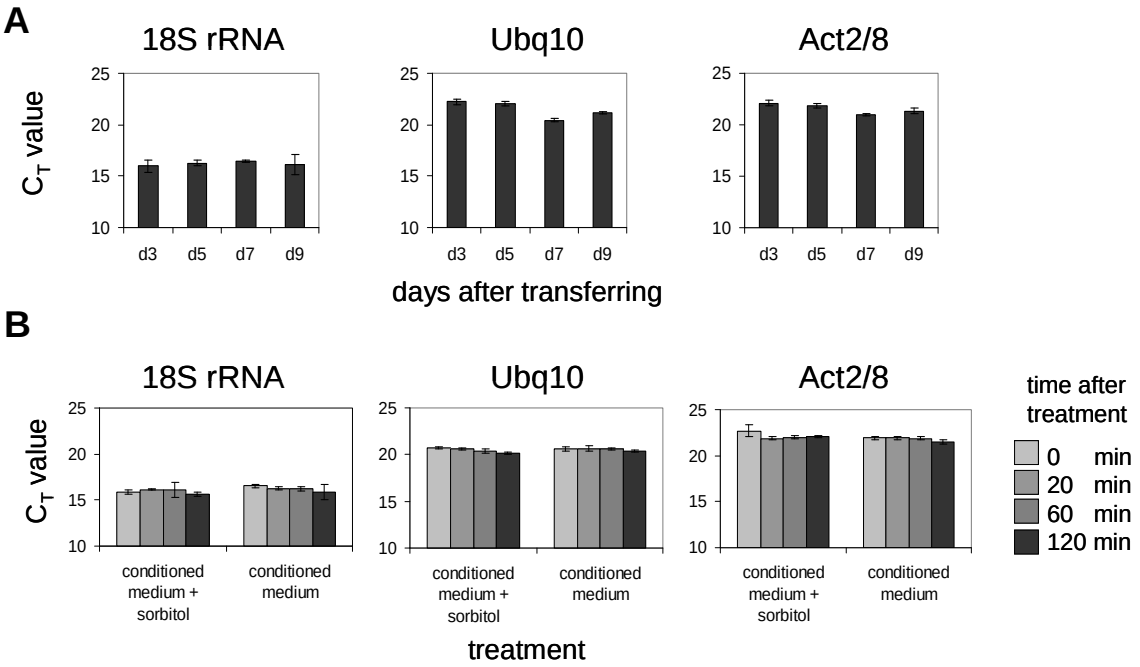

Figure 8. Analysis of the reference genes.
C_T values of the reference genes (18S rRNA, Ubq10 and Act2/8, as indicated) from both experiments (**A.** days after transferring and **B.** time course after hyperosmotic stress) were plotted. The bars represent the mean $\pm$ std deviation of C_T values from triplicated reactions and 2 independent biological replicates.

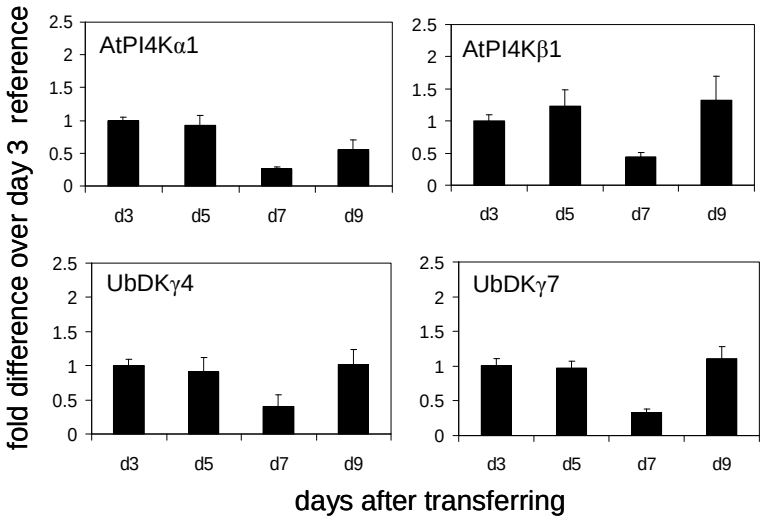

Figure 9. Analysis of gene expression in Arabidopsis cells grown in suspension culture.
Data for the indicated genes (AtPI4α1, AtPI4Kβ1, UbDKγ4 and UbDKγ7) were plotted as mean $\pm$ std deviation of fold change compared to the reference sample d3. Data were normalized against Ubq10.

Interestingly however, at d 9 in the transcript level of some genes went back up to d 3 levels (Figure 9). In the experiment with hyperosmotic treatment again no significant changes in gene expression were observed (Figure 10).

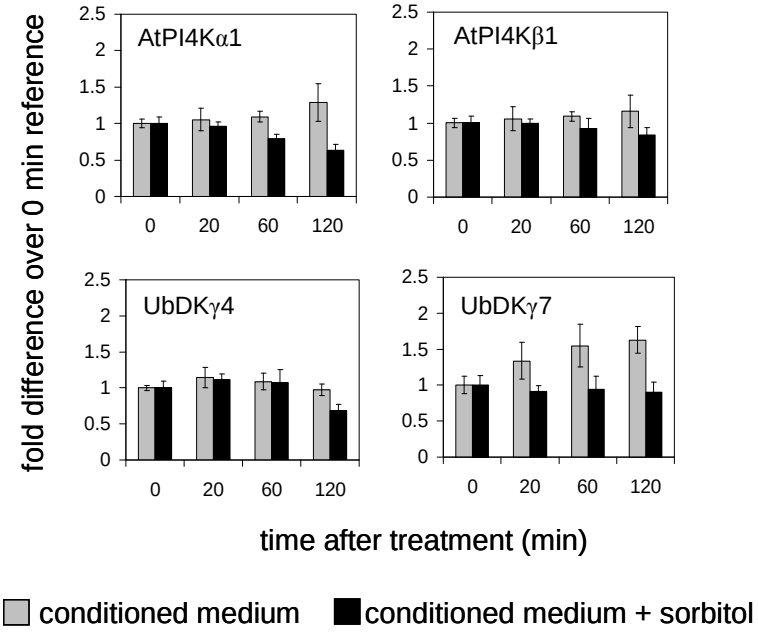

Figure 10. Analysis of gene expression in Arabidopsis cells exposed to hyperosmotic stress.
Data for the indicated genes (AtPI4α1, AtPI4Kβ1, UbDKγ4 and UbDKγ7) were plotted as mean +/- std deviation of fold change compared to the reference sample 0 min. Data were normalized against Ubq10.

APPENDIX 3

Analysis of PI4K activity associated with the products of *lateral root development* (lrd) alleles of AtPI4Kα1

The results presented here are part of a collaboration between Dr. Jocelyn Malamy (University of Chicago), her Ph.D. student Dana MacGregor and myself (*unpublished*). My contribution was to optimize the expression of the recombinant proteins in Sf9 insect cells and perform the lipid kinase assays.

Dr. Malamy and her group have identified Arabidopsis genes responsible for osmotic regulation of lateral root development using a forward genetic screen. This screen identified many recessive mutations which confer a more highly branched root system to plants. They have further characterized two of these mutants, named *lateral root development1* and *2* (*lrd1* and *lrd2*). Both mutants show increased levels of lateral root initiation and of primordia that develop into lateral roots. *lrd2* plants show increased branching under all of the conditions tested. Mapping experiments have identified *lrd2* (A, B and AB forms) as alleles of AtPI4Kα1.

The coding sequence of the *lrd2*A, *lrd2*B and *lrd2*AB was cloned into pFastBac HT plasmid for production of recombinant His-tagged enzymes in insect (*Sf9*) cells. We used the Bac-to-Bac Baculovirus Expression System (Life Technologies/Gibco-BRL) according to the manufacturer's recommendation. *Sf9* cell maintenance, generation of recombinant baculoviruses, transfection and activity assays were performed according to Stevenson-Paulik et. al. (2003).

We found that *lrd2*A, *lrd2*B and *lrd2*AB encode functional PI4Ks and that their activity is indistinguishable from that of the AtPI4Kα1 produced from the cDNA reported by Stevenson-Paulik et. al. (2003) (Figure 11). Our observation is consistent with the fact that the mutations in the *lrd2* alleles are not in the catalytic PI3/4K domain.

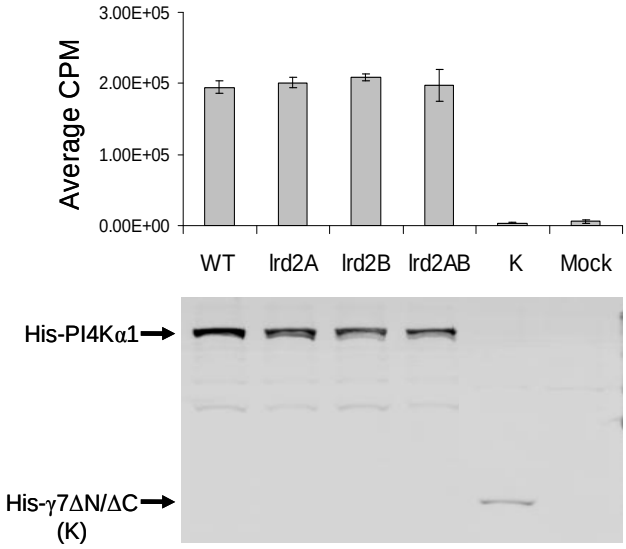

Figure 11. *lrd2* mutant alleles of AtPI4Kα1 encode active PI4K
Sf9 cells expressing *lrd2*A, *lrd2*B and *lrd2*AB and wild type *AtPI4Kα1* were lysed and sonicated, and the cleared lysates were assayed for PI4K activity. The averages +/- std deviation of duplicate samples from two independent experiment are shown (*upper panel*). Lower panel: 30 μg of lysates from the corresponding insect cells were separated by SDS-PAGE and blotted onto PVDF membrane. Proteins were visualized with a monoclonal anti-Penta·His™ antibody (Qiagen GmbH, Hilden, Germany) as described in **Chapter 2**. **(K =** His-γ7ΔN/ΔC which is a truncation of UbDKγ7 (**Chapter 4** – Figure 1) with no lipid kinase activity that was used here as a control in addition to the Mock transfected cells.

APPENDIX 4

UbDKγ4 phosphorylation sites and other *in vitro* substrates

UbDKγ4 phosphorylation sites

As part of the biochemical characterization of UbDKγ4, we determined the *in vitro* phosphorylation sites of the recombinant UbDKγ4 using mass spectrometry. GST-UbDKγ4 was produced in *E. coli* and affinity purified as described in **Chapter 2**. Protein phosphorylation reactions were performed with GST-UbDKγ4 in the presence and absence of ATP. The products of the reactions were separated by SDS-PAGE and the corresponding bands were excised and subjected to in-gel tryptic digestion with the resulting peptides extracted and analyzed by LC/MS/MS. The results, summarized in Table 6, indicate that UbDKγ4 is heavily phosphorylated in the interdomain region (between UBL2 and PI3/4K domains – **Chapter 4**). Half (4 out of 8) of the identified sites are in Ser residues between aa 185 and 264. The fact that many of the phosphorylation sites are present in this interdomain sequence may explain, at least in part, why that sequence (absent in the truncation ΔUBL1/UBL2) is necessary for autophosphorylation *in vitro* (**Chapter 2** – Figure 3).

Of interest, 6 sites were found in samples from both reactions, with and without ATP and one site was found in the sample from reactions performed in the absence of ATP (Table 6). This observation suggests that these sites are phosphorylated before the affinity purification of the enzyme. This can happen either as result of activity of a bacterial protein kinase or (most likely) as a result of autophosphorylation of UbDKγ4 inside the *E. coli*. Consistent with this finding that the recombinant purified UbDKγ4 is phosphorylated, we found that pre-incubation with ATP prior to doing the binding assays with UbDKγ4 (as in **Chapter 2** – Figure 4C) did not make any detectable difference in the binding partners recovered (Figure 12).

Unexpectedly, a Tyr residue (Table 6) was phosphorylated. Because no other PIKK or PI3/4K has Tyr kinase activity, we assume this Tyr phosphorylation results from a bacterial kinase.

Arabidopsis CDC48 phosphorylation

Mammalian CDC48, known as p97 or valosin-containing protein (VCP), is targeted for phosphorylation by protein kinases. Two different kinases were identified as using p97/VCP as a substrate, Akt kinase and DNA-PK (Klein et al., 2005; Livingstone et al., 2005). The latter is a PIKK (see **Chapter 1 and 2**) that targets Ser784 of p97/VCP. We have shown that AtCDC48c interacts *in vitro* with UbDKγ4 (**Chapter 2**). Here we asked whether AtCDC48 could be phosphorylated by UbDKγ4 like AtUFD1, another UbDKγ4 interacting protein. We found that AtCDC48 is phosphorylated *in vitro* by UbDKγ4 (Figure 13).

Zea mays UFD1 phosphorylation

During the process of searching for UbDKγ4 interacting proteins and putative substrates, we tested whether an N-terminal fragment of *Zea mays* UFD1 (ZmUFD1) (a kind gift from Dr. Rebecca Boston's lab) could be an UbDKγ4 *in vitro* substrate. Protein phosphorylation assays as described before using recombinant UbDKγ4 and the ZmUFD1 fragment revealed that UbDKγ4 can phosphorylate the ZmUFD1 fragment (Figure 14).

Recombinant protein production, purification and phosphorylation assays for both AtCDC48 and ZmUFD1 fragment were performed as described in early chapters (**2** an **4**).

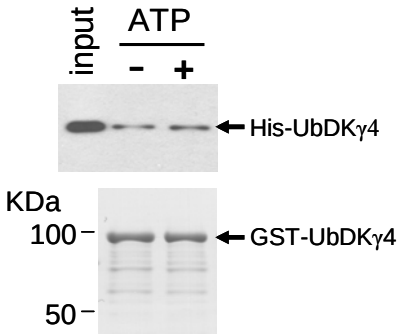

Figure 12. Pre-incubation with ATP does not affect UbDKγ4 intermolecular interaction.
GST-UbDKγ4 immobilized on glutathione-Sepharose beads was used as bait in pull-down assays containing His-UbDKγ4 as prey. GST-UbDKγ4 and His-UbDKγ4 were pre-incubated together in phosphorylation reaction conditions with or without ATP (as indicated). Bound His-UbDKγ4 was detected by immunoblotting with anti His-tag antibody (*upper panel*). GST-UbDKγ4 was visualized by Amido Black staining of the membrane (*lower panel*). The *input* lane corresponds to 20% of the amount of His-UbDKγ4 originally used in each binding assay.

Table 6. Identification of UbDKγ4 *in vitro* phosphorylation sites as determined by LC/MS/MS analysis.

Peptide[a]	Calc. $[M+H]^{+b}$	Meas. $[M+H]^{+c}$	Chg.[d]	Xcorr[e]	ΔC_n[f]	Ions[g]	Phosphoryl-ation Site	Reaction + / - ATP
R.DY*GVSEGNILHLVLK.L	1737.9	1736.5	2	4.496	0.195	28/42	pY93	+ ATP
R.DYGVS*EGNILHLVLK.L	1737.9	1736.8	2	3.761	0.241	26/42	pS96	both
R.EAKS*IVPPK.K	1049.1	1048.6	2	1.831	0.251	14/24	pS217	both
K.KLS*LEPVVVNSK.A	1393.5	1393.3	2	2.823	0.399	21/33	pS225	both
K.LSLEPVVVNS*K.A	1265.4	1265.7	2	3.164	0.377	22/30	pS233	both
K.DM#IQS*ASDGLK.S	1261.3	1260.6	2	1.60	0.115	11/30	pS247	- ATP
R.SSEGT*GGAYFM#QGPSGNK.F	1871.8	1871.0	2	4.689	0.089	28/51	pT265	both
K.KGT*KVGEGALR.E	1196.3	1196.1	2	2.933	0.373	20/30	pT312	both

[a]The amino acid residues appearing before and after the periods correspond to the residues proceeding and following the peptide in the protein sequence. Based on the product ion spectrum, phosphoseryl, phosphothreonyl and phosphotyrosyl residues are determined as indicated by S*, T* and Y*, respectively. Met sulfoxide is denoted as M#.

[b]The average mass calculated is based upon the peptide sequence.

[c]Deconvoluted mass determined from the observed centroid mass-to-charge (*m/z*) ratio at the reported charge state.

[d]Charge state of the observed precursor ion.

[e]SEQUEST cross-correlation score (Xcorr) of the peptide is based on the degree of overlap between the product ion spectrum to the theoretical distribution of b and y ions for the peptide.

[f]SEQUEST difference of cross correlation scores (ΔC_n) is the "difference" between the top two Xcorrs for a given product ion spectrum.

[g]The total number of b and y ions (identified/theoretical).

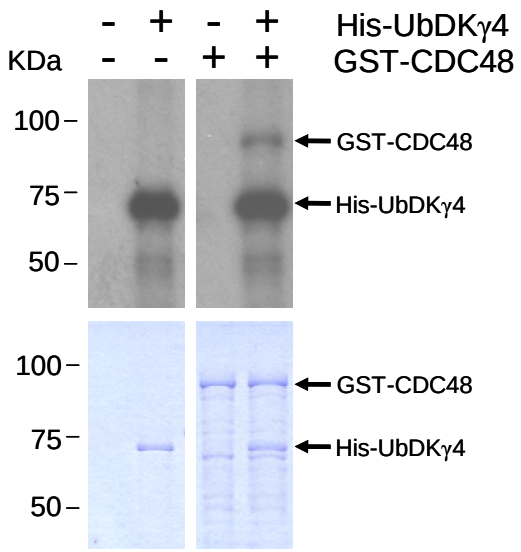

Figure 13. UbDKγ4 phosphorylates AtCDC48.
Protein phosphorylation assays were performed as described in Chapter II with no substrate or 1 µg of GST-CDC48 in reactions carried out in the presence or absence of 3 µg of His-UbDKγ4. GST-CDC48 was immobilized onto the glutathione Sepharose affinity beads and His-UbDKγ4 free in the supernatant was partially removed prior to the electrophoresis. The products of the reactions were resolved by SDS-PAGE. The ^{32}P-labeled proteins were revealed by autoradiography (*upper panel*) and the protein amounts by Coomassie blue staining (*lower panel*).

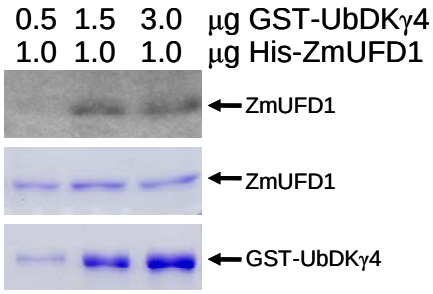

Figure 14. AtPI4Kγ4 phosphorylates UFD1. Increasing amounts of partially purified GST-AtPI4Kγ4 produced in *E. coli* were used in reactions containing ATP and recombinant UFD1 from maize. The products of the reactions were resolved by SDS-PAGE. The ^{32}P-labeled proteins were revealed by autoradiography (*upper panel*) and the protein amounts by Coomassie blue staining (*lower panel*).

APPENDIX 5

Effect of lipids on UbDKγ4 kinase activity

Lipid can regulate activity of protein kinases. Phosphoinositide-dependent kinases (PDKs) are the best known examples of protein kinases that can respond to the presence of phospholipids. Lipid regulation provides a mechanism for the PDKs to integrate membrane bound signaling with protein phosphorylation cascades (Alessi, 2001). PDK homologs have been found in plants, and they have been implicated in signal transduction mechanisms (Anthony et al., 2004).

We asked whether UbDKγ4 protein kinase activity could be affected by the presence of lipids. To investigate this we used recombinant GST-UbDKγ4 (**Chapter 2**) in phosphorylation assays with histone as substrate. We compared levels of histone phosphorylation across reactions with triton (X-100) or triton plus phosphatidylinositol (PtdIns), phosphatidic acid (PtdOH), phosphatidylcholine (PtdCho) or diacylglycerol (DAG) (Figure 15). Differences were marginal (~25 %) for the presence of all lipids tested, except PtdIns where histone phosphorylation was more than 50 % higher compared to the control reaction. Although the experiment has been repeated twice, more data are needed to compare the effects at different lipid concentrations and with a mixture of lipids, before any conclusions can be made.

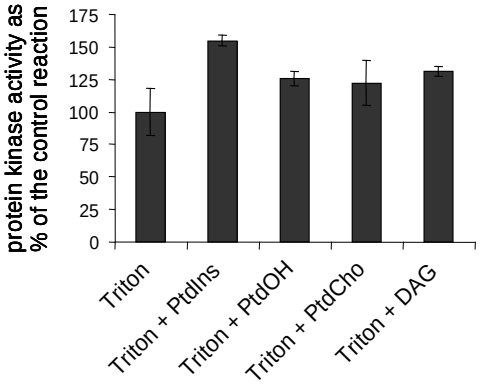

Figure 15. Effect of lipids on UbDKγ4 protein kinase activity.
GST-UbDKγ4 was used in protein kinase reactions containing [γ-^{32}P]ATP and histone (**Chapter 2**). The reactions were conducted in the presence of 0.01% Triton X-100 combined with different lipids as indicated in a final concentration of 15 μM of each lipid. Histone phosphorylation was measured as described by Zhang et. al. (2001). Briefly, phosphorylated histone in the reaction supernatant was spotted in P81 filter disks, non-incorporated ATP was removed by washing with 0.05 % phosphoric acid and the activity measured by scintillation counting. Data are presented as a percentage of the reaction in absence of lipid. Bars are average +/- std deviation of 4 replicates from two independent experiments.

APPENDIX 6

Phylogenetic analyses and expression studies reveal two distinct groups of calreticulin isoforms in higher plants

Staffan Persson, Magnus Rosenquist, Karin Svensson, **Rafaelo M. Galvão**, Wendy F. Boss and Marianne Sommarin

Department of Plant Biochemistry, Lund University, 22100 Lund, Sweden (S.P., K.S., M.S.); Department of Pathology, Beth Israel Deaconess Medical Center, Harvard Medical School, Boston, MA 02215 (M.R.); and Botany Department, North Carolina State University, Raleigh, NC 27695 (R.G., W.F.B.)

My contribution to this work was the gene expression analysis by RNA blotting of calreticulin 3 (CRT3) in different tissues of maize plants. The corresponding manuscript has been published:

Persson S, Rosenquist M, Svensson K, Galvao R, Boss WF, Sommarin M (2003) Phylogenetic analyses and expression studies reveal two distinct groups of calreticulin isoforms in higher plants. Plant Physiol 133: 1385-1396.

References

Alessi DR (2001) Discovery of PDK1, one of the missing links in insulin signal transduction. Colworth Medal Lecture. Biochem. Soc. Trans. 29: 1-14.

Anthony RG, Henriques R, Helfer A, Meszaros T, Rios G, Testerink C, Munnik T, Deak M, Koncz C, Bogre L (2004) A protein kinase target of a PDK1 signalling pathway is involved in root hair growth in Arabidopsis. Embo J 23: 572-581.

Barylko B, Wlodarski P, Binns DD, Gerber SH, Earnest S, Sudhof TC, Grichine N, Albanesi JP (2002) Analysis of the catalytic domain of phosphatidylinositol 4-kinase type II. J. Biol. Chem. 277: 44366-44375.

Bays NW, Hampton RY (2002) Cdc48-Ufd1-Npl4: stuck in the middle with Ub. Curr Biol 12: R366-371.

Boss WF, Davis AJ, Im YJ, Galvao RM, Perera IY (2006) Phosphoinositide metabolism: towards an understanding of subcellular signaling. Subcell Biochem 39: 181-205.

Boudsocq M, Lauriere C (2005) Osmotic signaling in plants. Multiple pathways mediated by emerging kinase families. Plant Physiol. 138: 1185-1194.

Cantley LC (2002) The phosphoinositide 3-kinase pathway. Science 296: 1655-1657.

Cantrell DA (2001) Phosphoinositide 3-kinase signalling pathways. J Cell Sci 114: 1439-1445.

Carpenter CL, Cantley LC (1996) Phosphoinositide kinases. Curr Opin Cell Biol 8: 153-158.

Chen Q, Boss WF (1990) Short-Term Treatment with Cell Wall Degrading Enzymes Increases the Activity of the Inositol Phospholipid Kinases and the Vanadate-Sensitive ATPase of Carrot Cells. Plant Physiol. 94: 1820-1829.

Cockcroft S, De Matteis MA (2001) Inositol Lipids as Spatial Regulators of Membrane Traffic. Journal of Membrane Biology 180: 187-194.

DeWald DB, Torabinejad J, Jones CA, Shope JC, Cangelosi AR, Thompson JE, Prestwich GD, Hama H (2001) Rapid accumulation of phosphatidylinositol 4,5-bisphosphate and inositol 1,4,5-trisphosphate correlates with calcium mobilization in salt-stressed arabidopsis. Plant Physiol 126: 759-769.

Drobak BK, Watkins PA (2000) Inositol(1,4,5)trisphosphate production in plant cells: an early response to salinity and hyperosmotic stress. FEBS Lett 481: 240-244.

Fruman DA, Meyers RE, Cantley LC (1998) Phosphoinositide Kinases. Annual Review of Biochemistry 67: 481-507.

Fu H, Girod PA, Doelling JH, van Nocker S, Hochstrasser M, Finley D, Vierstra RD (1999) Structure and functional analysis of the 26S proteasome subunits from plants. Mol Biol Rep 26: 137-146.

Glickman MH, Rubin DM, Fried VA, Finley D (1998) The regulatory particle of the Saccharomyces cerevisiae proteasome. Mol Cell Biol 18: 3149-3162.

Johnson ES, Ma PCM, Ota IM, Varshavsky A (1995) A proteolytic pathway that recognizes ubiquitin as a degradation signal. J. Biol. Chem. 270: 17442-17456.

Klein JB, Barati MT, Wu R, Gozal D, Sachleben LR, Jr., Kausar H, Trent JO, Gozal E, Rane MJ (2005) Akt-mediated valosin-containing protein 97 phosphorylation regulates its association with ubiquitinated proteins. J Biol Chem 280: 31870-31881.

Klusener B, Young JJ, Murata Y, Allen GJ, Mori IC, Hugouvieux V, Schroeder JI (2002) Convergence of calcium signaling pathways of pathogenic elicitors and abscisic acid in Arabidopsis guard cells. Plant Physiol 130: 2152-2163.

Livak KJ, Schmittgen TD (2001) Analysis of relative gene expression data using real-time quantitative PCR and the $2^{-\Delta\Delta CT}$ method. Methods 25: 402-408.

Livingstone M, Ruan H, Weiner J, Clauser KR, Strack P, Jin S, Williams A, Greulich H, Gardner J, Venere M, Mochan TA, DiTullio RA, Jr., Moravcevic K, Gorgoulis VG, Burkhardt A, Halazonetis TD (2005) Valosin-containing protein phosphorylation at Ser784 in response to DNA damage. Cancer Res 65: 7533-7540.

Mikami K, Katagiri T, Iuchi S, Yamaguchi-Shinozaki K, Shinozaki K (1998) A gene encoding phosphatidylinositol-4-phosphate 5-kinase is induced by water stress and abscisic acid in Arabidopsis thaliana. Plant J 15: 563-568.

Perera IY, Heilmann I, Boss WF (1999) Transient and sustained increases in inositol 1,4,5-trisphosphate precede the differential growth response in gravistimulated maize pulvini. Proc Natl Acad Sci U S A 96: 5838-5843.

Roth MG (2004) Phosphoinositides in constitutive membrane traffic. Physiol. Rev. 84: 699-730.

Stevenson-Paulik J, Love J, Boss WF (2003) Differential regulation of two Arabidopsis type III phosphatidylinositol 4-kinase isoforms. A regulatory role for the pleckstrin homology domain. Plant Physiol. 132: 1053-1064.

Stevenson JM, Perera IY, Heilmann I, Persson S, Boss WF (2000) Inositol signaling and plant growth. Trends Plant Sci 5: 252-258.

Toker A, Cantley LC (1997) Signalling through the lipid products of phosphoinositide-3-OH kinase. Nature 387: 673-676.

van Nocker S, Deveraux Q, Rechsteiner M, Vierstra RD (1996) Arabidopsis MBP1 gene encodes a conserved ubiquitin recognition component of the 26S proteasome. Proc Natl Acad Sci U S A 93: 856-860.

Zhao X-H, Bondeva T, Balla T (2000) Characterization of recombinant phosphatidylinositol 4-kinase β reveals auto- and heterophosphorylation of the enzyme. J. Biol. Chem. 275: 14642-14648.

Zhang H, Shi X, Hampong M, Blanis L, Pelech S (2001) Stress-induced inhibition of ERK1 and ERK2 by direct Interaction with p38 MAP kinase. J. Biol. Chem. 276: 6905-6908.